

Crosstalk of gene polymorphisms with RNA and protein phenotypic characteristics

Rudan, Marina

Doctoral thesis / Disertacija

2018

Degree Grantor / Ustanova koja je dodijelila akademski / stručni stupanj: **University of Zagreb, Faculty of Science / Sveučilište u Zagrebu, Prirodoslovno-matematički fakultet**

Permanent link / Trajna poveznica: <https://um.nsk.hr/um:nbn:hr:217:625111>

Rights / Prava: [In copyright](#) / [Zaštićeno autorskim pravom.](#)

Download date / Datum preuzimanja: **2024-07-17**



Repository / Repozitorij:

[Repository of the Faculty of Science - University of Zagreb](#)





University of Zagreb

FACULTY OF SCIENCE
DEPARTMENT OF BIOLOGY

Marina Rudan

**CROSSTALK OF GENE POLYMORPHISMS
WITH RNA AND PROTEIN PHENOTYPIC
CHARACTERISTICS**

DOCTORAL THESIS

Zagreb, 2018.



Sveučilište u Zagrebu

PRIRODOSLOVNO MATEMATIČKI FAKULTET

BIOLOŠKI ODSJEK

Marina Rudan

**POVEZANOST GENSKIH POLIMORFIZAMA
S FENOTIPSKIM KARAKTERISTIKAMA
MOLEKULA RNA I PROTEINA**

DOKTORSKI RAD

Zagreb, 2018.

This doctoral thesis has been carried out at the Mediterranean Institute for Life Sciences in Split and supervised by Professor Miroslav Radman and Anita Kriško, PhD in the frame of the Doctoral programme of Biology of the University of Zagreb. Some experiments were carried out also in: (i) the Department of Biology at the Faculty of Science of the University of Zagreb; (ii) the Division of Molecular Medicine, Rudjer Bošković Institute, Bijenička 54, 10000 Zagreb; (iii) the Institut für Zellbiochemie, Universitätsmedizin Göttingen, Humboldtallee 23, D-37073 Göttingen, Germany; (iv) the Molecular Systems Group, MRC London Institute of Medical Sciences (LMS), Du Cane Road, London W12 0NN, United Kingdom; (v) the Molecular Systems Group, Institute of Clinical Sciences (ICS), Faculty of Medicine, Imperial College London, Du Cane Road, London W12 0NN, United Kingdom; (vi) the Single Molecule Imaging Group, MRC London Institute of Medical Sciences (LMS), Imperial College London, Hammersmith Hospital Campus, London, United Kingdom.

Acknowledgment

I would like to express my gratefulness to my advisor, Prof. Miroslav Radman for his tremendous knowledge, motivation and inspirational discussions. His approach to science and simplicity to represent its intricacy is remarkable. I would also like to express my particular appreciation to my mentor Dr. Anita Kriško and thank her for the faith she had in me and for accepting me into her lab. Her constant support and guidance helped me a lot during my PhD and have enable me to grow as a research scientist.

My sincere thanks goes to Dr. Tobias Warnecke who participated in a notable part of my research. His comments and knowledgeable advice were priceless. I would like to thank the rest of my thesis committee: Prof. Biljana Balen, Dr. Davor Zahradka and Prof. Đurđica Ugarković for their insightful comments, suggestions and support.

I would also like to thank Jelena Ružić for everything she did at Medils, for her kindness and her strength. Many thanks goes to Prosper, Branka, Irena, Ljilja and Lora.

I thank all the labmates, especially Musa for being always ready to help. I am also very happy I had a chance to share the office with my colleagues Tea, Matea, Anita and Marina. I thank them for providing the stimulating working environment and for all the joyful moments we have shared together. Special thanks goes to Tea for her laboratory and personal support, her consideration and warm heart.

Thanks to all my friends for understanding why I did not have always time for them.

More than anyone else I would like to thank my family: my parents and my sister for being my biggest support. I am so grateful I have you in my life and I appreciate all the love and time we share together.

CROSTALK OF GENE POLYMORPHISMS WITH RNA AND PROTEIN PHENOTYPIC CHARACTERISTICS

MARINA RUDAN

Mediterranean Institute for Life Sciences

Meštrovićevo šetalište 45, Split

Both RNA and protein molecules can misfold into non-functional conformations. Since DNA is transcribed into RNA to direct the biosynthesis of proteins, functional cells require the maintenance of DNA, RNA and protein homeostasis. Here, it is explored whether DNA polymorphisms can impact upon RNA and protein conformation to the extent of displaying phenotypic changes. It has been found that this is a multifaceted process. Mutation-induced protein conformational changes can modify protein interactions and determine protein susceptibility to oxidation. Moreover, it was showed that deleterious mutations can be buffered at the transcript level with RNA chaperones (DEAD-box RNA helicases and cold shock proteins) acting as phenotypic suppressors of mutations and enhancing cellular fitness. These results also highlight the importance of mRNA quality control in eukaryotes and its potential to modulate cellular metabolic activity and lifespan. This research underscores the importance of studying systems-level crosstalk among DNA, RNA and protein maintenance, rather than studying individual processes separately.

113 pages, 44 figures, 10 tables, 151 references, original in English

Keywords: polymorphism, carbonylation, RNA chaperones, mutation buffering, RNA splicing, retrograde response

Supervisor: Prof. emeritus Miroslav Radman, Mediterranean Institute for Life Sciences

Reviewers: Prof. Biljana Balen; Dr. Davor Zahradka; Dr. Tobias Warnecke

Doctoral thesis accepted

Sveučilište u Zagrebu

Doktorska disertacija

Prirodoslovno-matematički fakultet

Biološki odsjek

POVEZANOST GENSKIH POLIMORFIZAMA S FENOTIPSKIM KARAKTERISTIKAMA MOLEKULA RNA I PROTEINA

MARINA RUDAN

Mediteranski institut za istraživanje života

Meštrovićevo šetalište 45, Split

Molekule RNA i proteini se mogu pogrešno smotati u nefunkcionalne konformacije. Budući da se za biosintezu proteina DNA prepisuje u RNA, funkcionalne stanice zahtijevaju održavanje homeostaze DNA, RNA i proteina. U ovom radu je istraženo mogu li DNA polimorfizmi utjecati na konformaciju molekule RNA i proteina, te rezultirati fenotipskim promjenama. Otkriveno je da je ovo iznimno složen proces, tijekom kojeg konformacijske promjene proteina izazvane mutacijama molekula DNA mogu modificirati interakcije proteina i odrediti njihovu osjetljivost na oksidaciju. Također, pokazano je da štetne mutacije mogu biti puferirane na razini transkripcije pomoću RNA šaperona (DEAD-box RNA helikaza i 'cold shock' proteina), koji djeluju kao fenotipski supresori mutacija i poboljšavaju stanični fitness. Ovi rezultati naglašavaju značaj kontrole kvalitete mRNA u eukariotima i njen potencijal za modulaciju stanične metaboličke aktivnosti te životnog vijeka. Ovo istraživanje ističe važnost proučavanja cjelokupnog sustava DNA, RNA i proteina, te njihove međusobne komunikacije umjesto analize staničnih procesa pojedinačno.

113 strana, 44 slike, 10 tablica, 151 literaturnih izvoda, originalno na engleskom jeziku

Ključne riječi: polimorfizam, karbonilacija, RNA šaperoni, puferiranje mutacija, RNA izrezivanje, retrogradni odgovor

Mentor: Prof. emeritus Miroslav Radman, Mediterranean Institute for Life Sciences

Ocjenjivači: Izv. prof. dr.sc. Biljana Balen; dr. sc. Davor Zahradka; Tobias Warnecke, PhD

Doktorski rad prihvaćen

Prošireni sažetak doktorske disertacije

Mutacije nastaju u stanicama kao promjene u sekvenci molekule DNA, potiču evoluciju i uzrok su mnogih bolesti. Pri prepisivanju i prevođenju, mutacije mogu utjecati na stabilnost molekula RNA i funkcionalnost proteina i stoga imati učinke na fenotip. Jedna od teorija starenja ističe akumulaciju oštećene DNA kao glavni uzrok starenja (Freitas and de Magalhaes, 2011). Postoje mnogi primjeri bolesti koje su uzrokovane izravno utjecajem pojedinačnih nukleotidnih polimorfizama (Bessenyei et al., 2004). Mutacije također mogu dovesti do supstitucije aminokiselina i na taj način uzrokovati povećanu osjetljivost proteina na karbonilaciju (Dukan et al., 2000), koja je ireverzibilni tip oksidacijskog oštećenja. Proteinska karbonilacija se akumulira tijekom starenja te se može smatrati biomarkerom mnogih bolesti povezanih sa starenjem.

Pitanje postavljeno u ovom istraživanju je: mogu li mutacije akumulirane na nivou molekule DNA biti puferirane pomoću RNA šaperona? Da bi bile u potpunosti funkcionalne, molekule RNA se također moraju smotati u trodimenzionalnu strukturu. Budući da se nerijetko događaju greške u ovom procesu (Herschlag, 1995), molekule RNA zauzimaju dugoživuće alternativne strukture (Downs i Cech, 1996) koje zahtijevaju pomoć RNA-vezujućih proteina (RNA šaperona). Kao i proteinski šaperoni, RNA šaperoni stabiliziraju nativne strukture i/ili pomažu u ponovnom smatanju krivo smotanih vrsta (Russell, 2008). Pokazano je da proteinski šaperoni mogu puferirati mutacije koje utječu na proteinsku stabilnost i tako maskirati njihove fenotipske posljedice (Queitsch et al., 2002; (Burga et al., 2011); (Fares et al., 2002). U kontekstu održavanja strukture RNA, od posebnog interesa su DEAD-box RNA helikaze (DBRH), koje odmataju zavojnice RNA i tako mogu umanjiti greške smatanja (Pan i Russell, 2010). Također, mnoge DBRH, uključujući RhlB komponentu degradosoma bakterije *E. coli* i eukariotski faktor inicijacije eIF4A, uključene su u smatanje i razmatanje različitih molekula RNA te bi mogli djelovati kao širok spektar mutacijskih pufera.

Dobiveni rezultati pokazuju da povećana ekspresija DEAD-box RNA helikaza (RhlB, SrmB i CsdA) poboljšava fitness mutatora *E. coli* iz 40.000 generacije (40k). Na taj se način, po prvi puta, pokazala sposobnost RNA šaperona u puferiranju štetnih mutacija. Ovaj fenomen je demonstriran i u drugom soju bakterije *E. coli* sniženog fitnessa, $\Delta mutH$, koji je poboljšan povećanom ekspresijom DBRH (RhlB, SrmB i CsdA). Nakon što je utvrđeno da ne postoji niti jedna identična mutacija između sojeva 40k i $\Delta mutH$, zaključeno je da RNA šaperoni puferiraju

širok spektar supstrata. Kako bi se ispitala molekularna osnova puferiranja, identificirane su mutacije koje djeluju štetno na stanični fitnes pojedinačno: mutacija u genu *lamB* (iz liste mutacija u soju *ΔmutH*) i sinonimna mutacija u genu *rplS* (iz liste mutacija u soju 40k). Kompeticijskim eksperimentima pokazano je puferiranje ovih štetnih učinaka uz pomoć pojačane ekspresije DBRH. Mehanistička raznolikost puferiranja dokazana je i pojačanom ekspresijom „cold-shock“ proteina CspA, koji je poboljšao fitnes u oba soja, 40k i *ΔmutH*.

Ispitani su korisni učinci RNA helikaza i u eukariotskim stanicama. Stoga, drugi dio ove disertacije uključuje proučavanje DEAD-box RNA helikaze Mss116, kodirane u jezgri kvasca *S. cerevisiae*, eksprimirane u mitohondrijima i potrebne za učinkovito izrezivanje mitohondrijskih introna grupe I i II. Od ukupno 13 introna u mtDNA, sedam ih se nalazi u genu *COXI*, koji kodira za podjedinicu I citokrom c oksidaze, a pet u genu *COB*, koji kodira citokrom b (Kennell et al., 1993).

Pretpostavljeno je da izrezivanje introna još jedan izvor pogrešaka u kontekstu stanične homeostaze, posebno u kontroli kvalitete mRNA i proteina, stoga je testirano može li učinkovitije i preciznije izrezivanje na razini mRNA ili potpuno uklanjanje introna iz mtDNA rezultirati poboljšanim staničnim fitnesom. Doista, fenotip bez introna (*I₀*) uključuje povećanu količinu zrelih mRNA komponenti dišnog lanca *COXI* i *COB* te ima pozitivan učinak na životni vijek kvasca. Učinkovitije izrezivanje introna iz gena *COXI* i *COB* pomoću RNA helikaze Mss116 također je rezultiralo produženim kronološkim životnim vijekom, što ukazuje na važnu ulogu kontrole kvalitete RNA u životnom vijeku kvasca *S.cerevisiae*.

Sojevi kvasca s uklonjenim mitohondrijskim intronima (*I₀*) ili s pojačanom ekspresijom Mss116, pokazivali su dulje generacijsko vrijeme, produljeni kronološki životni vijek, fuziju mitohondrija, povišenu potrošnju kisika, veću razinu ATP-a i povećanu razinu zrelih mRNA proteina *COXI* i *COB* u usporedbi s divljim tipom. Delecija gena *RTG2* u testiranim sojevima kvasca dovodi do smanjene razine potrošnje kisika i ATP-a, te smanjenog mitohondrijskog volumena i mase, što dokazuje da su ove fenotipske promjene kontrolirane aktivacijom retrogradnog odgovora. Ovi rezultati naglašavaju važnost održavanja homeostaze molekule RNA u normalnom staničnom funkcioniranju.

Jedno od pitanja postavljenih u ovom istraživanju je da li se pojava genskih polimorfizama, evoluiranih experimentalno u kontinuiranim bakterijskim kulturama, reflektira u polimorfizmu oksidacije proteina. Richard Lenski je tijekom experimenta „*E.coli* long term evolution experiment“, kojega je započeo 1988. godine, sačuvao brojne generacije bakterijskih kultura

koje su evoluirale tijekom vremena. Ova zbirka predstavlja bogat skup mutacija koje nam mogu pomoći u razumijevanju molekularne osnove proteinske otpornosti i osjetljivosti na oksidacijska oštećenja. Mutatorski sojevi, koji su nastali rano u ovoj experimentalnoj evoluciji *in vitro*, zajedno s ne-mutatorima i zajedničkim pretkom predstavljaju idealni modelni sustav za proučavanje utjecaja različitih vrsta mutacija na oksidacijsku osjetljivost proteina, te njihovih fenotipskih učinaka.

Cilj ovog projekta je bio odvojiti proteine exprimirane tijekom exponencijalnog rasta pretka, mutatora i ne-mutatora koristeći metodu dvodimenzionalne oxi-diferencijalne gel elektroforeze (engl. two dimensional Oxi-differential gel electrophoresis, 2D Oxi-DIGE). Ova metoda omogućuje učinkovito detektiranje oksidativnog oštećenja proteina (karbonilacije) i njihove ekspresije na istom gelu, obilježavajući ih različitim fluorescentnim bojama. Istovremenim označavanjem karboniliranih proteina specifičnim fluorescentnim bojama (mutatora i ne-mutatora u usporedbi s pretkom), oni s višom ili nižom razinom karbonilacije identificirani su spektrometrijom masa.

Koristeći 2D Oxi-DIGE identificirano je 39 proteina iz mutatorskog soja bakterije *Escherichia coli* (*E. coli*) s povećanom razinom karbonilacije, od kojih 10 nosi mutaciju u kodirajućim genima i 25 proteina sa sniženom razinom karbonilacije, od kojih 6 nosi mutaciju u kodirajućim genima. Također su identificirani proteini s povećanom razinom karbonilacije (kao što je ATP sintaza) u mutatorskom soju u usporedbi s pretkom i ne-mutatorom čiji kodirajući geni ne nose mutaciju, ali proteini koji su im interakcijski partneri nose, što ukazuje na indirektan učinak genskih polimorfizama na karbonilaciju proteina.

Table of content:

| | |
|--|----|
| 1. INTRODUCTION | 1 |
| 2. LITERATURE REVIEW | 4 |
| 2.1. Cellular fitness and homeostasis | 4 |
| 2.2. RNA folding..... | 4 |
| 2.2.1. Proteins with RNA chaperone activity..... | 5 |
| 2.3. Protein folding..... | 8 |
| 2.3.1. Protein chaperones | 9 |
| 2.3.2. Mutation buffering..... | 10 |
| 2.4. <i>E. coli</i> long term evolution experiment..... | 11 |
| 2.5. Aging..... | 13 |
| 2.5.1. The hallmarks of aging..... | 13 |
| 2.5.1.1. Genomic instability..... | 13 |
| 2.5.1.2. DNA damage theory of aging | 14 |
| 2.5.1.3. Proteostasis theory of aging..... | 15 |
| 2.5.2. DNA polymorphisms..... | 16 |
| 2.5.3. Oxidative stress | 17 |
| 2.5.3.1. The free radical theory of aging | 17 |
| 2.5.3.2. Protein carbonylation..... | 18 |
| 2.6. Yeast as a model organism in aging | 19 |
| 2.6.1. Replicative and chronological lifespan..... | 20 |
| 2.6.2. <i>S. cerevisiae</i> mitochondria..... | 22 |
| 2.6.2.1. <i>S. cerevisiae</i> mitochondrial genome | 22 |
| 2.6.2.1.1. Group II introns | 24 |
| 2.6.2.2. Retrograde response..... | 26 |
| 3. MATERIALS AND METHODS | 28 |
| 3.1. Bacterial strains, plasmids, and growth conditions..... | 28 |
| 3.2. Mutant proteins | 31 |
| 3.3. Competition assays..... | 31 |
| 3.4. Introduction of point mutations into ancestral genetic backgrounds..... | 31 |
| 3.5. Determination of relative chaperone levels..... | 33 |
| 3.6. Yeast strains and growth conditions | 34 |
| 3.7. Gene deletion..... | 34 |

| | | |
|--------|--|----|
| 3.8. | Insertion of point mutations into the promoter regions | 35 |
| 3.9. | Chronological lifespan measurement..... | 36 |
| 3.10. | Replicative lifespan measurement | 36 |
| 3.11. | Respiration measurement | 37 |
| 3.12. | Flow cytometry..... | 37 |
| 3.13. | Measurement of the Mss116 overexpression level | 37 |
| 3.14. | Assessment of mitochondrial membrane potential and mass..... | 38 |
| 3.15. | Evaluation of the mitochondrial morphology and protein import machinery..... | 38 |
| 3.16. | ROS measurement..... | 39 |
| 3.17. | RNA extraction..... | 39 |
| 3.18. | Quantitative real-time PCR..... | 39 |
| 3.19. | Single cell generation time measurement | 41 |
| 3.20. | Single molecule RNA-FISH and imaging..... | 42 |
| 3.21. | Protein extraction for 2D Oxi-DIGE | 43 |
| 3.22. | 2D Oxi-DIGE | 44 |
| 3.23. | Gel imaging and analysis | 44 |
| 4. | RESULTS..... | 45 |
| 4.1. | RNA chaperones buffer deleterious mutations in <i>E.coli</i> | 45 |
| 4.1.1. | Overexpression of DEAD-box RNA helicases enhances fitness of a low-fitness strain | 45 |
| 4.1.2. | RNA chaperones buffer distinct mutations in a second low-fitness strain | 47 |
| 4.1.3. | Pinpointing individual deleterious mutations buffered by RNA chaperones..... | 50 |
| 4.1.4. | Fitness gains upon overexpression of <i>cspA</i> suggest diverse mechanisms of buffering | 54 |
| 4.2. | Removal of self-splicing introns from <i>S. cerevisiae</i> mitochondria triggers the retrograde response | 58 |
| 4.2.1. | Deletion of self-splicing introns from <i>S. cerevisiae</i> mitochondria lead to hyper-fusion phenotype | 58 |
| 4.2.2. | Deletion of self-splicing introns from <i>S. cerevisiae</i> mitochondria activate the retrograde response | 64 |
| 4.2.3. | Overexpression of Mss116 RNA helicase phenocopies <i>lo</i> strain..... | 74 |
| 4.3. | Long-term accumulation of gene polymorphisms and their effect on protein oxidability in <i>E.coli</i> | 81 |
| 4.3.1. | Elucidating correlation between <i>E.coli</i> genomic mutations and level of proteome carbonylation (preliminary results)..... | 81 |
| 4.3.2. | Identification of proteins with increased/decreased carbonylation levels in mutator strain compared with ancestor and non-mutator..... | 85 |
| 5. | DISCUSSION | 91 |
| 6. | CONCLUSIONS | 95 |

| | |
|---------------------------|-----|
| 7. REFERENCES | 98 |
| 8. CURRICULUM VITAE | 112 |

1. INTRODUCTION

Mutations are changes in DNA sequence which occur constantly in the cells, drive evolution and cause diseases. When transcribed and translated, they may have an impact on RNA and protein stability and functionality accounting for their particular phenotypic effects. The DNA damage theory of aging posits that accumulated DNA damage leads to accelerated aging (Freitas and de Magalhaes, 2011). There are many examples of diseases caused directly by the impact of single nucleotide polymorphisms (SNPs) on cellular phenotype (such as inborn genetic diseases) (Bessenyei et al., 2004). Mutations can also lead to subtle protein misfolding due to synonymous substitutions whose eventual phenotype is conditional. Here it was studied how mutations with adverse phenotype effect can be rescued at the RNA and the protein level in two model organisms, namely *Escherichia coli* and *Saccharomyces cerevisiae*. Preliminary results aiming at discerning molecular basis of oxidative damage were also introduced.

First part of this research was addressing the question: can weak deleterious mutations accumulated at DNA level be buffered at the RNA level? Such a process would be of major interest in the research of RNA homeostasis involvement in cellular fitness; however, it would also implicate selective pressure at RNA level rarely considered by biologists. To be fully functional, RNA molecules must also fold into three-dimensional structures. Secondary structure of RNA has a similar stability as a native one and therefore frequently adopting misfolded structures (Herschlag, 1995). Proteins with RNA chaperone activity can facilitate conformational rearrangements of this long-lived misfolded species by stabilizing the native fold or refolding the misfolded structures (Russell, 2008).

Similar to RNA chaperone-assisted RNA folding, protein chaperones assist other proteins to achieve and maintain their native structures, enabling them to function properly. Phenotypic effects of harmful mutations that modify protein structure and function can be masked by protein chaperones. Phenomenon of mutation buffering was demonstrated by release of cryptic genetic variations as the result of heat shock protein 90 inhibition (Queitsch et al., 2002; Rohner et al., 2013; Rutherford and Lindquist, 1998) and by rescued fitness of *E. coli* mutator strains due to GroEL overproduction (Fares et al., 2002). DEAD box RNA helicases (DBRHs) have a role in the unfolding of RNA duplexes and thus facilitating folding errors. Considering them as

buffers of deleterious mutations that affect RNA stability, they are focus of this part of the thesis.

The results presented here reveal identification of individual mutations that lead to decreased fitness and are buffered with RNA chaperones. With this result, a novel research area have opened with multiple research directions, whereby the identification of mutations whose phenotype can be buffered at RNA level is only one of them.

An additional question is whether beneficial effects of RNA helicases upon cellular functioning are limited to prokaryotes or extended also to eukaryotic cells. Therefore, the second part of this thesis includes the study of DEAD-box RNA helicase Mss116, encoded in *S. cerevisiae* nucleus, expressed in mitochondria and required for efficient splicing of mitochondrial group I and group II introns. From a total 13 introns in the *S. cerevisiae* mtDNA, 7 are found in *COX1* gene, encoding for a subunit I of cytochrome c oxidase and 5 in *COB* gene, encoding cytochrome b (Kennell et al., 1993).

It was hypothesized that splicing is another source of errors in the context of cellular maintenance, specifically in the mRNA and protein quality control. Therefore, it was tested if more efficient and accurate splicing at mRNA level, or complete removal of introns from DNA, may result in improved cellular fitness. Indeed, the intronless phenotype includes increased amount of *COX1* and *COB* mature mRNA components of the respiratory chain, and has beneficial effect on yeast lifespan. These results promote the RNA maintenance as a potential hallmark of aging, underscoring its importance in normal cellular functioning.

Third, started to address the question whether the emergence of gene polymorphisms, evolved experimentally in continuous bacterial cultures, is reflected in the polymorphism of protein oxidability, measured by level of protein carbonylation. Protein carbonylation is an irreversible type of oxidative damage, accumulates during aging and can be considered as a biomarker of many age-related diseases. Mutations can also increase protein susceptibility to carbonylation (Dukan et al., 2000).

Richard Lenski started the *E. coli* long term evolution experiment project in 1988 by archiving numerous intermediate cultures over numerous generations. This collection presents a rich source of mutations whose penetrance to the level of proteins could facilitate our understanding of the molecular basis of protein resistance and sensitivity to oxidative damage. Since mutator strains emerged spontaneously early in the experiment of *in vitro* evolution, together with non-

mutator derived from the same ancestor, it was an ideal model system to study the impact of different levels of diverse mutations on proteins – their oxidability and phenotypic effects.

Using two-dimensional gel electrophoresis proteins expressed during exponential growth in the ancestor, mutator and non-mutator were separated. By simultaneous labelling of proteins and their carbonylation with specific fluorescent dyes, proteins with higher or lower carbonylation levels (in mutator and non-mutator, compared with the ancestor), were identified by mass spectrometry. The availability of genome sequences allowed matching each acquired mutation to its position in the genome and differential carbonylation at the protein level.

2. LITERATURE REVIEW

2.1. Cellular fitness and homeostasis

In order to have a functional cell, all biological processes must be in an equilibrium, homeostasis. Following the central dogma of molecular biology, there are three main components in the cell: DNAs, RNAs and proteins. DNA carries information that is transcribed into mRNA and translated into protein. Therefore, it is crucial to maintain DNA integrity and preserve the fidelity of gene expression.

An important element of cellular homeostasis is responsible for proper functioning of RNA molecules (“ribostasis”). RNAs have wide range of cellular activities, from translating genetic information into functional proteins to catalyzing some biochemical reactions and processing posttranscriptional modification to maintain the functional stability of RNA. However, the majority of functional molecules are proteins underscoring the importance of cellular proteostasis (protein homeostasis) that is accomplished by cellular mechanisms involved in protein synthesis, folding, trafficking, aggregation and protein degradation. A failure in any of these systems can lead to a disease or progression of ageing. A loss of homeostasis can affect cellular phenotype, i.e., fitness (Hartl, 2016).

2.2. RNA folding

RNA molecules are able to fold into many different structures, and as such, can perform multiple tasks in a cell. Building blocks of the RNA structure are nucleotides and each RNA nucleotide consists of three parts: ribose sugar, a phosphate group and a nitrogenous base. There are four basic secondary structural elements in RNA: helices, loops, bulges, and multi-branched loops (Fig 1.). The helices are A-form Watson-Crick duplexes; the loops, bulges and multi-branched loops are all non-Watson-Crick regions terminated by one or more helices. In the process of folding, RNAs can become trapped in alternative structures, which are as stable as the native one. Beside this kinetic problem, there is also a thermodynamic one when it comes to a single tertiary structure among the competing ones (Herschlag, 1995). The importance of understanding RNA properties led to the discovery of its catalytic properties and involvement in replication, intron splicing and translational regulation (Giegé et al., 1998).

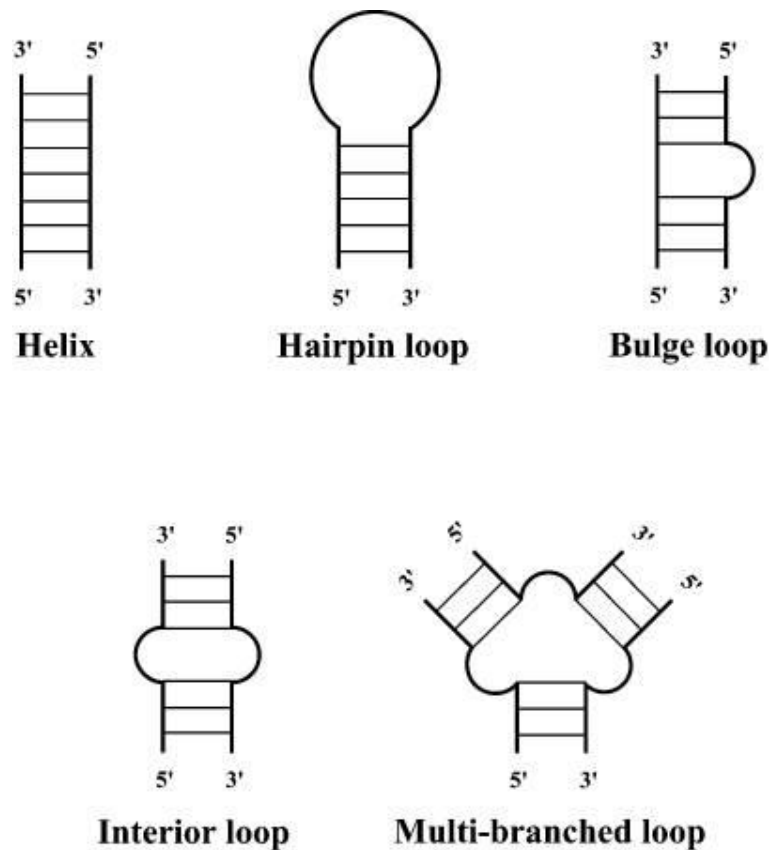


Figure 1. Elements of RNA secondary structure: helix, hairpin loop, bulge loop, interior (internal) loop and multi-branched loop. Adopted from Ding and Lawrence, (2003).

2.2.1. Proteins with RNA chaperone activity

RNA misfolding is common and it frequently produces long-lived alternate structures that require the assistance of RNA-binding proteins for timely resolution. It is clear that, in the cellular environment, RNA molecules profit from the assistance of several classes of non-specific RNA binding proteins that have been described as “chaperones” (Herschlag, 1995) (Fig 2.). Proteins with RNA chaperone activity prevent misfolding or resolve misfolded RNA species and after the RNA has been folded into its native structure, the protein becomes dispensable and dissociate (Herschlag, 1995). Such proteins are present from bacteria to humans and some of them are: virus-encoded RNA chaperones, ribosomal proteins, cold shock proteins (CSPs), *E. coli* translation initiation factor 1, *E. coli* transcriptional regulator StpA and heteronuclear ribonucleoproteins (Semrad, 2011).

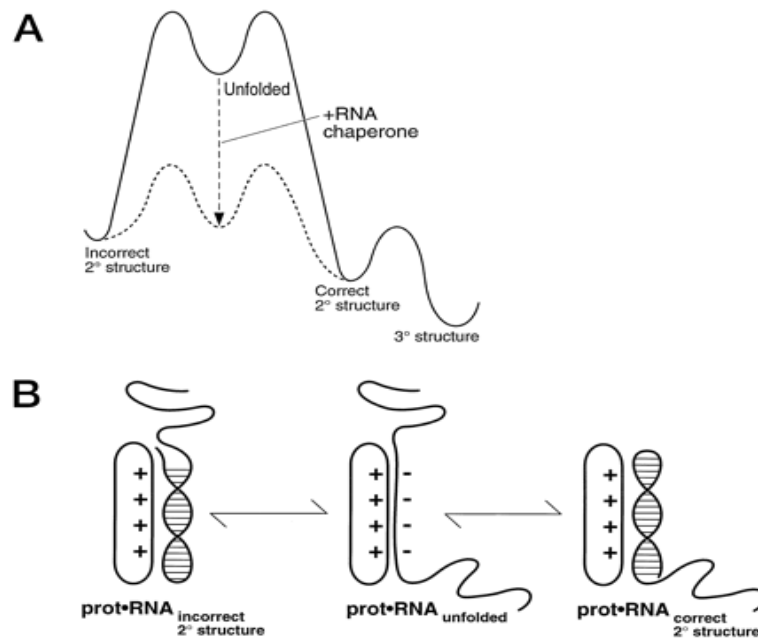


Figure 2. RNA folding and the effect of RNA chaperones. Adopted from Herschlag, (1995).

Cold shock proteins are expressed during temperature decline, involved in transcription, mRNA stability and translation. After a cold shock (from optimal 37°C to 15°C), *E. coli* cells immediately stop dividing and protein synthesis is repressed, but various CSPs are produced. There are nine members of the CSP family, CspA to CspI. The major ones, CspA, CspE and CspC facilitate transcription and translation of some proteins interacting non-specifically with RNA molecules and destabilizing mRNA structures. They act as transcriptional antiterminators enabling expression of genes dependent on CSPs at low temperature (Bae et al., 2000).

Another group of proteins involved in RNA folding are RNA helicases. They are highly conserved proteins and have important roles in RNA metabolism (Tanner and Linder, 2001). Classification is based on comparative sequence and functional analysis: helicases that form oligomeric rings, superfamilies (SFs) 3 to 6 and those that do not form rings, SFs 1 and 2 (Singleton et al., 2007). Largest family within the superfamily 2 are DEAD-box proteins with nine conserved motifs among which is Walker B motif that contains amino acid sequence Asp-Glu-Ala-Asp (DEAD) and non-conserved C terminal extension (Linder et al., 1989).

The *E.coli* genome codes for 5 DEAD-box proteins – RhlB, RhlE, SrmB, CsdA and DbpA – involved in ribosome biogenesis, RNA turnover and translation initiation. In this thesis focus was on RhlB, SrmB and CsdA.

The RhlB protein is a part of the RNA degradosome, a multienzyme complex, along with endoribonuclease RNaseE and PNPase, polynucleotide phosphorylase (Py et al., 1996).

SrmB protein stabilizes certain mRNAs and is involved in the assembly of the 50S ribosomal subunit at low temperatures (Charollais et al., 2003).

CsdA, cold shock DEAD-box protein A, participates in ribosome biogenesis. When overexpressed in S2 mutant, it restores the incorporation of S2 and S1 ribosomal proteins into the ribosome (Moll et al., 2002). CsdA is involved in mRNA degradation after cold shock (Prud'homme-Généreux et al., 2004) and is homologous to eukaryotic initiation factor eIF4A (Lu et al., 1999).

Saccharomyces cerevisiae possess RNA helicases involved in nuclear transcription, mRNA splicing, translation, transport, quality control mechanisms in gene expression, folding of self-splicing RNA introns and RNA decay (Fig 3.). The *S. cerevisiae* genome codes for 26 DEAD-box proteins and most of them have homologs in mammalian cells.

Mss116 is a nuclear encoded DEAD-box RNA helicase, required for efficient splicing of mitochondrial group I and II introns (Halls et al., 2007). Although, under near physiological conditions, some of these introns self-splice *in vitro*, *in vivo* their self-splicing abilities (efficiency) depends on intron-encoded maturases or nuclear-encoded proteins like Mss116 (Fedor and Williamson, 2005). The mechanism of Mss116 in intron splicing involves binding to RNA to stabilize on-pathway intermediates and RNA duplex unwinding to disrupt misfolded secondary structures (Del Campo et al., 2009; Fedorova and Pyle, 2012; Russell et al., 2013).

Involvement of Mss116p in splicing is, at least in part, independent of mitochondrial translation, as splicing of the bi1 (first intron of *COB*), ai5 γ (seventh intron of *COXI*) and ω (the only intron of the *LSU-rRNA*) introns does not require a maturase.

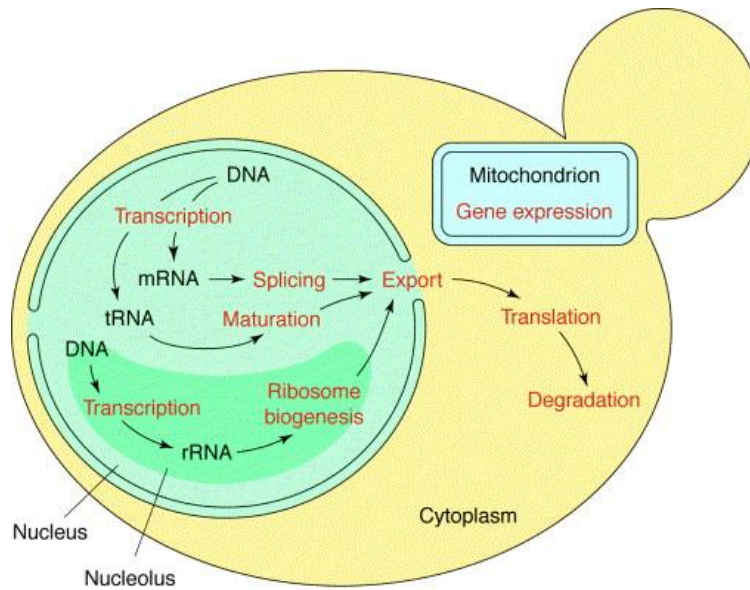


Figure 3. Cellular processes (shown in red) that require RNA helicases. Adopted from de la Cruz et al., (1999).

2.3. Protein folding

Proteins are molecules built as amino acid chains and are involved in almost all biological functions. To fulfil this biological role they must fold into a favourable three-dimensional structure, the native state, where interactions between protein residues are most stable and are thus able to find the lowest energy structure (Anfinsen, 1973; Dinner et al., 2000). During this process, proteins encounter energetic barriers, which can result in partially folded states or folding intermediates (Fig 4.). Accumulation of misfolded proteins often leads to the formation of insoluble aggregates. Aggregation can lead to formation of amyloid fibrils, oligomers or amorphous aggregates which can be toxic for the cell.

Protein folding and unfolding are key to their specific interactions and catalysis and, therefore, play a substantial role in translocation across membranes, regulation of the cell cycle, the immune response and secretion (Radford and Dobson, 1999). Since such major processes depend on the protein folded state, its impairment can lead to various diseases (Thomas et al., 1995). Cystic fibrosis, Huntington's disease, Alzheimer's and Parkinson's diseases are some of pathologies known to be directly associated with deposition of specific misfolded proteins forming aggregates in, or outside, the cell (Dobson, 2001).

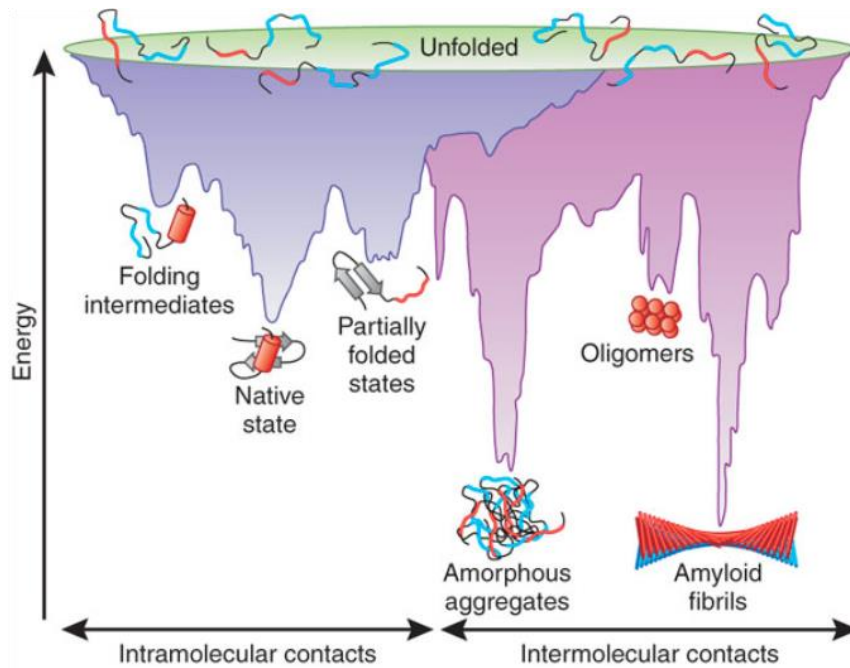


Figure 4. Energy landscape scheme of protein folding and aggregation. The purple surface shows the multitude of conformations ‘funneling’ to the native state via intramolecular contacts and the pink area shows the conformations moving toward amorphous aggregates or amyloid fibrils via intermolecular contacts. Both parts of the energy surface overlap. Aggregate formation can occur from intermediates populated during *de novo* folding or by destabilization of the native state into partially folded states and is normally prevented by molecular chaperones. Cell-toxic oligomers may occur as off-pathway intermediates of amyloid fibril formation. Adopted from Hartl and Hayer-Hartl, (2009).

2.3.1. Protein chaperones

Protein folding depends on a group of proteins, molecular chaperones, found in all three domains of life, which help other proteins to fold properly. Molecular chaperones function in preventing protein misfolding and aggregation, typically by shielding hydrophobic surfaces exposed by proteins in their non-native states (Hartl and Hayer-Hartl, 2009). Chaperones have essential roles in assisting the folding, assembly and transport of newly synthesized polypeptides (Hartl et al., 2011). During stress conditions in a cell protein misfolding and aggregation is frequent and the activity of chaperones is required. Known as heat-shock proteins (HSPs), chaperones are classified according to their molecular weight: HSP40, HSP60, HSP70,

HSP90, HSP100 and the small HSPs (15–30 kDa). In *de novo* protein folding and refolding, chaperones HSP70, HSP90 and chaperonin HSP60 act in the ATP-dependent manner, unlike some small HSPs that do not use ATP in preventing unfolded proteins to aggregate. Protein chaperones are also characterized according to their localization: cytosolic and organelle-specific chaperones.

2.3.2. Mutation buffering

During evolution, mutations arising in the genome are a driving force potentially leading to the emergence of new protein functions and can alter protein stability. Nonsynonymous mutations alter the amino acid sequence of a protein and synonymous mutation code for the same amino acid. Detrimental mutations that are highly destabilizing will not become fixed, although mutations that are introducing a new function have been shown to mainly decrease protein stability (Tokuriki et al., 2008). Destabilizing effects of mutations can be buffered by the structure maintenance effects of protein chaperones, thereby supporting the preservation of genetic diversity (Fares et al., 2004; Rutherford, 2003). Here are some experimental evidences for this phenomenon:

Rutherford and Lindquist (1998) reported buffering capacity of heat shock protein HSP90 using *Drosophila melanogaster* as a model organism. Mutated version of Hsp90 gene (Hsp83) resulted with impaired Hsp90 function and led to developmental abnormalities of flies. These experiment provided a new outlook of chaperones in evolution.

Tokuriki and Tawfik (2009) performed *in vitro* mutagenesis of four enzymes, three clients of GroEL/ES *E. coli* chaperonin, glyceraldehydophosphate dehydrogenase from *E. coli* (GAPDH), human carbonic anhydrase 2 (CA2), a variant of *Pseudomonas sp.* phosphotriesterase (PTE) and *E. coli* triose phosphate isomerase (TIM), which is not a GroEL/GroES client (Chapman et al., 2006; Kerner et al., 2005). Randomly mutated enzyme-encoding genes were transformed to *E. coli* carrying plasmid for GroEL/ES overexpression. Using such system, they aimed to examine buffering of destabilizing and adaptive mutations in the presence and absence of GroEL/ES overexpression. In the presence, results showed that folding of enzyme variants carrying mutations were improved comparing to the wild type enzymes and genetic diversity promoted (Tokuriki and Tawfik, 2009).

To investigate mutation buffering, Casanueva et al. (2012) used *Ceanorhabditis elegans* as a model organism to overexpress the transcription factor heat shock factor 1 (HSF-1), a regulator of the environmental stress response. They crossed the hsf-1 transgenic animals with strains carrying diverse mutations that affect development, which results in reduced mutation penetrance. Overexpression of this specific chaperone masked phenotypic consequences of mutations, such as: body morphology effect, larval and embryonic lethality, male gonad migration defect etc. This phenomenon was observed in all developmental stages of *C. elegans* with the protection ranging from 18 to 88% (Casanueva et al., 2012).

2.4. *E. coli* long term evolution experiment

In 1988, Richard Lenski started the "*E. coli* long-term evolution experiment" (LTEE) by continuously growing 12 parallel cultures from *E. coli* B laboratory strains, REL606 and REL607, which differ only in the *araA* genetic marker encoding for L-arabinose isomerase (Sniegowski et al., 1997). The *E. coli* B strain REL606 has a mutation in the *araA* gene that renders it unable to utilize the sugar L-arabinose. Strain REL607 is a spontaneous revertant of REL606 containing a single point mutation that restores the ability to metabolize L-arabinose. This marker is selectively neutral in a variety of conditions and can be used to determine the relative frequencies of Ara⁻ (REL606-derived) and Ara⁺ (REL607-derived) cells in a mixture for competition assays or marker divergence experiments. Ara⁻ and Ara⁺ cells form red and white colonies, respectively, on tetrazolium arabinose (TA) plates, because utilization of the sugar rather than only the tryptone and yeast extract components of this medium causes the excretion of acetic acid, acidifying the area surrounding the colony and changing the tetrazolium indicator colour from red to white. Within a few thousand generations, four cultures became mismatch repair deficient mutators adapting faster to the minimal growth medium by mutating at over a 100-fold increased mutation rate (Sniegowski et al., 1997; Wielgoss et al., 2013). The populations reached the milestone of 60,000 generations in April 2014. Every 75th day (~500 generations), the evolving populations themselves are stored away in the ultra-low freezer at -80 °C. Richard Lenski and his team sequenced the genomes of *E. coli* clones sampled at generations 500; 1,000; 1,500; 2,000; 5,000; 10,000; 15,000; 20,000; 30,000; 40,000 and 50,000, so they could examine the rate and mode of genomic evolution. They identified 45 mutations in the 20K clone (20,000 generation), which include 29 single-nucleotide polymorphisms and 16 deletions, insertions and other polymorphisms (DIPs). 22 point

mutations that were found in coding regions in the 20K clone are non-synonymous. In total they found 14,572 mutations; 500 insertions of insertion sequence (IS) elements; 726 deletions and 1,132 insertions each ≤ 50 base pairs (bp) (small indels); and 267 deletions and 45 duplications each >50 bp (large indels). After 50,000 generations, average genome length declined by 63 kb ($\sim 1.4\%$) relative to the ancestor. At this time point, six populations evolved hypermutable phenotypes with the defect in mismatch repair system or in removal of oxidized nucleotides (Sniegowski et al., 1997; Wielgoss et al., 2013). Figure 5a presents the total number of mutations over time in all 12 populations. Figure 5b represents number of mutations to a smaller scale for six populations before they evolved hypermutability and the six ones that did not become mutators.

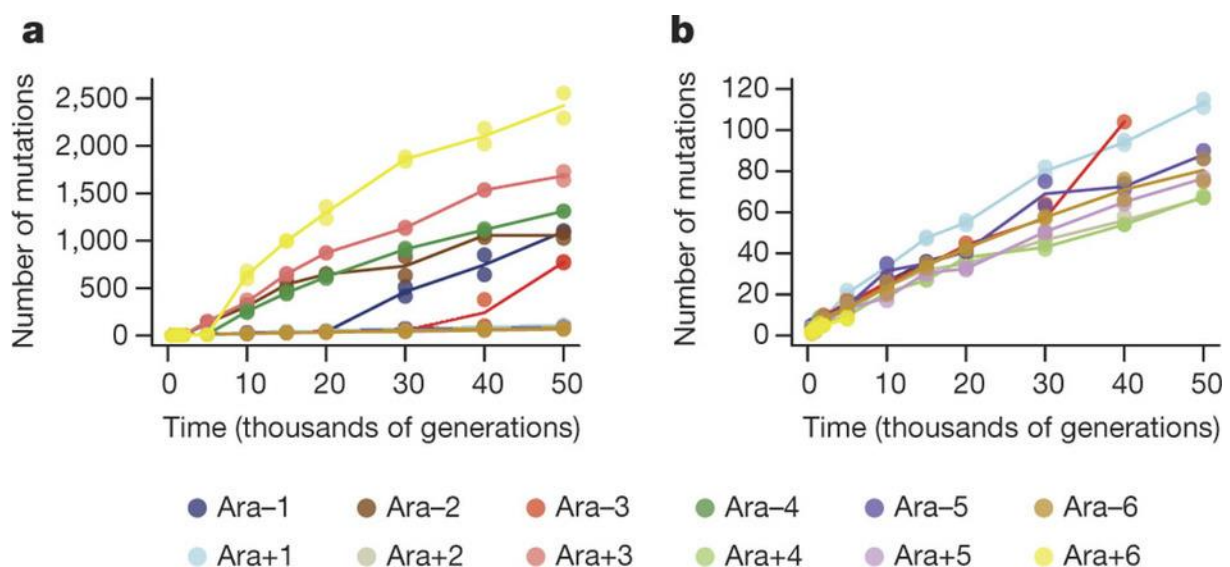


Figure 5. Total number of mutations over time in the 12 LTEE populations. a) Total mutations in each population. b) Total mutations rescaled to reveal the trajectories for the six populations that did not become hypermutable for point mutations and for the other six before they evolved hypermutability. Each symbol shows a sequenced genome; some points are hidden behind others. Each line passes through the average of the genomes from the same population and generation. Adopted from Tenaillon et al., (2016).

In addition, another strain that accumulated mutations during short-term evolution (evolved $\Delta mutH$) and its ancestor (MG1655) were also sequenced in the purpose of better understanding of the results. The MG1655-derived sequences were kindly provided by Dr. Tobias Warnecke, as well as a mutation identifications of MG1655 and REL606-derived strains.

2.5. Aging

Aging is a large-scale process present in almost all species, from fungi to humans. It is a progressive impairment of physiological functions followed by a steep increase in morbidity and mortality with age (De Magalhaes, 2011). There are two main groups of aging theories: first stating that aging is programmed into the body, and second emphasizing environmental impact on living organisms, which accumulate damage that causes aging at widely different levels with chronological age, but similarly with biological age (fraction of life span). Understanding the molecular processes of aging can provide means for prevention or delay of age-related diseases. However, there are many unanswered questions concerning the causes of aging, notably genetics versus life style.

2.5.1. The hallmarks of aging

Experts have defined nine cellular and molecular hallmarks of aging: genomic instability, telomere attrition, epigenetic alterations, loss of proteostasis, deregulated nutrient sensing, mitochondrial dysfunction, cellular senescence, stem cell exhaustion, and altered intercellular communication (López-Otín et al., 2013). Increased DNA damage accumulation can lead to different kinds of premature aging diseases, such as Werner syndrome, Ataxia telangiectasia, Bloom syndrome and Rothmund–Thomsom syndrome (Burtner and Kennedy, 2010).

2.5.1.1. Genomic instability

The integrity and stability of DNA is crucial for lasting cellular homeostasis and perpetuation of life because genes are required for the renewal of proteins that are generally short-lived. Such homeostasis can be disrupted exogenously by physical, chemical and biological agents, as well as endogenously including DNA replication errors, spontaneous hydrolytic reactions and reactive oxygen species (ROS) (Hoeijmakers, 2009). Those kinds of damage include point mutations, double strand breaks, translocations, deletions and can result in tumorigenesis or even cell death because of the loss of genes or loss of gene function due to macro and micro-mutations.

2.5.1.2. DNA damage theory of aging

DNA has a central role in life and its modifications can have enormous impact because function and structure provided by proteins depends on genes. DNA is subject to damage and mutations. When a gene mutation occurs, it will be copied into mRNA sequence that will be translated into an altered, often dysfunctional, protein (unless the mutation is a neutral mutation that does not alter amino acid sequence). DNA damage, on the other hand, caused by different physical or chemical modifications, changes the structure of a double helix (Fig 6.). This scenario can lead to cell cycle arrest and trigger programmed cell death, be it programmed (apoptosis) or not (necrosis).

DNA damage theory of aging proposes that the accumulation of DNA damage is the main cause of deterioration in cellular fitness and aging process (Carrington, 2007; Szilard, 1959). Many researches have shown that DNA mutations increase with age and defects in DNA repair mechanisms can accelerate aging processes (Hasty et al., 2003; Vijg and Dollé, 2002). But, no increase in mutation frequency with age was detected in mouse brain that still ages (Stuart et al., 2000). May it be that mutations in other organs causes brain aging? Too many similar questions remain unanswered.

Rossi et al. (2007) showed that endogenous DNA damage accumulates with age in mice wild type stem cells and can lead to decline in stem cell function, while Hyun et al. (2008) reported that DNA repair capacity is higher in long-lived nematode *Caenorhabditis elegans* mutants with defects in the insulin/IGF-1 pathway than in wild type animals. But, why? What is the cause of age-related decay in DNA repair capacity? In general, genetic diseases caused by defects in DNA repair mechanism, known as progeroid syndromes, support the DNA damage theory of aging (Freitas and de Magalhaes, 2011).

There is also experimental evidence that does not support this theory. Narayanan et al. (1997) provided experiments with mice defective in mismatch repair endonuclease, PMS2, where mice nullizygous for *Pms2* resulted with 100-fold elevation in mutation frequency compared with both wild-type and heterozygous mice, but do not affect development nor accelerate aging.

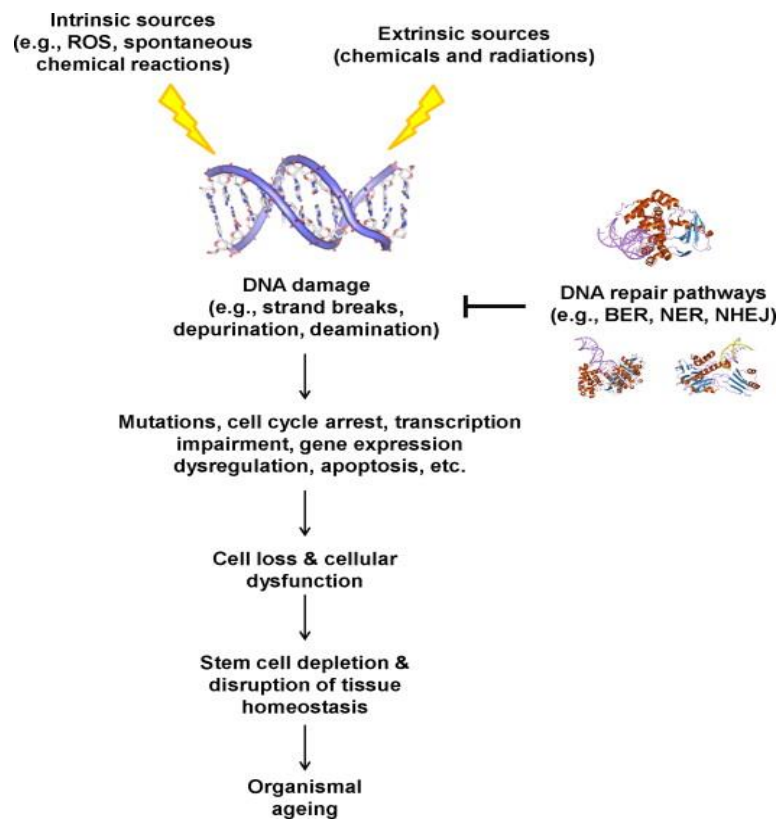


Figure 6. Overview of the DNA damage theory of ageing. Adopted from Freitas and de Magalhaes, (2011).

2.5.1.3. Proteostasis theory of aging

Proteostasis network includes processes of protein synthesis, folding, transport, localization, aggregation, degradation and has a role in maintaining proteome stably functional. During aging the processes of proteostasis are decaying and damaged proteins accumulate. To preserve protein homeostasis in the cell, molecular chaperones and the proteolytic system, which represent cellular protein quality control, have the most important function. The ubiquitin/proteasome system (UPS) is the main proteolytic system responsible for targeting damaged proteins (ubiquitination) and their degradation (Fig 7.). The 8 kDa regulatory protein, ubiquitin, is targeting proteasome substrates for degradation. The UPS system plays important role in lifespan; its activity is required for long-lived mutants to achieve maximal lifespan extension. *C. elegans* insulin/insulin-like growth factor-1-signaling (IIS) mutant extended lifespan is dependent on E3 ligase, a key component involved in proteolysis regulation (Ghazi et al., 2007). Molecular chaperones activity has also significant impact on longevity; their increased expression results in enhanced longevity (Koga et al., 2011; Lithgow et al., 1995;

Shama et al., 1998). Failure of protein quality control systems leads to proteopathies, protein conformational disorders, including neurodegenerative diseases and amyloidosis (Esser et al., 2004; Morimoto, 2008).

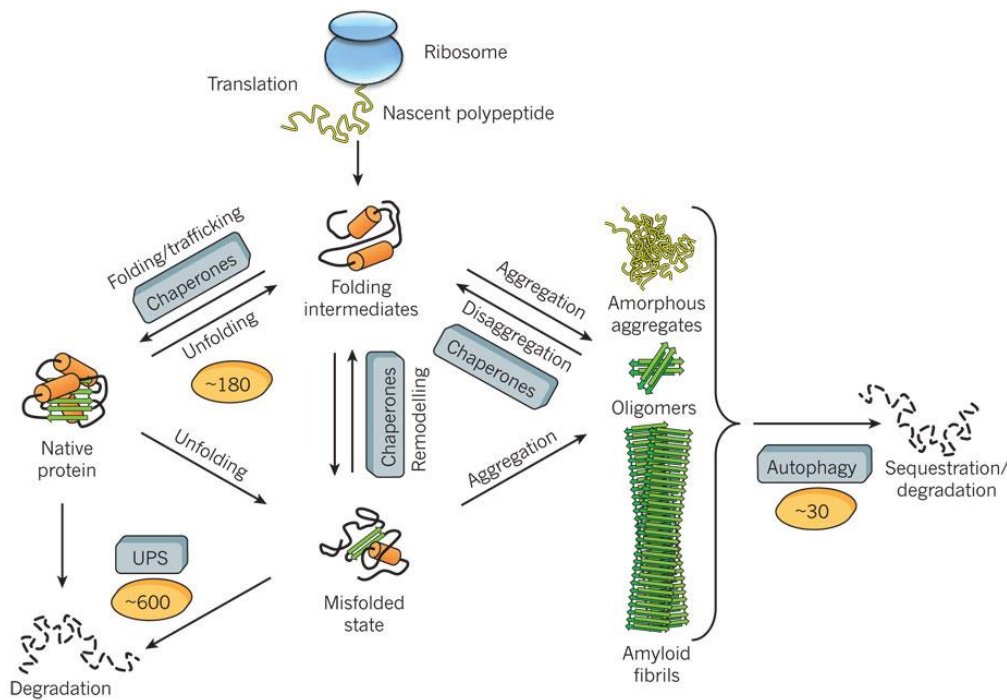


Figure 7. Protein fates in the proteostasis network. Adopted from Hartl et al., (2011).

2.5.2. DNA polymorphisms

DNA polymorphisms are variations in nucleotide sequence, predominantly single nucleotide polymorphisms (SNPs), high variability in repeat number of simple sequence motifs (mostly from mono- to penta-nucleotides) and much less frequent large deletions, inversions and duplications. Polymorphic variations do not necessarily affect the phenotype. There are several types of SNPs: they can be synonymous without affecting protein sequence, or non-synonymous leading to altered protein sequence, structure and in some cases even a function. SNPs are associated with different types of diseases. Some of the examples are: Alzheimer disease (Wolf et al., 2013), sickle cell anemia (Ingram, 1956), cystic fibrosis (Hamosh et al., 1992) and hyperlipidemia (Huertas-Vazquez et al., 2010). Cystic fibrosis is caused by the mutation in the cystic fibrosis transmembrane conductance regulator (*CFTR*) gene (Riordan et al., 1989).

2.5.3. Oxidative stress

Oxidative stress is a change in cellular redox system that occurs with imbalanced levels of prooxidants (production of ROS) and antioxidants. Although production of ROS is caused by some environmental changes or xenobiotics, it is also a product of a normal cellular oxidative metabolism. ROS are highly reactive molecular species, which include free radicals and nonradicals. Superoxide ($O_2^{\bullet-}$), hydroxyl radical (OH^{\bullet}), hydroperoxyl radical (HO_2^{\bullet}), nitric oxide (NO^{\bullet}), nitrogen dioxide (NO_2^{\bullet}), and peroxy (ROO^{\bullet}) are some of the small molecules that can damage nucleic acids, lipids, and proteins and alter their functions. Oxidative damage can target two different parts of a protein: the protein backbone and the amino-acid side chain. The first leads to fragmentation reactions and the second produces different oxidations products, such as carbonyl derivatives and alkoxy radicals.

2.5.3.1. The free radical theory of aging

The “free radical hypothesis” was first proposed by Harman in 1956. He proposed free radical oxidative damage of macromolecules as the main cause of aging (Harman, 1956). This hypothesis was later altered into “oxidative stress hypothesis”, but still maintains the argument that increase in ROS and failure of antioxidant defences result in impaired proteostasis, metabolic regulation, DNA repair, and ultimately leads to senescence-associated decrease in physiological fitness (Sies et al., 1985; Sohal and Allen, 1990). Cutler (1991) tested the hypothesis that antioxidants may increase longevity and found a positive correlation of specific antioxidants with lifespan of mammals. In 1997, scientists used rats (3-4 years lifespan) and pigeons (35 years lifespan) as model organisms. They measured oxygen consumption, H_2O_2 and free radical production that were all higher in heart mitochondria of the short-lived rats than in pigeons supporting the free radical theory of aging (Herrero and Barja, 1997). There are also experiments that do not support this theory. For example, naked mole rats are attractive organisms to study effects of oxidative damage on aging, since they live up to 30 years while ordinary rats live 3-4 years. Conversely to this theory, results showed that oxidative protein damage levels are higher in naked mole rat compared to Wistar laboratory rats (Harman, 1956).

2.5.3.2. Protein carbonylation

Protein carbonylation (PC) is a well-known marker for oxidative stress. It is a type of irreversible protein modification caused by ROS. PC includes a direct metal catalysed oxidative (MCO) attack on lysine, arginine, proline and threonine residues (“primary protein carbonylation”) (Fig 8.) or reactions via the addition of aldehydes, such as those generated from lipid peroxidation processes, to amino acid side chains (“secondary protein carbonylation”) (Butterfield and Stadtman, 1997; Grimsrud et al., 2008; Levine, 2002). Misfolded proteins are more susceptible to oxidation and result in higher levels of carbonylation compared to natively folded proteins (Dukan et al., 2000). Conformational stability also plays a major role in the susceptibility to oxidation. It is shown that the proteome of pathogenic bacteria is more resistant to oxidation than the proteome of non-pathogens due to its increased conformational stability (Vidovic et al., 2014).

Oxidative damage results in impaired protein function and elevated mutation rate (Krisiko and Radman, 2010, 2013). Protein carbonylation is increasing with the age of many species and has a significant damaging effect on cellular functions. Diseases associated with increased carbonylation include Parkinson’s disease, Alzheimer’s disease, cancer, cataractogenesis, diabetes, sepsis and autoimmune diseases (Dalle-Donne et al., 2003; Levine, 2002).

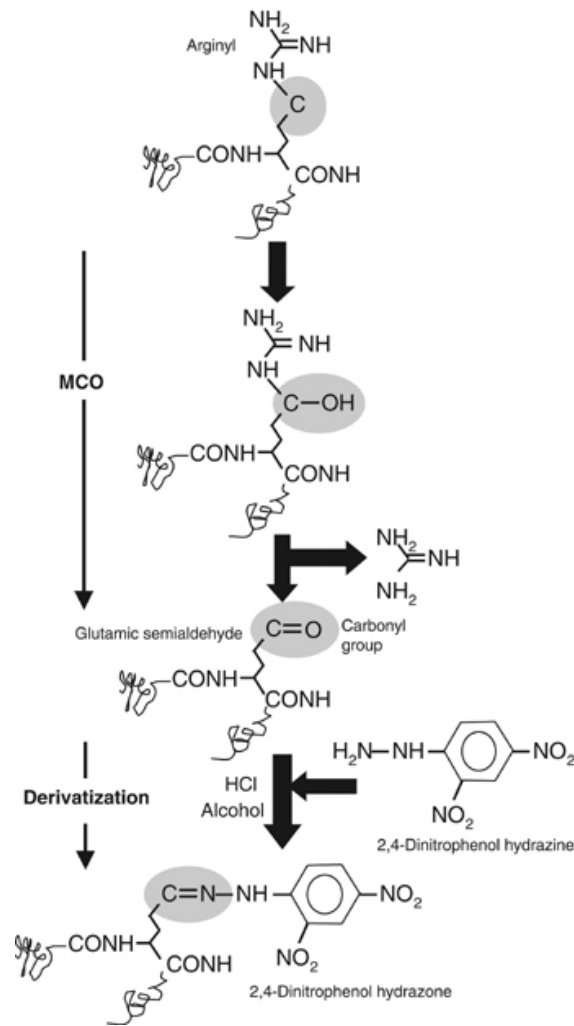


Figure 8. Carbonylation and derivatization of a protein amino-acid side chain. A scheme for the formation of glutamic semialdehyde from an arginyl residue is depicted as a consequence of an MCO. For detection, the carbonyl group, in this case glutamic semialdehyde, is subsequently derivatized by 2,4-dinitrophenol hydrazine. The resulting protein 2,4-dinitrophenol hydrazone can be detected by specific monoclonal or polyclonal antibodies (see Requena et al., 2001). Adopted from Nyström, (2005).

2.6. Yeast as a model organism in aging

Budding yeast *Saccharomyces cerevisiae* is a unicellular eukaryote used as a model organism in molecular biology and genetics. Since (i) it is inexpensive to grow yeast in large amounts of standard media (in which their doubling time is 1.5-2 hours at 30 °C), (ii) yeast genome size is small and completely sequenced (6000 genes) long ago (Goffeau et al., 1996). As it is largely

orthologous to the human genome, *S. cerevisiae* serves as an exquisite experimental model for studying aging. Fundamental cellular processes including DNA replication, transcription, mRNA translation, protein degradation and cell cycle are conserved in eukaryotic organisms through evolution and genetically manipulated yeast cells are used in experimental studies for better understanding of these processes. System of homologous recombination allows easy genetic manipulations, providing knockouts for a particular gene of interest.

S. cerevisiae can reproduce sexually and asexually, depending on the environmental conditions, and can exist in haploid and diploid state. Both states can undergo asexual reproduction (mitosis) called budding, which occurs when the ‘mother’ yeast cell produces a genetically identical new small cell (a bud). Under high stress conditions, diploid cells undergo sexual reproduction (meiosis) producing haploid spores. There are two mating types determined by two different alleles of the mating-type (*MAT*) locus and the protein encoded by the *HO* gene is an endonuclease responsible for the process of mating type switching by a gene conversion process. Haploid cell type *MATa* (**a** cell) can mate with the opposite mating type *MAT α* (α cell) forming a stable diploid *MATa/MAT α* (**a/a** cell).

2.6.1. Replicative and chronological lifespan

Yeast as a model organism for studying aging was introduced after the discovery that single yeast cell is mortal (Barton, 1950). A. Barton was the first person who separated each daughter cell from its mother cell and Mortimer and Johnston (1959) discovered decreasing number of divisions during individual cell lifespan. This is a definition of replicative lifespan (RLS) – number of buds produced by a single yeast cell (Fig 9.). The average number of buds generated by single cell is between 19 to 25 daughter cells. Experimentally, RLS can be measured by microdissection using agar plate with the yeast strain and a thin needle for removing buds under a microscope - method still used for lifespan analysis (Sutphin et al., 2011). Since *S. cerevisiae* cells divide asymmetrically, buds are smaller than the mother cell and can be visually distinguished under a microscope. After separation of a ‘daughter’ cell, chitin bud scars are formed on the surface of a mother cell and can be monitored to estimate the number of asymmetric divisions. New methods include microfluidic devices, a system based on chemical or mechanical trapping of mother cells, where daughter cells are removed by a flowing medium (Lee et al., 2012). It is also possible to quantify fluorescent signal during cell lifespan (Xie et al., 2012). Another interesting technique is Mother Enrichment Program (MEP), which disables

offspring to divide upon estradiol addition leading to linear growth of the population (Lindstrom and Gottschling, 2009).

Another approach to quantify lifespan of budding yeast is chronological lifespan (CLS), measured as the time during which non-dividing population survives under starvation conditions (Fig 9.). Yeast culture is grown in liquid medium, 2% glucose, until it reaches stationary phase; glucose from the medium is depleted, cell growth reduced and mitochondrial respiration activated (Longo, 1997). Yeast culture can be maintained in the medium depleted of 2% glucose (standard CLS method) or transferred to water during post-diauxic phase (extreme calorie restriction/starvation). Number of viable cells is estimated by plating different dilutions of culture on agar plates.

Kaeberline and his co-workers (2009) reported a molecular mechanism of chronological lifespan in aging. They found that decrease in the pH of the culture medium promotes yeast chronological aging, i.e. that increased CLS is result of reduced extracellular acetic acid (Burtner et al., 2009).

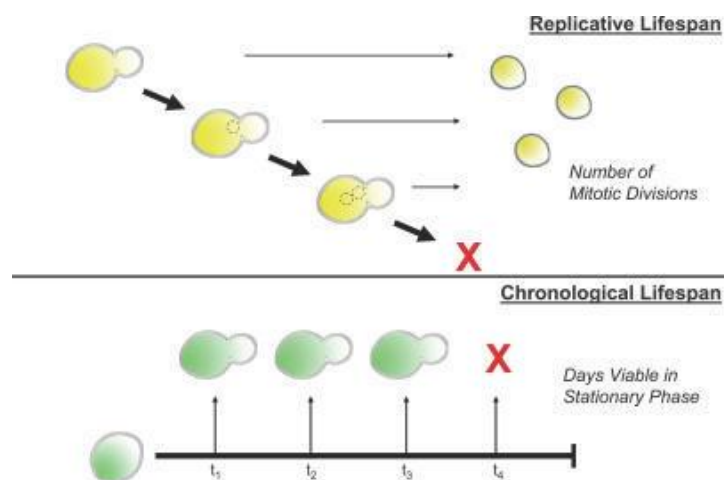


Figure 9. Schematic for yeast replicative and chronological aging. Replicative Lifespan (RLS) in yeast is measured by the number of mitotic divisions that can arise from a single mother cell. Replicative viability is calculated as the mean number of daughters produced from mothers of a particular strain background before senescence. Chronological Lifespan (CLS) is measured by the length of time cells in a stationary culture can remain viable. Viability is calculated by the fraction of the culture able to reenter the cell cycle after an extended state of quiescence. Adopted from Kaeberlein et al., (2007).

2.6.2. *S. cerevisiae* mitochondria

Like all eukaryotic organisms, *S. cerevisiae* possess mitochondria, organelles responsible for adenosine triphosphate (ATP) production. ATP is a cellular energy source required for many biological functions including DNA, RNA and protein synthesis, cell signalling, transport and cell division. Since yeast is a facultative anaerobe, ATP can be produced by respiration or fermentation. ATP produced by respiration is generated by oxidative phosphorylation (OXPHOS) on the inner mitochondrial membrane. The mitochondrion contains outer and inner membranes, inter-membrane space, cristae and matrix. Cristae are folds of the inner membrane that provide an increase in the surface area, enabling higher production of ATP molecules. Matrix is space surrounded by the inner membrane where mitochondrial DNA, enzymes, ribosomes and electron transport chain (ETC) are located.

The ETC system of *S. cerevisiae* includes NADH dehydrogenase (Ndi1p, Nde1-2p), which represent mammalian Complex I and four additional protein complexes: Complex II (Sdh1-4p), Complex III (Qcr1-9p), Complex IV (Cox1-11p) and Complex V (F1Fo ATP synthase), which together with cytochrome c and ubiquinone form OXPHOS system. Complex I-IV transfer electrons from NADH and FADH₂, produced in the Krebs cycle, to oxygen through ETC. Energy released in this process is used to transport protons across the inner mitochondrial membrane, out of the matrix, and to maintain an electrochemical potential ($\Delta\mu H$) composed of an electrical gradient ($\Delta\Psi$) and a pH gradient. During chemiosmosis, protons are transported back into the matrix by ATP synthase, the enzyme that uses the energy to phosphorylate ADP to ATP.

2.6.2.1. *S. cerevisiae* mitochondrial genome

Mitochondrial (mt) DNA in *S. cerevisiae* encodes for seven essential components of three respiratory chain complexes. The *COB* gene encodes for apocytochrome b (complex III), *COX1*, *COX2* and *COX3* genes encode for subunits I, II and III of the cytochrome c oxidase (complex IV) and *ATP6*, *ATP8* and *ATP9* genes encode for subunits 6, 8 and 9 of the F₀ component of the mitochondrial ATP synthase (complex V) (Fig 10.). Mitochondrial genome also encodes the small subunit 15S rRNA and the large subunit 21S rRNA of the mt ribosome, 24 tRNAs and RNA subunit of the RNase P (Foury et al., 1998). *S. cerevisiae* mitochondrial genome can also contain 7 introns in the *COX1* gene, 5 in the *COB* gene and 1 in the 21S rRNA. Yeast mtDNA is organized into dynamic nucleoprotein complexes termed the nucleoids. Each

cell contains 50-100 copies of mtDNA and each nucleoid up to 10 copies of mtDNA (Chen and Butow, 2005; Lipinski et al., 2010). Except for mtDNA and packaging proteins, significant part of the nucleoids is nuclearly encoded proteins which play an important role in maintenance of the mitochondrial genome. The nuclear genome of *S. cerevisiae* encodes about 200 proteins that participate in the maintenance and expression of the mitochondrial genome (Hong et al., 2007). Deletion of nuclear genes coding for mitochondrial DNA polymerase subunit Mip1p, DNA helicase Pif1p and some others involved in the mitochondrial DNA metabolism, leads to complete loss (ρ°) of mtDNA (Genga et al., 1986; Lahaye et al., 1991). Since ρ° yeast cells cannot perform respiration, they are unable to grow on non-fermentable carbon source, such as glycerol or ethanol. Due to mutations in mtDNA with functional replication and transcription, wild type (ρ^{+}) mtDNA turns into non-functional (ρ^{-}) with deficiency in protein synthesis (Mounolou et al., 1966). Both, complete loss and non-functional mtDNA result in the petite phenotype, small yeast colonies forming in the presence of fermentable carbon source, such as glucose. Although mitochondrial genome is not requisite for yeast survival, its function in synthesis of iron-sulphur is essential (Kispal et al., 2005).

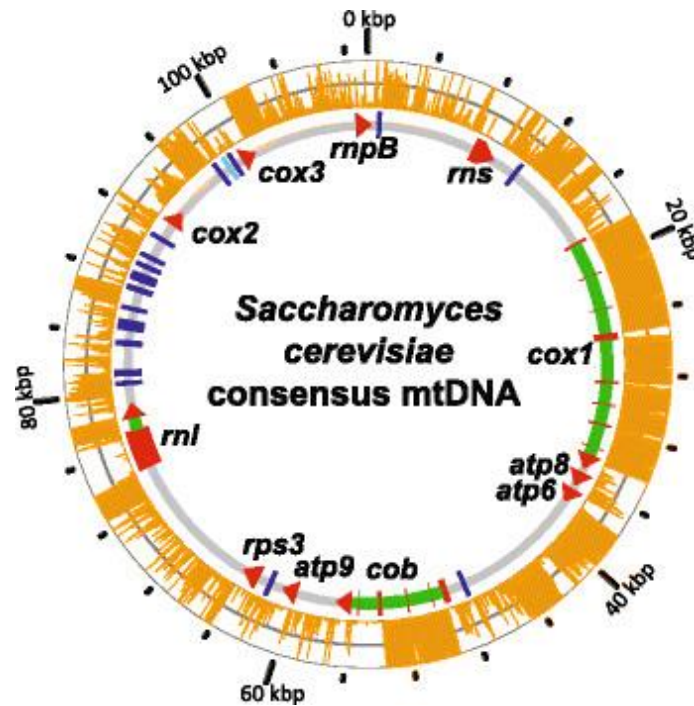


Figure 10. Consensus genome map of *S. cerevisiae* mtDNA. A consensus genome map based on the alignment of nine divergent mtDNAs illustrates the extensive polymorphisms across *S. cerevisiae* mtDNAs. The consensus sequence (~109 kbp) is substantially longer than the longest mtDNA in this alignment (~86 kbp) due to indel variation. Genes (red arrows), introns (green), and tRNAs (blue) are indicated. The light blue bar indicates a sole tRNA encoded on the light strand. The orange bars indicate the number of polymorphic sites within 100 bp windows, where the inner and outer edges of the circle represent 0 and 100, respectively. The grey line represents the genome-wide average of 51 polymorphic sites per window. Adopted from Wolters et al., (2015).

2.6.2.1.1. Group II introns

Introns are nucleotide sequences within genes, between two exons, that must be spliced out from the precursor messenger RNA (pre-mRNA) molecule to generate functional gene product. After introns are removed, exons are joined together to form a mature mRNA. Spliceosomal introns and tRNA introns are removed by spliceosomes and splicing endonucleases, respectively; group I and group II introns are ribozymes catalyzing their own RNA splicing. Out of 13 introns in the *S. cerevisiae* mitochondrial genome, 9 are group I and 4 group II introns. They are characterized by different splicing mechanisms, secondary and tertiary structures.

Group II introns are found in bacteria, archaeobacteria, mitochondria, and chloroplasts, but not in the nuclear genomes. They consist of catalytically active intron RNA (ribozyme) and an intron-encoded protein (IEP). Intron RNA contains six helical domains: I to IVa at the 5' end, IVb to VI at the 3' end. IEP contains four domains:

- RT (reverse transcriptase)
- X (maturase, RNA splicing)
- D (DNA binding)
- An endonuclease activity

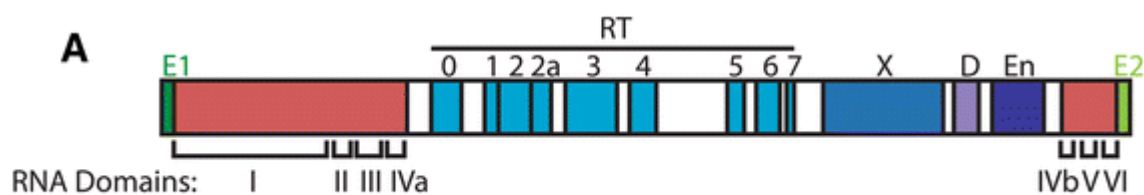


Figure 11. Genomic structure of a group II intron. The 2- to 3-kb sequence consists of RNA and protein portions. The intron RNA domains are depicted in red and demarcated with Roman numerals. Domains I to IVa are at the 5' end of the intron, while domains IVb to VI are at the 3' end. The IEP sequence is nested within the RNA's sequence and the domains are denoted by differently shaded blue boxes. The IEP contains a reverse transcriptase domain (RT) with motifs 0 to 7, a maturase domain (X, sometimes called X/thumb), a DNA-binding domain (D), and an endonuclease domain (En). Exons are shown in green. Adopted from Zimmerly and Semper, (2015).

Reverse transcriptase activity of IEPs enables introns mobility; acting as retroelements, introns are moving through the genome by copying themselves. IEPs, also known as maturases, play a role in splicing generating a mature mRNA. RNA splicing includes two trans-esterification reactions, first one forming intron-exon lariat and second one resulting with excised lariat and connected exons (Newman, 1998) (Fig 12.). After splicing, IEP remains bound to the excised intron RNA lariat forming a nucleoprotein complex that invades DNA sites.

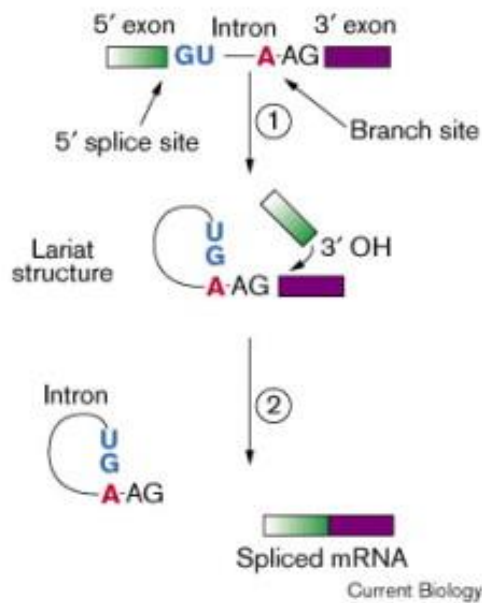


Figure 12. RNA splicing. Splicing of mRNA precursor involves two successive trans-esterification reactions. In the first reaction (1) the 2' OH of a specific adenosine (red) at the branch site near the 3' end of the intron attacks the 5' splice site (blue). This reaction releases the 5' exon (green; with a 3' OH terminus) and leaves the 5' end of the intron (blue) joined by a 2'-5' phosphodiester bond to the branch site adenosine (red); this intron–3' exon intermediate is therefore in the form of a lariat. In the second reaction (2) the 3' OH of the 5' exon intermediate (green) attacks the 3' splice site, producing the spliced mRNA and lariat-shaped intron products Adopted from Newman, (1998).

2.6.2.2. Retrograde response

Mitochondria are organelles responsible for the ATP production, fuel most cellular functions, and their maintenance is of a great importance. It is believed that they have evolved via endosymbiosis with pre-eukaryotic cells, followed by gene transfer into the nuclear genome and the majority of mitochondrial proteins are encoded in the nucleus. Consequently, communication between mitochondria and nucleus is crucial for the mitochondrial maintenance, therefore it includes the antegrade (nucleus to mitochondria) and the retrograde (mitochondria to nucleus) communication pathway.

Mitochondrial retrograde signalling pathway is activated when the mitochondrial dysfunction occurs. In *S. cerevisiae*, this includes three nuclearly encoded proteins: Rtg1p, Rtg2p and Rtg3p (Fig 13.). Retrograde pathway activator, Rtg2p, regulates translocation of Rtg1 and Rtg3

cytosolic proteins to the nucleus, which are transcriptional activators of nuclear genes that code for mitochondrial proteins (Sekito et al., 2000). This translocation depends on partial dephosphorylation of Rtg3p and binding of Rtg2p to Mks1p, a negative regulator of the retrograde response which can inhibit this signalling pathway by binding to Bmh1/2p (Liu et al., 2003).

Expression of about 400 genes are significantly altered in retrograde response (Epstein et al., 2001). Liu and Butow (1999) showed that expression of four genes involved in tricarboxylic acid (TCA) cycle are under the control of RTG1, RTG3 transcription factors when respiratory function is reduced. Those genes are: CIT1, ACO1, IDH1, and IDH2 coding for citrate synthase, aconitase and two subunits of mitochondrial NAD(+)-dependent isocitrate dehydrogenase, respectively.

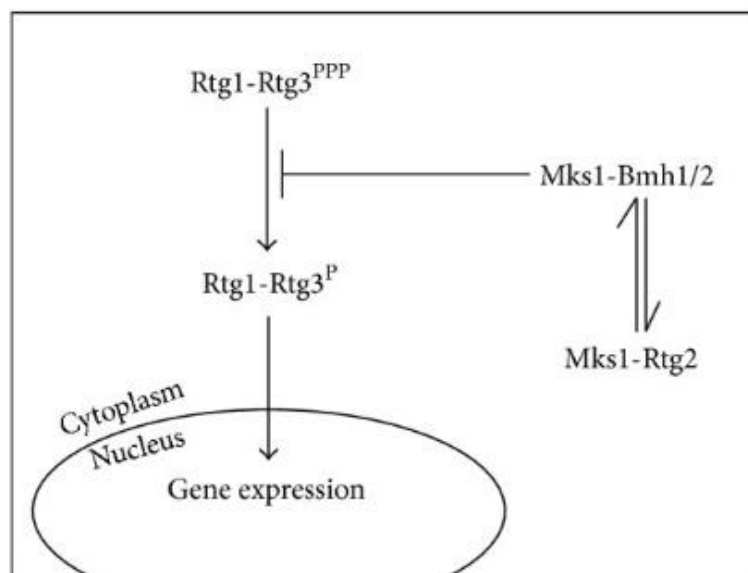


Figure 13. Simplified scheme of the RTG-dependent retrograde signaling pathway. In *S. cerevisiae* this pathway depends on three proteins. Rtg1 and Rtg3 form a transcription factor that translocates to the nucleus when the pathway is activated. In the nucleus, Rtg1 and Rtg3 control the expression of a set of genes that code for mitochondrial proteins. Rtg2 is an activator of the pathway that allows the nuclear translocation of Rtg1 and Rtg3. Adopted from da Cunha et al., (2015).

3. MATERIALS AND METHODS

3.1. Bacterial strains, plasmids, and growth conditions

The strains used in this research were derived either from the *E. coli* K12 MG1655 strain by laboratory evolution and P1 transduction and/or transformation, or from the REL606 strain and its descendants in the LTEE (Sniegowski et al., 1997). All strains used are listed in Table 1. Sequences of *cspA*, *rhlB*, *srmB*, and *csdA* inserted into pCA24N::Cam were obtained from the ASKA collection (<http://www.shigen.nig.ac.jp/ecoli/strain/>). For strain construction and subsequent experiments, bacteria were grown in Luria-Bertani (LB) medium at 37 °C. To distinguish competitors during competition assays, cells were plated onto tetracycline arabinose (TA) solid medium (Lenski, 1991).

Table 1. List of *E. coli* strains used in this study.

| Strain | Characteristics | Source, Reference or Construction |
|---------------|--|--|
| MG1655 | | Lab stock |
| Δ araA | <i>E. coli</i> MG1655 Δ araA ::Kan/Ara- | NBRP |
| MR01 | MG1655 Δ araA::Kan/Ara- | Transduction with P1(Δ araA ::Kan) |
| MR02 | MR01 pCA24N::Cam/Ara- | Transformation |
| MR03 | MG1655 pCA24N- <i>cspA</i> ::Cam/Ara+ | Transformation |
| MR04 | MG1655 pCA24N- <i>rhlB</i> ::Cam/Ara+ | Transformation |
| MR05 | MG1655 pCA24N- <i>srmB</i> ::Cam/Ara+ | Transformation |
| MR06 | MG1655 pCA24N- <i>csdA</i> ::Cam/Ara+ | Transformation |
| Δ mutH | MG1655 Δ mutH::Kan /Ara+ | Keio collection |
| MR07 | Δ mutH /Ara- | Selection on TA plates |
| MR08 | MR07 pCA24N::Cam/Ara- | Transformation |
| MR09 | Δ mutH pCA24N- <i>cspA</i> ::Cam/Ara+ | Transformation |
| MR10 | Δ mutH pCA24N- <i>rhlB</i> ::Cam/Ara+ | Transformation |

Table 1. (continued)

| Strain | Characteristics | Source, Reference or Construction |
|------------------------------|---|---|
| MR11 | $\Delta mutH$ pCA24N- <i>srmB</i> ::Cam/Ara+ | Transformation |
| MR12 | $\Delta mutH$ pCA24N- <i>csdA</i> ::Cam/Ara+ | Transformation |
| REL607 | <i>E. coli</i> B/Ara+ | (Wiser et al., 2013) |
| REL606 | <i>E. coli</i> B/Ara- | (Wiser et al., 2013) |
| MR13 | REL606 pCA24N::Cam/Ara- | Transformation |
| MR14 | REL607 pCA24N- <i>cspA</i> ::Cam/Ara+ | Transformation |
| MR15 | REL607 pCA24N- <i>rhlB</i> ::Cam/Ara+ | Transformation |
| MR16 | REL607 pCA24N- <i>srmB</i> ::Cam/Ara+ | Transformation |
| MR17 | REL607 pCA24N- <i>csdA</i> ::Cam/Ara+ | Transformation |
| REL 10953 | Ara+ | (Wiser et al., 2013) |
| MR18 | REL 10953/Ara- | Selection on TA plates |
| MR19 | MR18 pCA24N::Cam/Ara- | Transformation |
| MR20 | REL 10953 pCA24N- <i>cspA</i> ::Cam/Ara+ | Transformation |
| MR21 | REL 10953 pCA24N- <i>rhlB</i> ::Cam/Ara+ | Transformation |
| MR22 | REL 10953 pCA24N- <i>srmB</i> ::Cam/Ara+ | Transformation |
| MR23 | REL 10953 pCA24N- <i>csdA</i> ::Cam/Ara+ | Transformation |
| <i>de novo</i> $\Delta mutH$ | MG1655 $\Delta mutH$::Kan/Ara+ | Transduction with P1 ($\Delta mutH$::Kan) |
| MR24 | <i>de novo</i> $\Delta mutH$ /Ara- | Selection on TA plates |
| MR25 | MR24 pCA24N::Cam/Ara- | Transformation |
| MR26 | <i>de novo</i> $\Delta mutH$ pCA24N- <i>cspA</i> ::Cam/Ara+ | Transformation |
| MR27 | <i>de novo</i> $\Delta mutH$ pCA24N- <i>rhlB</i> ::Cam/Ara+ | Transformation |
| MR28 | <i>de novo</i> $\Delta mutH$ pCA24N- <i>srmB</i> ::Cam/Ara+ | Transformation |
| MR29 | <i>de novo</i> $\Delta mutH$ pCA24N- <i>csdA</i> ::Cam/Ara+ | Transformation |
| REL 8602A | Ara+ | (Wiser et al., 2013) |
| MR30 | REL 8602A/Ara- | Selection on TA plates |
| MR31 | MR30 pCA24N::Cam/Ara- | Transformation |

Table 1. (continued)

| Strain | Characteristics | Source, Reference or Construction |
|--------|--|--|
| MR32 | REL 8602A pCA24N- <i>cspA</i> ::Cam/Ara+ | Transformation |
| MR33 | REL 8602A pCA24N- <i>rhlB</i> ::Cam/Ara+ | Transformation |
| MR34 | REL 8602A pCA24N- <i>srmB</i> ::Cam/Ara+ | Transformation |
| MR35 | REL 8602A pCA24N- <i>csdA</i> ::Cam/Ara+ | Transformation |
| MR36 | MR01 pJ444-01::Amp/Ara- | Transformation |
| MR37 | MG1655 pJ444-01- <i>cspA</i> ::Amp F20L/Ara+ | Transformation |
| MR38 | MG1655 pJ444-01- <i>rhlB</i> ::Amp E166K/Ara+ | Transformation |
| MR39 | MG1655 pJ444-01- <i>srmB</i> ::Amp E158K/Ara+ | Transformation |
| MR40 | MG1655 pJ444-01- <i>csdA</i> ::Amp E157K/Ara+ | Transformation |
| MR41 | MG1655 Δ <i>mutH</i> ::Cam /Ara+ | Transduction with P1 (Δ <i>mutH</i> ::Cam) |
| MR42 | MR41/Ara- | Selection on TA plates |
| MR43 | MR42 pJ441-01::Kan/Ara- | Transformation |
| MR44 | MR41 pJ441-01- <i>cspA</i> ::Kan F20L /Ara+ | Transformation |
| MR45 | MR41 pJ441-01- <i>rhlB</i> ::Kan E166K/Ara+ | Transformation |
| MR46 | MR41 pJ441-01- <i>srmB</i> ::Kan E158K/Ara+ | Transformation |
| MR47 | MR41 pJ441-01- <i>csdA</i> ::Kan E157K/Ara+ | Transformation |
| MR48 | REL606 pJ441-01::Kan/Ara- | Transformation |
| MR49 | REL607 pJ441-01- <i>cspA</i> ::Kan F20L/Ara+ | Transformation |
| MR50 | REL607 pJ441-01- <i>rhlB</i> ::Kan E166K/Ara+ | Transformation |
| MR51 | REL607 pJ441-01- <i>srmB</i> ::Kan E158K/Ara+ | Transformation |
| MR52 | REL607 pJ441-01- <i>csdA</i> ::Kan E157K/Ara+ | Transformation |
| MR53 | MR18 pJ441-01::Kan/Ara- | Transformation |
| MR54 | REL 10953 pJ441-01- <i>cspA</i> ::Kan F20L /Ara+ | Transformation |
| MR55 | REL 10953 pJ441-01- <i>rhlB</i> ::Kan E166K/Ara+ | Transformation |
| MR56 | REL 10953 pJ441-01- <i>srmB</i> ::Kan E158K/Ara+ | Transformation |
| MR57 | REL 10953 pJ441-01- <i>csdA</i> ::Kan E157K/Ara+ | Transformation |

3.2. Mutant proteins

Mutations in the DEAD domain of *E. coli* DBRHs abolish or severely reduce helicase activity, as demonstrated for the *E. coli* DBRHs RhIB (Vanzo et al., 1998), DbpA (Elles and Uhlenbeck, 2007), and CsdA (Turner et al., 2007). Here, DBRH mutants in which the central glutamic acid residue has been recoded to yield lysine, a change known to abolish RhIB ATPase activity, which is required for helicase activity was used (Vanzo et al., 1998). Mutations in the nucleic acid-binding domain of CspA were previously evaluated for their impact on both nucleic acid binding and protein stability (Hillier et al., 1998). The F20L mutation was found to only weakly affect protein stability, but strongly reduce nucleic acid binding (Hilier et al., 1998) and was therefore chosen for this study. Plasmids carrying the mutated genes were constructed by and purchased from DNA2.0.

3.3. Competition assays

Pairwise competition experiments was performed to estimate the relative fitness of two competing *E. coli* strains as previously described (Lenski, 1991). Briefly, the two competitors were grown separately, mixed at an initial ratio of 1:1 and diluted 100-fold in the competition environment (LB supplemented with the relevant antibiotics for plasmid maintenance). Initial and final densities (after either 24 or 2 hr) were estimated by diluting and spreading the cells on indicator TA (tetrazolium and arabinose) plates, which allow the competitors to be distinguished through an arabinose-utilization marker, which is neutral under the conditions utilized (Lenski, 1988). Relative fitness was calculated as

$$w = \ln(A_f/A_i) / \ln(B_f/B_i),$$

where *A* and *B* are the densities of the two competitors, and *i* and *f* represent initial and final densities, respectively. One-sample *t*-tests was used to evaluate whether mean relative fitness differed from the null expectation of one.

3.4. Introduction of point mutations into ancestral genetic backgrounds

All point mutations detected in the evolved $\Delta mutH$ strain that were located in a gene of known function (i.e., not located in a y-gene) were individually introduced into the ancestral MG1655 background using a recombineering approach (Sawitzke et al., 2013). Briefly, single-stranded

oligonucleotides were designed, ~70 nt in length, that were complementary to the region of interest and carried the desired point mutation (Table 2.). They were transformed by electroporation into the TB56 (Ara⁺) and TB62 (Ara⁻) strains supplemented with pSIM6. In both TB56 and TB62 (kindly provided by Tobias Bergmiller), the native *mutS* promoter has been replaced with an *ara* promoter. In the presence of 0.2% arabinose, the strains have wild-type MutS levels, whereas in the presence of 0.2% glucose, MutS expression is repressed. Growing strains in LB medium supplemented with 0.2% glucose therefore increases the likelihood that oligo-born mutations are fixed due to impaired mismatch repair. Following electroporation, cells were grown overnight at 32 °C on LB agar plates supplemented with 0.2% arabinose, and the presence of mutations was confirmed by sequencing target regions from individual colonies on an ABI PRISM 310 Genetic Analyzer using the Big Dye Terminator 1.1 Cycle Sequencing kit (Life Technologies, Carlsbad, CA). The primers used for sequencing are listed in Table 3.

Table 2. Primers used for introducing point mutations.

| Primer name | Primer sequence |
|-----------------------------|---|
| rapA_Ok | GC GGC GCA GGT AGA GTT TGA AAC CTT TAA CCA CCA GCT TAA CGC GGT TAA CCG TCA CAC CGG CAG CAA ACT GGT T |
| cyoA_Ok | GTA CAG CCC GAA CTG GTC ACA CTC CAA TAA AGT GAA AGC TGT GGT CTG GAC GGT ACC TAT CTT AAT CAT |
| torA_Ok | GAT AAT GCC ACG GTT GGA GTG ATT GCC GTA CTG GCC GAG ATC GTT ACG CTC AAA CTG CGT GGT CGC AGG |
| osmC_Ok | CG CTG CGC CAA TCA GTT CTT CAG GGT TGG TTC TTT TTT CGC CTT CAA AAC GCG TGT TAA ATC CAT ACG GCT GTT G |
| lsrR_Ok | TG TTC AAA GTG AAG AAT GAA TTA TGA CAA TCA GCG ATT CGG CAA TTT CAG AAC AGG GAA TGT GTG AAG AAG AAC A |
| speC_Ok | TT TTA TGA CAC GCT GAC GCA GTA CGT TGA GAT GGG TAA CAG CAC CTT TGC TTG CCC TGG ACA TCA ACA TGG TGC GTT T |
| lamB_Ok | TG TAC ATC GGG CGA ATA CCG ACG GTC CAC CAC CTG GTC CCG TTG TCG TTA TCC CAG TTG ATA TCC TGG TAC ATA C |
| rplS_non- syn_Ok | CCA GAC TCA CTC TCC GGT AGT TGA CAG CAT TTC TAT CAA ACG TCG TGG TGC TGT TCG TAA AGC TAA ACT |

Table 3. Primers used for sequencing.

| Primer name | Primer sequence |
|-------------------------|-------------------------------------|
| rapA_fwd | TTC GTC GTC ACG AAT GTT CGG G |
| rapA_RC | CCT TTC TGG CGA TAC CGG TAG |
| cyoA_fwd | AAA GCG ATT TCA TTC ACG GTA GC |
| cyoA_RC | TTG CAG GCA CTG TAT TGC TCA GT |
| torA_fwd | ATC GAT GCG ATC CTC GAA CC |
| torA_RC | TTA TTC CAG AAG TCA TCA AAC GCT |
| osmC_fwd | TCG GAA TAT CCT GCT TAT CCT CG |
| osmC_RC | AAG GTA GAG GCA TCA ATA CCC G |
| lsrR_fwd | TTC CAG ACA GCC TTC AAA GCG |
| lsrR_RC | CTT TTA ATT TGT TCA TAA CCT TAG GTG |
| speC_fwd | TTT ATT CGC TGC CGA TGT GCC |
| speC_RC | CGG CAG TCG TCA TTA CCG C |
| lamB_fwd | GTG TCC TGA AGG GCT TTA ACA A |
| lamB_RC | AGC GTT ACC GGT GTA GTC GTA A |
| rplS_non-syn_fwd | AAT ATC CCA TAG CCA GTA ACA AG |
| rplS_non-syn_RC | GCA ACT TGA ACA AGA GCA GAT G |
| rplS_syn_fwd | CAC AGG GTT TAG GAA AAA AAT |
| rplS_syn_RC | GTA CCT TCC TTC CGT CCG G |

3.5. Determination of relative chaperone levels

Exponentially growing evolved $\Delta mutH$ strains overexpressing one of the four RNA chaperone proteins (CspA, RhlB, SrmB or CsdA) were pelleted by centrifugation and resuspended in UTC^{DTT} buffer containing 8 M urea, 2 M thiourea, 4% 3-[(3-cholamidopropyl)dimethylammonio]-1-propanesulfonate hydrate (CHAPS) and 10 mM dithiothreitol (DTT) supplemented with a mixture of protease inhibitors. Cells were incubated for 2 hr at room temperature followed by a 20-min centrifugation step at 12,000 × g. Protein concentrations were determined using the Bradford assay (Bradford, 1976). For each sample, 15 µg of total protein extract was loaded onto an acrylamide gel (6% stacking and 20% resolving gel) using

sodium dodecyl sulfate polyacrylamide gel electrophoresis (SDS-PAGE). 6X-His tagged CspA, RhlB, SrmB, and CsdA were detected by Western blotting using a mouse monoclonal anti-6X His tag antibody (Abcam, United Kingdom) followed by a goat anti-mouse polyclonal antibody conjugated to horseradish peroxidase (Abcam). Proteins were visualized on autoradiographic film using the Amersham ECL Advance chemiluminescence detection system (GE Healthcare Life Sciences, United Kingdom). ImageJ (Collins, 2007) was used to quantify the intensity of each chaperone band on the Western blot and normalized this intensity by the amount of total protein loaded into each lane (detected by Coomassie staining of the polyacrylamide gel and subsequent quantification with ImageJ). This normalized abundance allows comparing relative chaperone levels across experiments (Figure 23).

3.6. Yeast strains and growth conditions

Strain Y258 and the pBG1805 plasmid bearing *Mss116* for overexpression (*Mss116_{OE}*) were purchased from Thermo Scientific (Dharmacon). *Mss116^{E268K}* was purchased from DNA 2.0 and cloned into pBG1805 using standard cloning techniques (Sambrook et al., 1989). *Mss116_{OE}* and *Mss116^{E268K}* were overexpressed in the Y258 nuclear background. The nuclear background of the *I₀* strain is a161-U7¹³ and the corresponding intron-containing strain was used as the WT control for *I₀*. a161-U7 wild type and *I₀* were a gift from Dr. Alan Lambowitz.

All strains were grown on yeast extract-peptone-dextrose (YPD) medium with 2% (w/v) glucose, 1% (w/v) yeast extract, 2% (w/v) peptone and on -URA medium (same as YPD with uracil dropout supplement), at 30 °C with shaking. All experiments were performed on exponentially growing cells: cells were grown to OD 0.6-0.7 for WT, *I₀*, Δ Hap4, and Δ Rtg2 and to OD 0.9-1.0 for *Mss116_{OE}* and *Mss116^{E268K}*, harvested by centrifugation at 4,000 \times g for 5 minutes, washed and further treated as required.

3.7. Gene deletion

Deletion of Hap4 and Rtg2 was performed by following the protocol described in (Golik et al., 1995), using a hygromycin cassette for selection in the WT background and a nourseothricine cassette in the *I₀* background. Primers used for the deletions are listed in Table 4.

Table 4. Primers used for the deletion of Hap4 and Rtg2.

| Primer name | Primer sequence |
|---|---|
| Upstream flanking region of <i>rtg2</i> | |
| FW1_ <i>rtg2</i> | CAA ACC TCA CTA GAC GAC TAC |
| RC1_ <i>rtg2</i> | ATA GTC GAC AGA CAT CTA GTC TTT AAA TAC TTG |
| Downstream flanking region of <i>rtg2</i> | |
| FW2_ <i>rtg2</i> | GCA CGC CAA TTT TAA CCC TCT C |
| RC2_ <i>rtg2</i> | GCG ATA GTG ATA CCG AGA CTG A |
| Upstream flanking region of <i>hap4</i> | |
| FW1_ <i>hap4</i> | TCG ATT TTG CAG ATT GTT CTA AAA GTA AAT |
| RC1_ <i>hap4</i> | TAT CAG CTG AAA GTC TTT GCG GTC AT |
| Downstream flanking region of <i>hap4</i> | |
| FW2_ <i>hap4</i> | TAT GAG CTC AAT AGG CAT GTT GCA ATA |
| RC2_ <i>hap4</i> | TCT CTT GAC GTG TTT CAC CAT ACG |

3.8. Insertion of point mutations into the promoter regions

In order to introduce promoter-attenuating mutations into mitochondrial DNA, the protocol described in (Bonney et al., 2007) was followed. Briefly, a mutant fragment of mtDNA (in this case promoter sequences) flanked by WT mtDNA sequence is first transformed into a *rho*⁰ strain, which is then mated with a recipient *rho*⁺ strain. Upon mating, mitochondria from the two strains fuse and recombination between the two mtDNAs produces recombinant *rho*⁺ strains in which the new mtDNA sequence is integrated by double crossover. For transformation, tungsten powder was used as a carrier of DNA (Tungsten M-10 Microcarriers #1652266, BioRad). Bombardment was performed using the Biolistic PDS-1000/He particle delivery system (BioRad). Cells were transformed with linear DNA fragments obtained by ligation of each mutated promoter region with 500bp of up- and downstream flanking DNA (Table 5.). *Sac*I and *Sal*I restriction sites were added by PCR for ligation between the 3'-end of the upstream flanking region and the 5'-end of the promoter sequence, and 3'-end of the promoter sequence and 5'-end of the downstream flanking region, respectively. The mutations introduced here have been previously shown to reduce the strength of *cox1* and *cob* promoters (Turk et al., 2013).

Table 5. Primers for promoter point mutations insertion.

| Cox1 ATTGATATAAGTAATAGATA → ATTGAAATAAGTAATAGATA | |
|--|--|
| Upstream flanking region of cox1 promoter | |
| Primer name | Primer sequence |
| FW_u_cox1 | CCG GGA CTT ATA TAT TTA ATA CTA AAA A |
| RC_u_cox1 | AC TTA TTA TTT AAT ATT ATA TAT TAC TTT TTA GAGCTC AT |
| Downstream flanking region of cox1 promoter | |
| Primer name | Primer sequence |
| FW_d_cox1 | AT CAGCTG T AAT AAT AAT ATT ATT AAT ATT TTA TAT AAA TAA |
| RC_d_cox1 | AAT TAT TGT TAT ATC TAA AAG GAT AAT AAT ATA TTA |
| Cob TATTATATAAGTAATATATA → TATTAAATAAGTAATATATA | |
| Upstream flanking region of cob promoter | |
| Primer name | Primer sequence |
| FW_u_cob | ATA TTT AAA GAA GGA ATT GTT TAT ATA TAT TAA TAT |
| RC_u_cob | TTT CTT ATA ATT ATA TTA AGA TTA TAT ATA TAA ATA G GAG CTC AT |
| Downstream flanking region of cob promoter | |
| Primer name | Primer sequence |
| FW_d_cob | AT CAG CTG AAA ATA ATA TAA AAT AAT TAT AAT TCA ATT TAT ATA TTA A |
| RC_d_cob | ATA TAT AAT TAT TAT TAT TAT TAA TAA ATT ATA AAA ATA AAA |

3.9. Chronological lifespan measurement

All strains were grown to saturation as described above and pelleted at $4,000 \times g$ for 5 min. Cells were then washed twice and resuspended in sterile deionized water (10^6 cells in 10 mL in order to avoid cell growth on the debris of dead cells) and incubated at $30^\circ C$ with shaking. Every 2-3 days, cells were serially diluted and plated onto YPD plates in order to evaluate cell growth.

3.10. Replicative lifespan measurement

Replicative lifespan (RLS) was determined by micromanipulation for *Mss116^{OE}* and *Mss116^{E268K}* in the Y258 background, as well as for *Mss116^{OE}* in the Δ Hap4 and Δ Rtg2 nuclear backgrounds, counting the number of daughters produced by individual mother cells. It was not possible to reliably determine RLS for the *I₀* strain as daughter and mother cells could not be

separated in a timely manner, which is critical for RLS measurements. Wild type cells were incubated at 30 °C on YPD and mutants on -URA plates for the duration of the experiment. Using a microscope equipped with a microdissection apparatus suitable for *S. cerevisiae* (Singer Instruments), cells were transferred to defined places on agar plates and virgin daughter cells collected. Each cell was monitored continuously over several days every 60 - 90 min until all mother cells stopped budding. The total number of daughter cells was noted for each mother cell. The total number of monitored mother cells is as follows: 90 cells for the empty vector control, 86 cells for *Mss116_{OE}*, and 91 cells for the *Mss116^{E268K}*. The measurements were pooled from 3 independent experiments.

3.11. Respiration measurement

Oxygen uptake was monitored polarographically using an oxygraph equipped with a Clark-type electrode (Oxygraph, Hansatech, Norfolk, UK). Cells were harvested during exponential growth phase, spun and resuspended in growth medium (as above) at the density of 30×10^6 cells/mL. 500 μ L of culture were transferred to an airtight 1.5 mL oxygraph chamber. Cells were assayed in conditions closely similar to the ones in a flask culture (30 °C and stirring). Oxygen content was monitored for at least 4 min. To ensure that the observed oxygen consumption was due to the mitochondrial activity, complex III inhibitor antimycin (final concentration 10 μ g/mL) was routinely added to the cultures and compared to the rate observed without antimycin.

3.12. Flow cytometry

Flow cytometry was carried out on a Becton-Dickinson FACSCalibur machine equipped with a 488 nm Argon laser and a 635 nm red diode laser.

3.13. Measurement of the Mss116 overexpression level

The expression level of Mss116 in the *Mss116_{OE}* strain was measured by using a rabbit polyclonal anti-His tag antibody (Abcam, ab137839, 1:10000) and secondary IgG goat anti-rabbit labeled with Alexa 488 (Thermo Fisher Scientific, A11034, 1:2000). The signal obtained by flow cytometry (mean fluorescence over 10000 cells) was compared to the Mss116 tagged

with GFP (Thermo Scientific) endogenous expression level estimated by using flow cytometry measurement based on the GFP signal. The mean fluorescence intensity in Mss116_{OE} was normalized to the mean fluorescence intensity detected in wild type cells with endogenous expression of Mss116.

3.14. Assessment of mitochondrial membrane potential and mass

Variations of the mitochondrial transmembrane potential ($\Delta\Psi_m$) were studied using 3,3'-dihexyloxacarbocyanine iodide (DiOC6(3)). This cyanine cationic dye accumulates in the mitochondrial matrix as a function of $\Delta\Psi_m$ ²¹. Cells (1×10^6 /mL) were incubated in 1 mL culture medium containing 40 nM DiOC6(3) for 30 min in the dark at 30 °C with constant shaking. DiOC6(3) membrane potential-related fluorescence was recorded using FL1 height. A total of 10,000 cells were analyzed for each curve. The collected data was analyzed using FlowJo software version 7.2.5 to determine the mean green fluorescence intensity after each treatment. The results are expressed as a percentage of mean fluorescence of the control strain. As a negative control, in each experiment, aliquots of cells were preincubated with carbonyl-cyanide 4-(trifluoromethoxy)- phenylhydrazone (FCCP, Sigma) and antimycin (Sigma) at 100 μ M and 5 μ g/mL, respectively, 10 min before fluorescent dye staining, which leads to a collapse of mitochondrial membrane potential.

To measure mitochondrial mass, 10-N-Nonyl acridine orange (NAO) was used, a dye that binds to cardiolipin, a phospholipid specifically present on the mitochondrial membrane (Perry et al., 2011). Cells (1×10^6 /mL) were incubated in 1 mL culture medium containing 100 nM NAO for 30 min in the dark at 30 °C with constant shaking, followed by analysis on FACSCalibur flow cytometer with the same photomultiplier settings as used for DiOC6(3).

3.15. Evaluation of the mitochondrial morphology and protein import machinery

To image mitochondrial morphology, strains were transformed with a MitoLoc plasmid (Vowinckel et al., 2015) (a gift from Markus Ralser) according to a previously described protocol (Gietz and Schiestl, 2007), with the only difference that the cells were incubated with the plasmid overnight at room temperature. Microscope slides were prepared as follows: 150 μ L of YPD media containing 2% agarose was placed on a preheated microscope slide and cooled, before applying yeast cells to obtain a monolayer. The cells were centrifuged at $4000 \times g$ for

3 min, and resuspended in 50 μ L YPD. Once dry, the cover slip was placed, sealed, and mounted on a temperature-controlled Nikon Ti-E Eclipse inverted/UltraVIEW VoX (Perkin Elmer) spinning disc confocal setup, driven by Volocity software (version 6.3; Perkin Elmer). Images were recorded through a 60xCFI PlanApo VC oil objective (NA 1.4) using coherent solid state 488 nm and 543 nm diode lasers with a DPSS module, and a 1000 \times 1000 pixel 14-bit Hamamatsu (C9100-50) electron-multiplied, charge-coupled device (EMCCD). The exposure time was 100 ms for GFP and 300 ms for mCherry, at 5–10% laser intensity. The number of cells with cytosolic mCherry accumulation was counted manually. Approximately 1000 cells of each strain were examined. Images were analysed using ImageJ software with the MitoLoc plugin.

3.16. ROS measurement

Cells were incubated in the dark with 5 μ M MitoSOXTM red mitochondrial superoxide indicator (Molecular Probes) for 10 min at 30 °C and subsequently analyzed by flow cytometry. Fluorescence (excitation/emission maxima of 510/580 nm) of 10,000 cells resulting from the intracellular red fluorescence was measured in the FL2 channel. The collected data was analyzed using FlowJo software version 7.2.5 for Microsoft (TreeStar, San Carlos, CA, USA) to determine the mean green fluorescence intensity after each treatment. The results are expressed as the mean fluorescence across 10,000 cells.

3.17. RNA extraction

Total RNA was isolated using the NucleoSpin RNA kit (Macherey&Nagel) according to the manufacturer's instructions for up to 3 \times 10⁸ yeast cells, which includes incubation with 50–100 U of zymolyase for 1 hr at 30 °C. The quality of the resulting total RNA was tested on 1% agarose gels.

3.18. Quantitative real-time PCR

cDNA was synthesized from 1000 ng of total RNA using the iScriptTM cDNA Synthesis Kit (Biorad). The cDNA was 100-fold diluted, mixed with primer pairs for each gene and SYBRgreen (BioRad). All primer pairs were designed to have a melting temperature of 60 °C

and are listed in Table 6. The qPCR reaction was run on a QuantFlexStudio 6 (Life Technologies) using 40 cycles, after which the melting curves for each well were determined. Final fold change values were estimated relative to the UBC6 gene in the control strain replicates.

Table 6. Primers used for q-PCR.

| Systematic gene name | Standard gene name | FWD primer | RC primer |
|-----------------------------|---------------------------|---|--|
| YBL099W | ATP1 | ATGTTGGCTCGTACTGCTGCTATTC | GCAATACCATCACCGACTGCAAG |
| Q0085 | ATP6 | ATGTTTAATTTATTAATACATATA TTACATCACCATTA | TAAATAGCTTCTTGTGAAATTAATCA TCTTGAAC |
| YNR001C | CIT1 | ATG TCA GCG ATA TTA TCA ACA ACT AGC AA | GGT TTT ACC GTG TTC TTT CTT GAA TTT TTT A |
| Q0105 | COB | ATG GCA TTT AGA AAA TCA AAT GTG TAT TTA AGT T | TAT GCA CAT CTC TTA TAA TAT GTT CAA CAG A |
| Q0045 | COX1 | ATG GTA CAA AGA TGA TTA TAT TCA ACA AAT GC | ATT AAA GCA GGC ATT ACT AAG AAG AAA ATC A |
| Q0250 | COX2 | ATG TTA GAT TTA TTA AGA TTA CAA TTA ACA ACA TTC AT | GTC CAT GTT TAA TAT ATT TAT ATG CAA TAG GAT T |
| YGL187C | COX4 | ATG CTT TCA CTA CGT CAA TCT ATA AGA TTT TT | TCT AAC CTA GCT AAA CCA GTT TCT TGA T |
| YJR104C | SOD1 | ATG GTT CAA GCA GTC GCA GTG TTA AA | TTG AAA GGA TTG AAG TGA GGA CCA G |
| YHR008C | SOD2 | ATG TTC GCG AAA ACA GCA GCT GC | ATT GGT CAA CAG CAG TGT TGA ATC C |
| YER100W | UBC6 | ATG GCT ACA AAG CAG GCT CAC AAG | GGT TTG TAT GGA TAA TCA GAC GGG AA |
| YBR072W | HSP26 | ATG TCA TTT AAC AGT CCA TTT TTT G | TTA GTT ACC CCA CGA TTC TTG A |
| YJL159W | HSP150 | TGTCTCTCAAATTGGTGATGGTCAA | TCTTTGGGGCTAAAGTAGTGGTGGT |
| YOR136W | IDH1 | GCT TAA CAG AAC AAT TGC TAA GA | GTT GAT GAT TTC ATT CGT GAA GTC |
| YKL148C | SDH1 | ATG CTA TCG CTA AAA AAA TCA GCG CTC | TTG TAG CCC GCC TCG GCA AG |
| YLL041C | SDH2 | ATG TTG AAC GTG CTA TTG AGA AGG AAG | TTG ATC TTT AAC AGC GCA TCA AGT ACC |
| YCR005C | CIT2 | ATG ACA GTT CCT TAT CTA AAT TCA AAC AGA A | TCC CTG GAA TAC CTC TCA TAC CAC |
| YBR179C | FZO1 | TCG TGG AGC TCA CTC AAG AA | GGT ACA CGC AAA ACA TCA CG |

Table 6. (continued)

| Systematic gene name | Standard | | |
|----------------------|--------------|---|---|
| | gene name | FWD primer | RC primer |
| YLL001W | DNM1 | GAA TCG AAG CAA ACG AAG GA | CTC TCG GTC AGT GGA GGT TC |
| YIL065C | FIS1 | GGA CGC ATA CGA ACC ACT CT | ATT CTC GTC TAC GGG ACT CG |
| Q0050 | aI1 | TTT ACA TGG TAA TTC ACA ATT ATT TAA TG | AAT ACA GCA TGA CCA ACT ACT AAA A |
| Q0055 | aI2 | GGT CAT GCT GTA TTA ATG ATT TTC T | CCA ATT AAA GCA GGC ATT ACT AAG A |
| Q0060 | aI3 | GCT TTA ATT GGA GGT TTT GGT AAC | GTA GCT CCA ATT ATT AAT GGT AAT AAA TA |
| Q0065 | aI4 | TAC GAG CAT TTA TTT TGA TTC TTT GGT | GAA TAA TTA AAA TAT ATA CTT CAG GGT G |
| Q0070 | aI5 α | CAA CAG GAA TTA AAA TTT TCT CAT GAT TA | TTG AAC CAC CAT GGA TTA GAG C |
| Q0075 | aI5 β | TCA TTA GAT GTA GCA TTC CAC GAT | AAT GTC CCA CCA CGT AGT AAG T |
| | aI5 γ | TAC TAC GTG GTG GGA CAT TTT C | AAT AGC ACC CAT TGA TAA TAC ATA GT |
| | bI1 | GGT TAT TGT TGT GTT TAT GGA CAG A | ACC TCA ATG TGA CAA TTG TGA TAG |
| Q0110 | bI2 | TGT CAC ATT GAG GTA ATA TAA ATA TCG | CTG AGA ATA AAT TAG TAA TAA CTA GTG C |
| Q0115 | bI3 | TTG TAT CTT GAT TAT GAG GTG GGT T | GGA TTA GAG GGT TAG ATA CTG AG |
| Q0120 | bI4 | ATT CTA TTC ACC TAA TAC TTT AGG TCA | GAT TAC CAG GAA TAT AGT TAT CAG GA |
| | bI5 | ATC CTT TAG TAA CAC CAG CAT CTA T | AAT GGT AAT AAG TAT CAT TCA GGT ACA |

3.19. Single cell generation time measurement

Individual cells (approximately 100 for each strain) were placed on agar plates of appropriate growth medium, as described above, using a micromanipulator. Next, an image of each original mother cell was taken every 10 minutes for 8-9 hours. The images were then analysed and division time of each cell was extracted.

3.20. Single molecule RNA-FISH and imaging

Yeast cultures were grown as described above, fixed with 37% formaldehyde for 45 min at room temperature, digested with 2.5 μ L of zymolyase (Zymo Research, 2000 U) at 30 °C for 60 min and permeabilized with 70% ethanol overnight at 4 °C. Cells were hybridized in the dark at 30 °C using Stellaris RNA-FISH probes (Biosearch Technologies). 45 probes targeting intron aI2 and 40 probes targeting intron aI5b cox1 were coupled to Quasar 670 dye (red). 43 probes targeting cox1 exons were coupled to Quasar 570 dye (green). All probes are listed in Table 7. Yeast cells were placed on microscope slides with Vectashield Mounting Medium and imaged with an Olympus IX70 wide-field fluorescence microscope. A series of z-stacks was acquired with a step size of 0.3 μ m. The images were analysed using Image J. The number of green (exon), red (intron) and yellow (colocalized) foci was manually counted and normalized per 100 cells in each of three biological replicates. At least 300 cells were analyzed per replicate per strain.

Table 7. RNA-FISH probes used for targeting aI2, aI5b and cox1 exons

| aI2 intron | aI5 β intron | exons |
|-------------------------|------------------------|-------------------------|
| GTGCGCCGTTTCGCTTAATTT | ATTAATTTAATAAGTGTCGTGC | ATGGTACAAAGATGATTATAT |
| CTGTATTGAAGTGTTAATTGAT | GGTTATATATATATATATATTA | CAACAAATGCAAAAGATATTG |
| TATCTCTGTTTATTCAATTAAT | GCTAACGGGGAAACTCTTATAA | GTATTATATTTTATGTTAGC |
| CTTTACCGTATCATTTTGGTTC | GACAATCCCGTGATAACTTTAA | TTTTTAGTGGTATGGCAGG |
| TTAGTAGTAACATACATAGTAT | GTATTGTAGAGACTAAACGTG | CAGCAATGTCTTTAATCATTAG |
| GATACGTAAACCATATGGCTTA | GATTTTAATATTATTTAAATAT | GCACCTGGTTCACAATATTAC |
| GGGGCCAACCTCAACGGGGACA | GAGATAGTCCAATCTTATATG | GGTAATTCACAATTATTTAATG |
| GCATGCCATAAAAGCGCTGGAG | CAATTAATATCTCCTTTTGGG | GTAGTTGGTCATGCTGTA |
| CAGCCAGCGCAAGGTAAGAACT | GTTCCGGTCCCTGGTCCGGCC | GTAATGCCTGCTTTAATTG |
| GTCTTCATAGTACCCAAATTTA | CGAAACTAAAGATATTAAG | TATTTATTACCATTAATAATTG |
| GTGAGATACTTTAGTACTTTAT | GAATCAATTATAAATAATTATA | GCTACAGATACAGCATTTC |
| GCAAGGAAGGAAGACAGTTTAG | GATAATTATACTGAAGAAGAAA | GAATTAATAACATTGCTTTTTG |
| GATTAATACTACGGATTTTTTC | CTGGATTATTTGAAGGAGATGG | GTATTACCTATGGGGTTAG |
| GAAAATAATCATAATAAACTTG | GTTTTTCAATTACTTTTTCTTT | GTTTAGTTACATCAACTTTAG |
| GTCAGATATTAGAATGTTATTA | GATGTTTTATTAGCTAATTATT | GAATCAGGTGCTGGTACAGGG |
| GGTTCTAATAATATTACCTTAG | GTCTTTATTTTAAAAATTGGTC | CTGTCTATCCACCATTATC |
| GGATTAATATTTTCATATTTAAA | CAGCTAAATATAATTTTAATAA | CTATTCAGGCACATTCAGGACC |
| CTAAAGATATTAACACTAATAT | CAGCTGTAAATGAAATATTAT | GTGTAGATTTAGCAATTTTTGC |
| GAAATTCCTAAAACATCTGGAG | GAAGTATTTATAAATTATATTA | CATTTAACATCAATTTTCATCAT |
| GACCTTTAAGTGTTGGAAATCC | GGTAAATTATTAACATATAAAA | GGTGCTATTAATTTTCATTG |
| TTGTACAAGAAAGTATGAGAAT | CCTTGATTAACAGGTTTAAAT | CAACATTAATATGAGAAC |

Table 7. (continued)

| aI2 intron | aI5β intron | exons |
|--------------------------------|-------------------------------------|------------------------|
| GGAATTCCTCAAGGTAGTGTG | CATAAAAATAGTCAATGATTAA | GTATGATCAATTTTCATTAC |
| GAGGTAGAAATCCAATTTATAA | GTCCGGCCCCGCCCCCGCG | CGTTCTTATTATTATTATC |
| GATTAGATTAAGAGACCATTAC | GCGGACCCCAAAGGAGATATTA | CCTGTATTATCTGCTGGT |
| GGTGTAAATGGGTTCTCATAATG | CTTGGTGGTATTTTAAAAAGAG | GAAGTATCAGGAGGTGGTGACC |
| GGGTATGATGTAAAAGTTACAC | CTGGTGCTACAGCTTATATTTA | GAGCATTATTTTGATTCTTTGG |
| GGGTTAGACATCATACTAGTTT | GCTCAATCATCAAAAGCTATA | CACCCTGAAGTATATATTTT |
| GCCCCATTAGAAGTATTGTAA | CCTTTTATTGAATATTTTAAT | GGCTTCAATTGGATTATTAGG |
| GGCTATTGTTCTCATGGTATT | CCATTAAGTCTTAGAAGATATA | GGATTAGATGCAGATCTTAGAG |
| CCCAGAGGGGTTGGAAGATTAA | CAATATTTATTATTAATATTG | GCTCTAATCCATGGTGGTTC |
| GGTAGAGGTATTATAAACTATT | CTTATTAATAAATAAATAAATTA | GGGTGGTTTAACTGGTGTGCC |
| GGTAGAATTACATACATTTTAT | CTTAATCTTTATTAATATTA | CTTACTACGTGGTGGGAC |
| GTTGATCCTCATTCAAAAGTTA | GAATTAATATTATTACAAAGTG | CTATGTATTATCAATGGGTGC |
| GATTCTAATTATACACCTGATG | CTTTAGAAAATAAAAAATG | GCAGGATACTATTATTGAAG |
| GATAGATATAAATATATGTTAC | GAGTTAAAATTATTATTAATAA | GGGGCTAATGTTATTTTC |
| GTGGTATTTGTCAAATTTGTGG | CTTCATTATAACAATATCG | GGTATTAATGGTATGCCTAG |
| CATCACGTAAGAACATTAAATA | GATAATATTAAGAGTAAAT | GATTATCCTGATGCTTTCGCAG |
| CTATCTGTAAAACATGTCATTT | CTTAAAGTGTTAATTTAA | GTCGCTTCTATTGGTTCATTC |
| GTTTCATCAAGGTAAATATAATG | ATATTCTTTTTTTTTTATG | GATCAATTAGTTAATGGATTAA |
| CAGGTTTATAATAATTATTAT | | GCACCTGATTTTGTAGAATC |
| CTATTAATATGCGTTAAATGG | | CACCAGCTGTACACTCATTAA |
| GCCGTATGATATGAAAGTATC | | CACCAGCTGTACAATCTTAA |
| CGGTTCGGAGAGGGCTCTTTTA | | |
| GATAGGTTTGCTACTCTAC | | |
| GCCCCATTAGAAGTATTGTAA | | |
| GGCTATTGTTCTCATGGTATT | | |
| CCCAGAGGGGTTGGAAGATTAA | | |
| GATAGGTTTGCTACTCTAC | | |

3.21. Protein extraction for 2D Oxi-DIGE

Bacterial cultures were grown up to exponential phase (OD₆₀₀=0.4) in LB medium, each strain in four replicates. After centrifugation (7,155 x g, 15 min, 4 °C) pellets were treated with 500 μ L of UTC (8M urea, 2M thiourea, 4% CHAPS, 5 mM DTT) buffer, each and homogenized by vortexing and by extensive pipeting. Contaminant DNA was broken by sonication (10 seconds, 3 times) on ice. Protein concentration was measured after centrifugation (16,000 x g, 30 min, 4 °C) by Bradford method (Bradford, 1976) from the supernatant and subjected to second sonication for 10 s in order to break remained genomic DNA.

3.22. 2D Oxi-DIGE

Internal standard (IS) was prepared using an aliquot of each samples of the experiment. For each sample, 300 µg of proteins was prepared for carbonyls derivatization. pH was adjusted to 4.0. Samples were derivatized by 0.5 mM final CF647DI-Hydrazide (Biotium Inc. USA), 60 min incubation (4 °C). Samples were immediately precipitated with trichloroacetic acid (TCA) and acetone. Protein pellet homogenised in UTC buffer (without DTT) (9,300 x g overnight 4 °C). pH was adjusted on 8.5 followed by minimal tagging with Cy3NHS. All the samples were tagged with 400 pmol Cy3NHS (50 µg of CF647-Hydrazide prior tagged proteins) and Internal Standard (1850 µg of IS) was tagged with Cy2NHS. For each 2D gel, 50 ug of protein extract (Cy3NHS and CF647Hydrazide labelled) was mixed with 50 ug of Internal Standard (Cy2NHS labelled).

Proteins were separated by isoelectric focusing on Immobiline DryStrip (Serva, 24 cm, pH3-10) in an IPGPhor3 (GE Health Care, Little Chalfont, UK) following separation according to molecular weight with Ettan Dalt System electrophoresis (GE Health Care, Little Chalfont, UK) in 8-18% polyacrilamide gradient gel. Following completion of the electrophoresis, gels were scanned with Typhoon FLA9500 system (GE Health Care, Little Chalfont, UK).

3.23. Gel imaging and analysis

Images were analyzed using SameSpots 2D analysis software (TotalLab, UK). All the gels were automatically aligned onto one reference gel (Cy2NHS internal standard labeled sample) and then manually corrected to ensure proper alignment. Differentially expressed proteins labelled with Cy3NHS (1.5 fold change, $p \leq 0.05$, ANOVA) between mutator strain, ancestor and non-mutator were included for liquid chromatography/mass spectrometry identification. Carbonylated spots signal (CF647 Hydrazide signal) was normalized and Relative Modification index (RMI) was calculated. Statistically significant spots ($p \leq 0.05$ (ANOVA) and 1.5 RMI) were selected for further identification. Spots of interest were excised from gel using a semiautomatic picking device according to manufacturer instruction (Screen Picker, LabConsult Inc., Belgium).

4. RESULTS

4.1. RNA chaperones buffer deleterious mutations in *E.coli*

This part of my thesis is already published in eLife journal (Rudan, M., Schneider, D., Warnecke, T., & Krisko, A. (2015). RNA chaperones buffer deleterious mutations in *E. coli*. *Elife*, 4, 1-16.).

4.1.1. Overexpression of DEAD-box RNA helicases enhances fitness of a low-fitness strain

Mutations that affect protein folding can be buffered by protein chaperones. This phenomenon results with no change in the phenotype. The hypothesis in this research proposed mutation buffering on the RNA level by RNA chaperones. More precisely, it was suggested that maintaining RNA structure and increasing its stability by DBRHs could mask the detrimental effects of mutations. To test this hypothesis, competition experiments between certain *E.coli* strains were performed and their relative fitness measured. The *E. coli* REL606 strain, which is the ancestor of the long-term evolution experiment (LTEE), and two evolved mutS mutator strains with deficiency in mismatch repair system were used. Mutator strains were sampled from a lineage after ~20,000 (20k) and ~40,000 (40k) generations of adaptation to a minimal glucose-limited medium (Sniegowski et al., 1997).

During this evolution experiment under conditions of weak selection, 40k strain accumulated deleterious mutations and resulted with decreased fitness compared with its ancestor (Figure 14A). The 20k strain did not show any deviation in fitness compared to the ancestor (Figure 14A). Since mutS mutation arose ~3,000 generations into the LTEE (Sniegowski et al., 1997), it is present in both 20k and 40k strains and it is not responsible for reduced fitness in 40k strain.

Three DEAD box RNA helicases, RhlB, CsdA and SrmB, were selected to test the aforementioned hypothesis. Since mutator strain sampled from 40,000 generation showed compromised fitness, plasmids carrying a selected *E. coli* DBRH gene (either rhlB, csdA, or srmB) were introduced into its background. The same was done with the ancestor and the 20k strain for control experiments. Each transformed strain was competed against a strain of the same genotype but bearing an empty control plasmid. Overexpression in the ancestral and the 20k backgrounds had limited effects on competitive fitness, while overexpression of each

DBRH enhanced fitness of the mutationally compromised 40k genotype (Figure 14B). To confirm this buffering effect is due to helicase activity of DBRHs, plasmid carrying the mutation that rendered the respective helicase domain catalytically inactive were introduced. In each case, the central glutamic acid residue of the DEAD motif has been substituted with lysine (E166K, E157K, and E158K). For each DBRH tested, fitness gains were abolished (Figure 14B), suggesting that helicase and therefore RNA remodelling activities are essential for buffering.

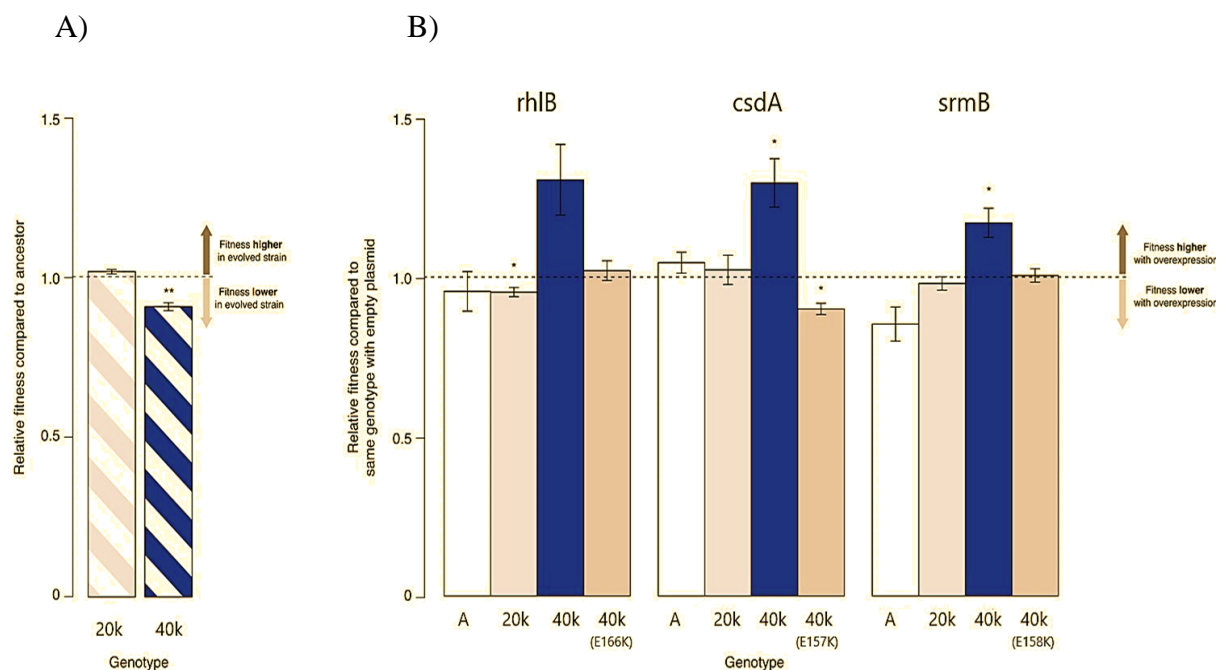


Figure 14. Relative fitness of *E. coli* REL606-derived strains.

A) Relative fitness of the 20k and 40k genotypes, each competed against their REL606 ancestor.
 B) Relative fitness of ancestral and evolved genotypes overexpressing one of three DEAD box RNA helicases (DBRHs) compared with identical strains carrying the empty control plasmid. E166K, E157K, and E158K: competitions in the 40k background where plasmids carried mutated versions of the respective DBRH. In each case, the central glutamic acid residue of the DEAD motif has been recoded to lysine, compromising the helicase activity. Bar heights indicate mean relative fitness across four biological replicates, with each mean derived by averaging over four technical replicates. Error bars represent standard errors of the mean. ** $p < 0.01$, * $p < 0.05$ (one-sample *t*-test). Based on and adopted from Rudan et al., (2015).

It was also tested whether fitness rescue occurs in stationary phase as a result of strain survival or if it is already present in exponential phase. Same competition experiments were performed for 20k and 40k strains compared to ancestor and selected DBRHs in the 40k background. Mixed cultures of competitors were plated after 2 hours (mid-exponential phase) and resulted with similar buffering effects as the ones in stationary phase (Figure 15).

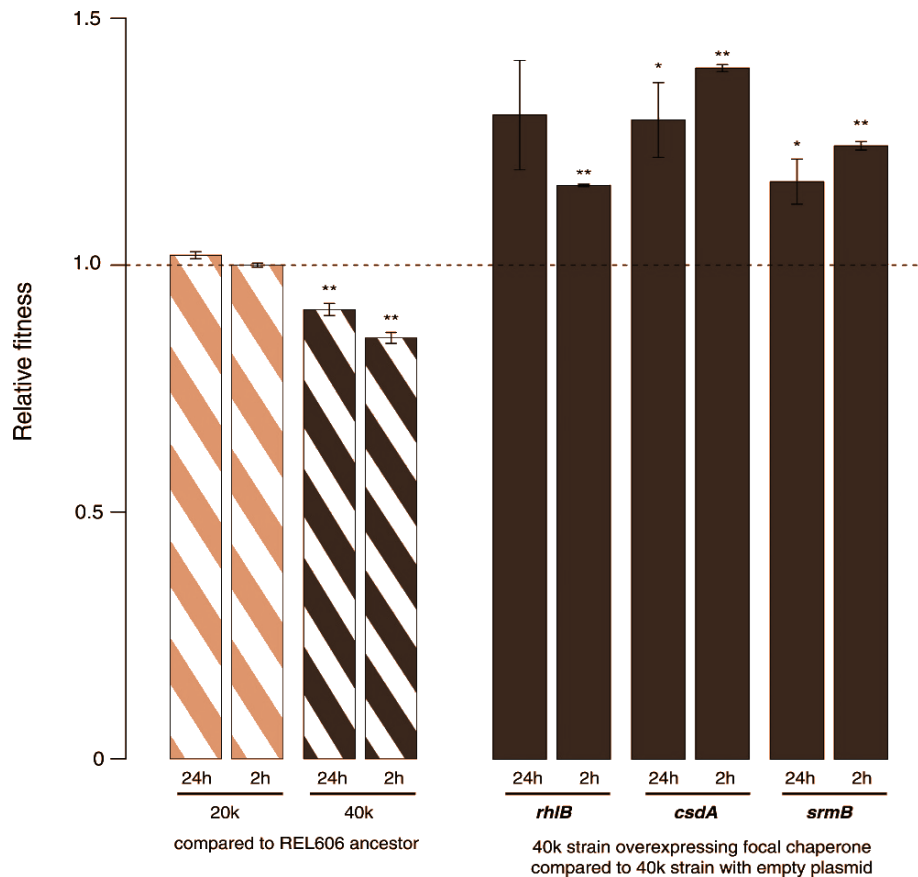


Figure 15. Relative fitness in competition experiments terminated in mid-exponential phase (REL606). Based on and adopted from Rudan et al., (2015).

4.1.2. RNA chaperones buffer distinct mutations in a second low-fitness strain

It is known for chaperones responsible for *de novo* protein folding and refolding to function in ATP-dependent manner. They recognize exposed hydrophobic amino-acid side chains that are buried in the native state (Hartl et al., 2011) and this non-specific pathway allows buffering to occur across a wide range of substrates. In order to examine does the DBRH-mediate buffering occur in a second low-fitness strain and test whether it encompasses diverse target substrates,

MG1655-derived *mutH* deletion ($\Delta mutH$) strain was used, a mutator with deficient mismatch repair system allowing different mutations to accumulate. This strain was sampled after a relatively short period of laboratory evolution (~500 generations) and, in competition experiments, it displayed reduced fitness compared with its ancestor (Figure 16A). Upon overexpression of specific DBRH gene (*rhIB*, *csdA* or *srmB*), $\Delta mutH$ experienced fitness gains as the previous *mutS* mutator strain did (Figure 16B). To confirm that fitness effects were not directly related to the *mutH* deletion, *mutH* was deleted in the ancestral MG1655 background *de novo*. Fitness of the *de novo* $\Delta mutH$ strain was not reduced compared with the deletion-free ancestor (Figure 16A).

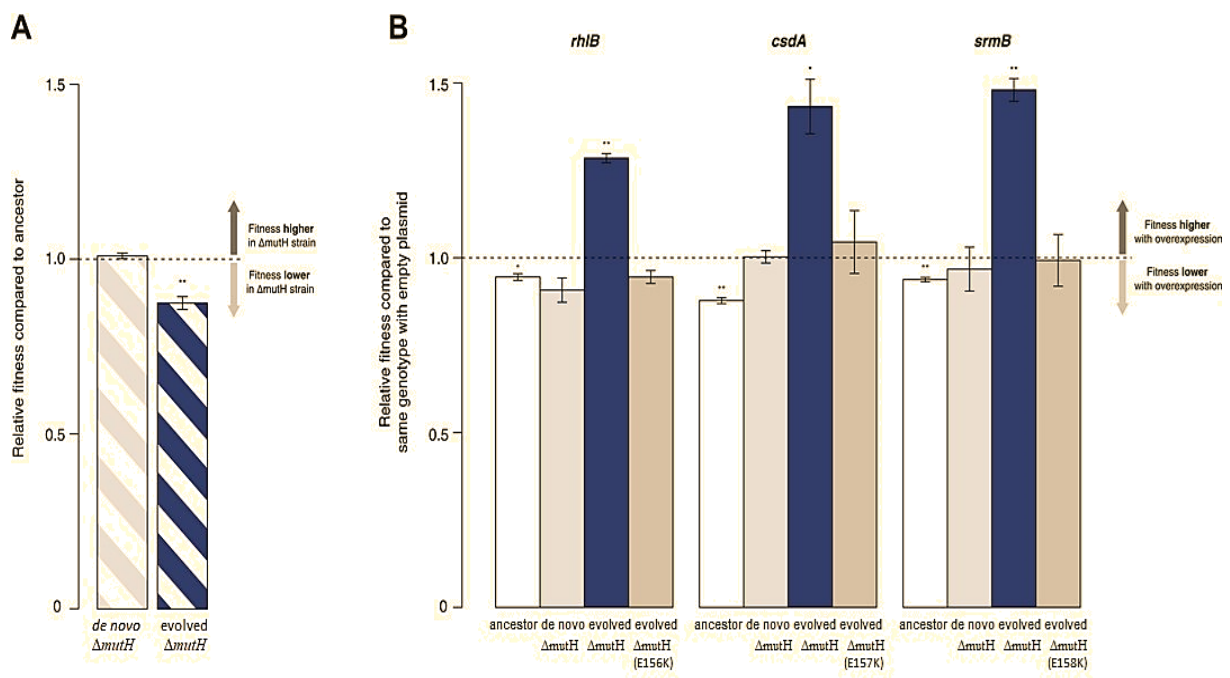


Figure 16. Relative fitness of *Escherichia coli* MG1655-derived strains.

A) Relative fitness of the evolved and *de novo*-constructed $\Delta mutH$ strains, each competed against their MG1655 ancestor. B) Relative fitness of ancestral, evolved, and *de novo* $\Delta mutH$ genotypes overexpressing one of three DEAD box RNA helicases compared with identical strains carrying the empty control plasmid. E166K, E157K, and E158K, bar heights and error bars are as described in Figure 14. ** $p < 0.01$, * $p < 0.05$ (one-sample *t*-test). Based on and adopted from Rudan et al., (2015).

To examine effect of DBRHs on fitness during different bacterial growth phases, competitions experiments with evolved *ΔmutH* terminated in the mid-exponential phase (after 2 hr) were performed. Results showed similar buffering effects as the ones in stationary phase (Figure 17).

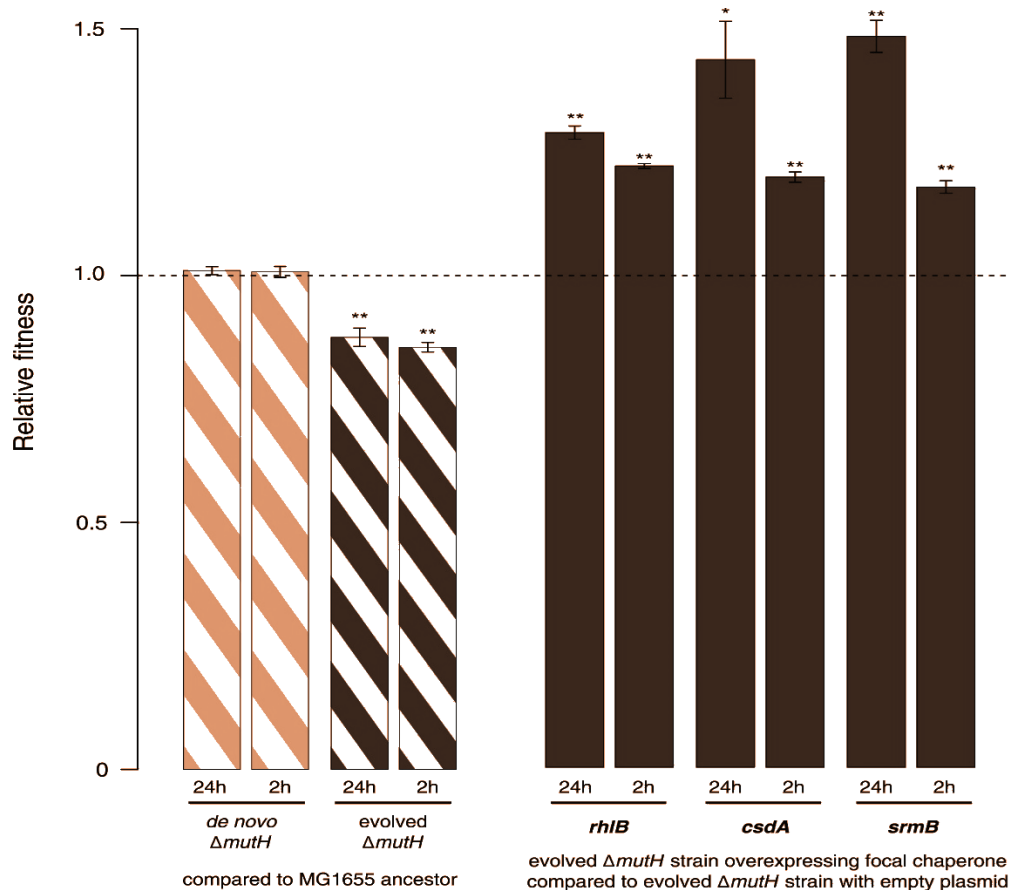


Figure 17. Relative fitness in competition experiments terminated in mid-exponential phase (MG1655). Based on and adopted from Rudan et al., (2015).

After confirmed mutation buffering of these three RNA helicases in a second low-fitness strain, it was necessary to rule out the buffering of identical mutations across strains. For this purpose the genomes of the evolved *ΔmutH* strain and its laboratory ancestor were sequenced (Chapter 2.4). 20k and 40k strains were already sequenced carrying 667 single nucleotide polymorphisms in coding sequences of 755 in total and 1163/1291, respectively. In the evolved *ΔmutH* it was found significantly fewer mutations compared with the 40k strain, more precisely 12 SNPs in coding sequences (Table 8). While evolved *ΔmutH* do not contain large deletions, except the *mutH* deletion itself, 20k strain possess one and 40k four of them. More importantly, there were

no identical point mutations or indels in the two evolved strains, implying buffering of independent mutations. This might be indicative of a general rather than gene- or pathway-specific buffering mechanism and is consistent with DBRHs being broad-spectrum catalysts of RNA remodelling that recognize and target misfolded substrates through a non-specific mechanism of action (Jarmoskaite et al., 2014).

Table 8. Number of mutations in evolved mutator strains compared with their respective ancestors.

| Strain | • SNPs (CDS/total) | □ Small indels (CDS/total) | Large deletions |
|----------------------|--------------------|----------------------------|-----------------|
| 20k | 667/755 | 86/129 | 1 |
| 40k | 1163/1291 | 128/183 | 4 |
| Evolved <i>ΔmutH</i> | 12/12 | 0/2 | 0± |

• SNP, single-nucleotide polymorphism; CDS, coding sequence

□ ≤ 4 bp

± Excluding the *ΔmutH* deletion itself

4.1.3. Pinpointing individual deleterious mutations buffered by RNA chaperones

In order to justify buffering of mutations that compromise mRNA stability by DBRHs and eventually reveal its molecular mechanism, mutations that are individually deleterious and subject to fitness improvement by chaperone overexpression were identified. Since evolved *ΔmutH* strain carries only 12 point mutations, each mutation was tested as a candidate for DBRH-mediated buffering separately. Out of 12 mutations, seven of them are located in a gene of known function (*hepA*, *torA*, *lamB*, *cyoA*, *osmC*, *lsrR* and *speC*) and five are located in *y*-genes. Recombineering approach was used, also known as homologous recombination-mediated genetic engineering, to individually introduce each of 7 mutations into the MG1655 genome. After constructing strains with specific mutations, competition experiments in which each strain was compared against MG1655 were performed. Results displayed one strain with impaired fitness, the one with a mutation in the *lamB* gene (Figure 18A). By overexpressing DBRHs, this strain revealed fitness increase (Figure 18A). Maltose outer membrane protein, coded by *lamB* gene, is involved in the transport of maltose and maltodextrins. It becomes

derepressed under glucose-limiting conditions to maximize sugar uptake. Mutants with *lamB* deletion are outcompeted by reference strains when grown on glucose (Death et al., 1993), suggesting a possible cause of fitness loss in our strain. Same type of competition experiments were performed terminating in the exponential phase and results were consistent with the previous ones, verifying *lamB* as a driver of fitness loss in this strain (Figure 19).

Due to the large number of mutations in the second mutator strain, 40k, it was difficult to test each mutation as a candidate for DBRH-mediated buffering, so focus was on two mutations in the essential ribosomal protein gene *rplS*: one synonymous (*rplS*^{syn}) and one non-synonymous (*rplS*^{nonsyn}). Both mutations are present in the 40k strain but not in the 20k one. It is known that some synonymous mutations in ribosomal protein genes, such as *rplA* and *rpsT* in *Salmonella typhimurium*, can strongly compromise fitness (Lind et al., 2010). Therefore, competitions between the REL606 ancestor and strains carrying either the *rplS*^{syn} or *rplS*^{nonsyn} mutation were performed. Results showed no effect on fitness in the presence of *rplS*^{nonsyn} mutation, but *rplS*^{syn} mutation has a deleterious effect and was rescued by DBRH overexpression (Figure 18). Additional results for competitions terminated in mid-exponential phase (after 2 hr) are shown in Figure 20.

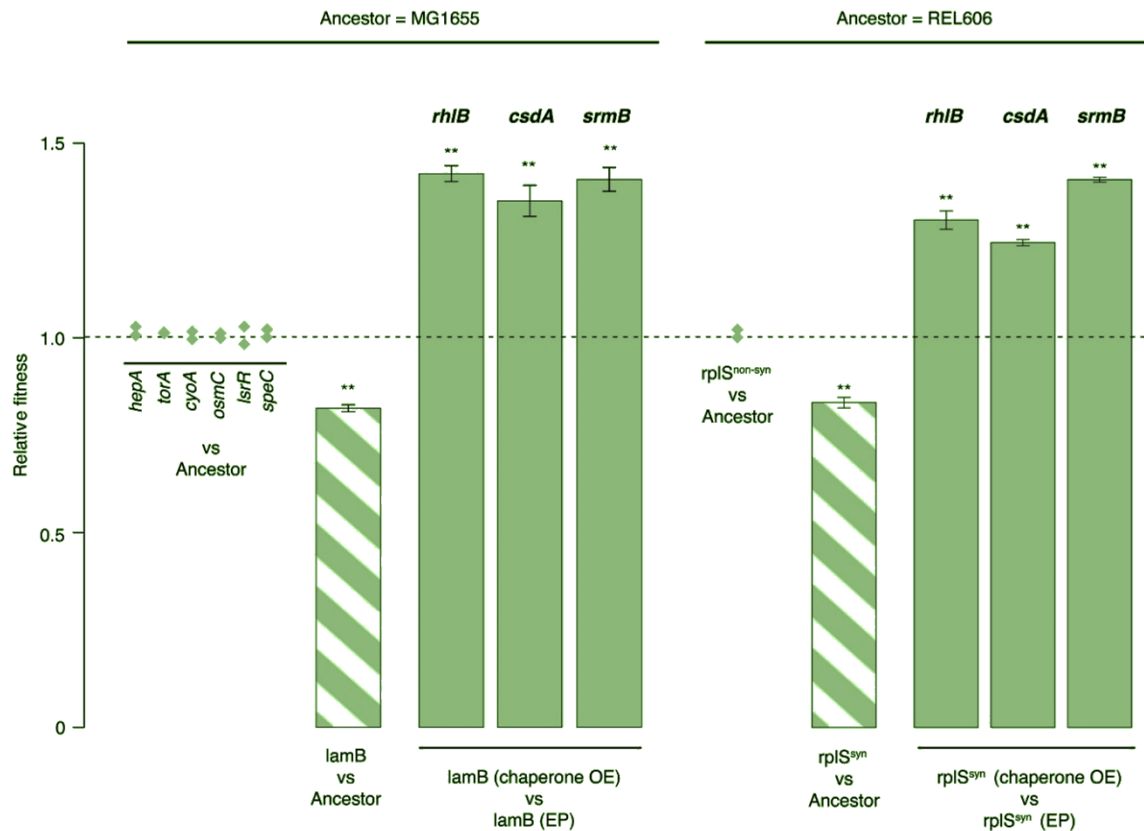


Figure 18. Fitness effects and buffering of individual mutations.

Relative fitness of strains carrying single point mutations introduced into the relevant ancestral background competed against the respective ancestor. Initial screening for fitness defects involved two biological replicates (diamonds). For the two mutations, where the initial screen suggested a measurable fitness deficit, *lamB* and *rplS^{syn}*, all competitions were carried out in quadruplicate. Bar heights and error bars are as described in Figure 14. ** $p < 0.01$, * $p < 0.05$ (one-sample t -test). OE: overexpression; EP: empty plasmid. Based on and adopted from Rudan et al., (2015).

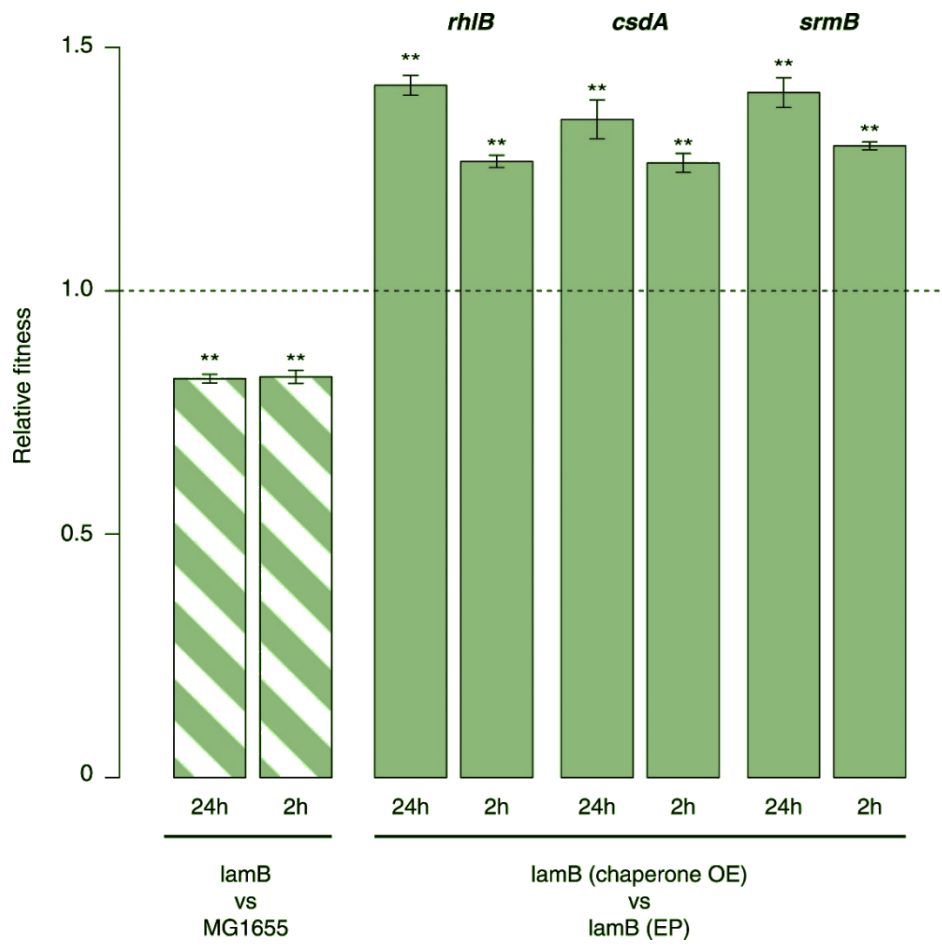


Figure 19. Relative fitness in competition experiments terminated in mid-exponential phase (*lamB*). OE: overexpression; EP: empty plasmid. Based on and adopted from Rudan et al., (2015).

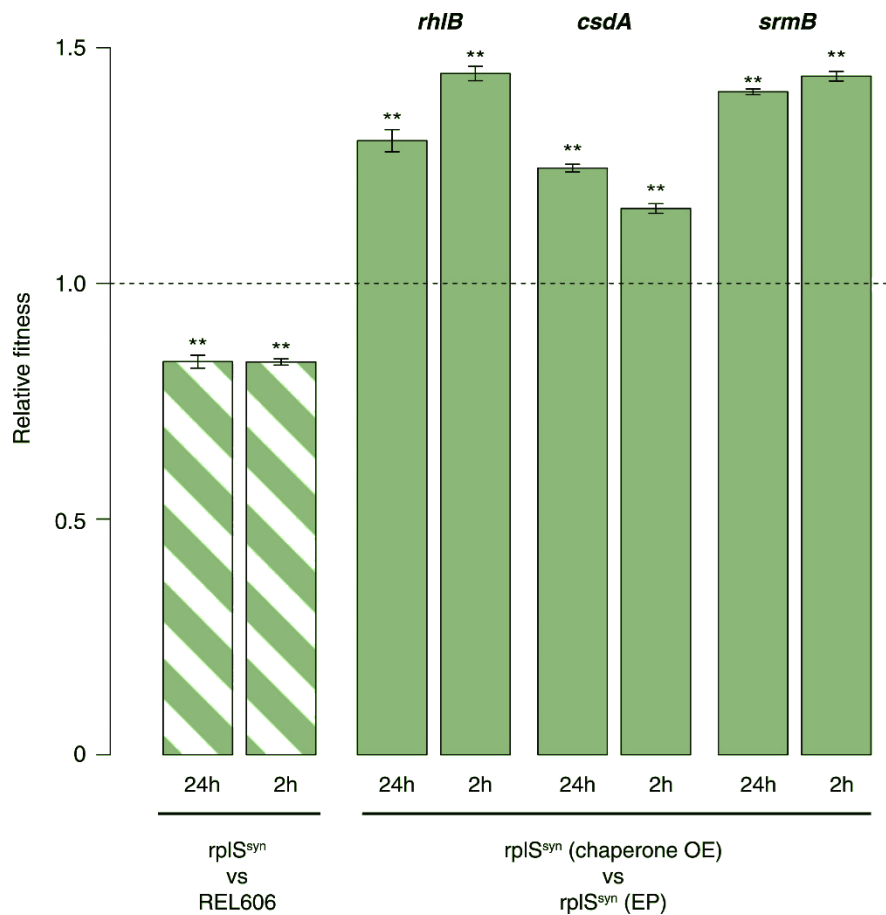


Figure 20. Relative fitness in competition experiments terminated in mid-exponential phase (*rplS^{syn}*). OE: overexpression; EP: empty plasmid. Based on and adopted from Rudan et al., (2015).

4.1.4. Fitness gains upon overexpression of *cspA* suggest diverse mechanisms of buffering

Along with DBRHs, some other chaperones also assist in RNA folding, so different mechanisms could be involved in mutation buffering. In order to investigate mechanistic variety in buffering, the cold shock protein CspA which inhibit the formation of misfolded RNA secondary structures by stabilizing single-stranded RNA (Jiang et al., 1997) was selected. Plasmids overexpressing *cspA* gene were introduced into the 20k and 40k strains and their ancestor and then competition experiments performed against the same genotype with empty plasmid. Relative fitness of compromised 40k strain was improved. The same set of experiments was done with MGG1655 derived strains. Evolved *ΔmutH*, second low-fitness strain, has also experienced fitness gain by overexpressing CspA (Figure 21). By contrast,

overexpression of a mutant version of CspA with severely reduced nucleic acid-binding activity (Hillier et al., 1998) did not confer fitness benefits upon overexpression (Figure 21). Figure 22 is demonstrating relative fitness in competition experiments terminated in mid-exponential phase and 24 hours overexpressing CspA in 40k, evolved $\Delta mutH$, rplS^{syn} and lamB mutant.

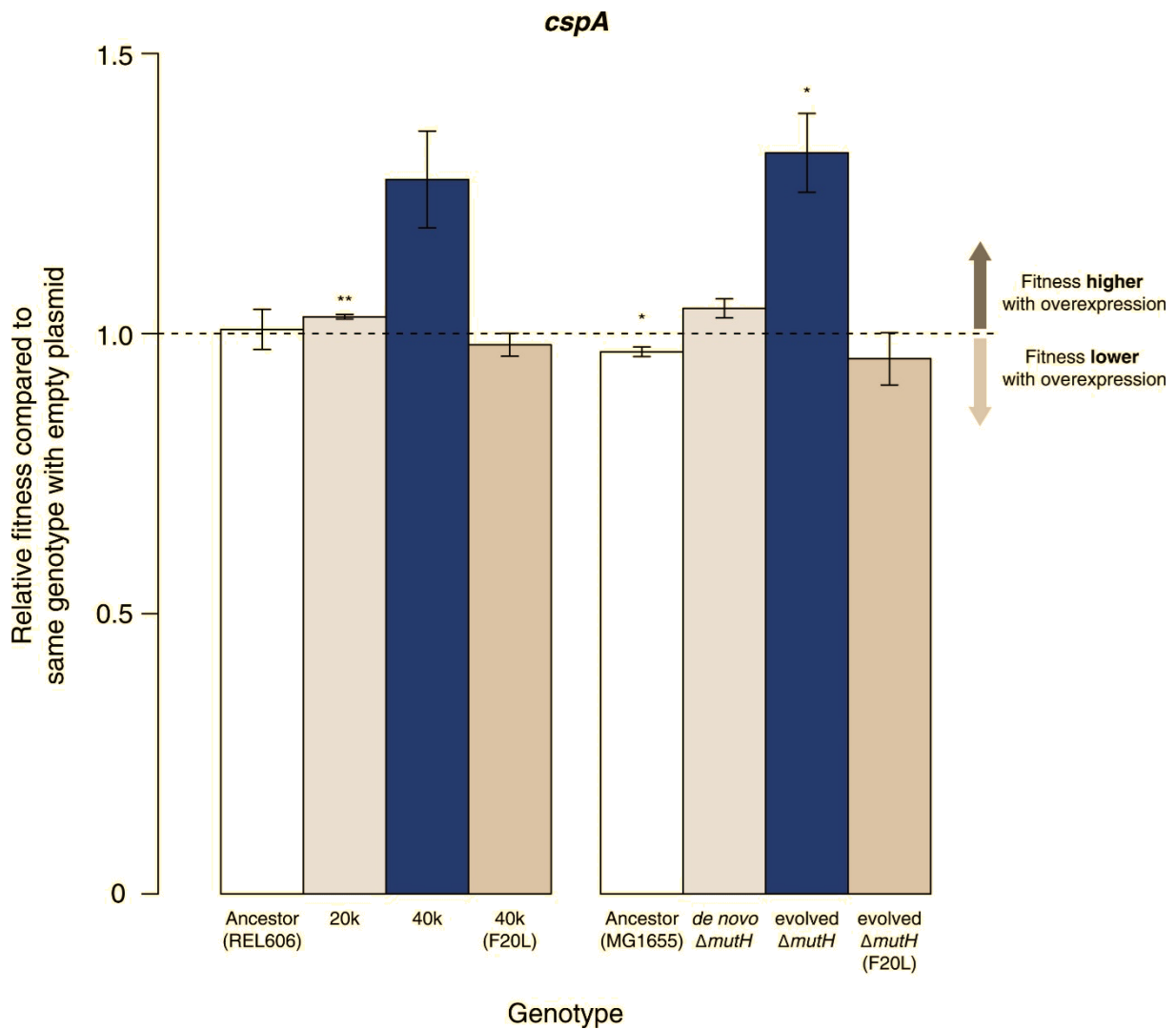


Figure 21. Effects of CspA overexpression on relative fitness.

Relative fitness of REL606- and MG1655-derived strains overexpressing CspA compared with strains of the same genotype carrying the empty control plasmid. F20L: competitions in the 40k and evolved $\Delta mutH$ backgrounds, respectively, where plasmids carried a mutated version of the *cspA* gene yielding a protein with compromised nucleic acid binding ability (Hilier et al., 1998). Bar heights and error bars are as described in Figure 14. ** $p < 0.01$, * $p < 0.05$ (one-sample *t*-test). Based on and adopted from Rudan et al., (2015).

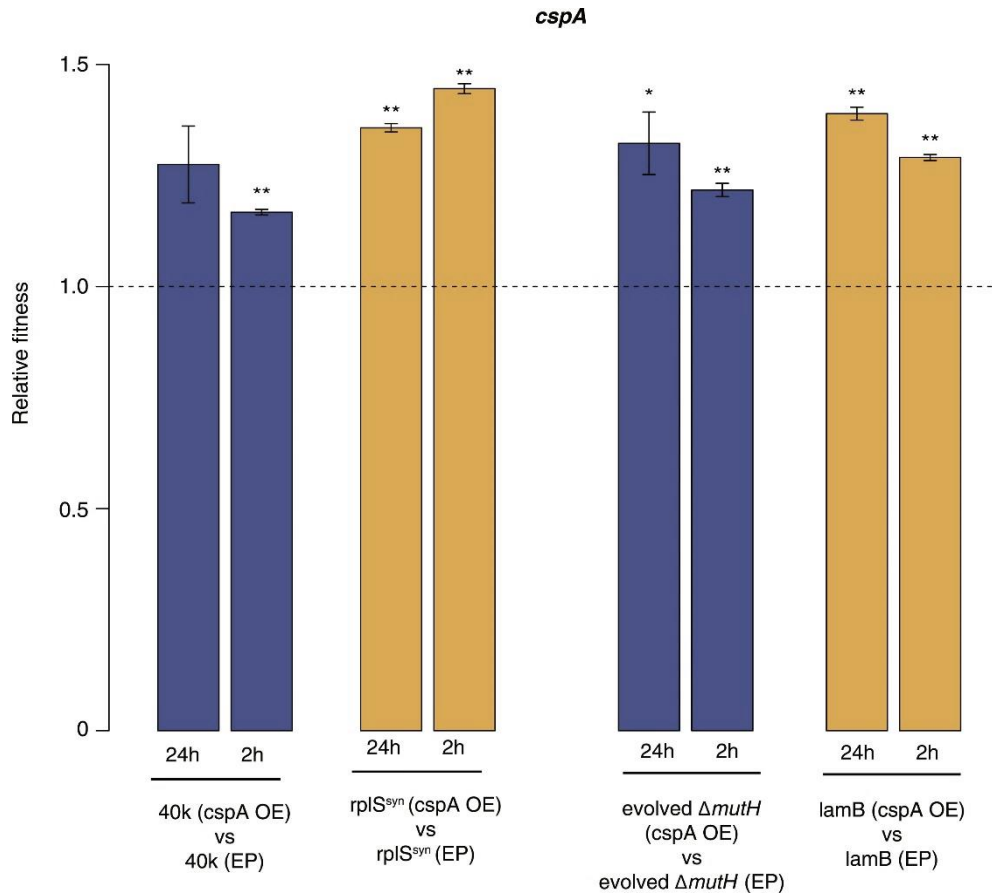


Figure 22. Relative fitness in competition experiments terminated in mid-exponential phase (*cspA*). OE: overexpression; EP: empty plasmid. Based on and adopted from Rudan et al., (2015).

Although CspA levels are relatively low compared with overexpressed DBRHs (~fourfold and ~twofold reduced relative abundance compared with CsdA and RhlB/SrmB, respectively, Figure 23), buffering still occurs likely because CspA is subject to negative autoregulation (Bae et al., 1997).

Hunger et al. demonstrated association of DBRHs and cold shock proteins in preventing the formation of unfavourable structures (Hunger et al., 2006). Therefore, it is not surprised that the RNA chaperones mediated buffering include identical substrates.

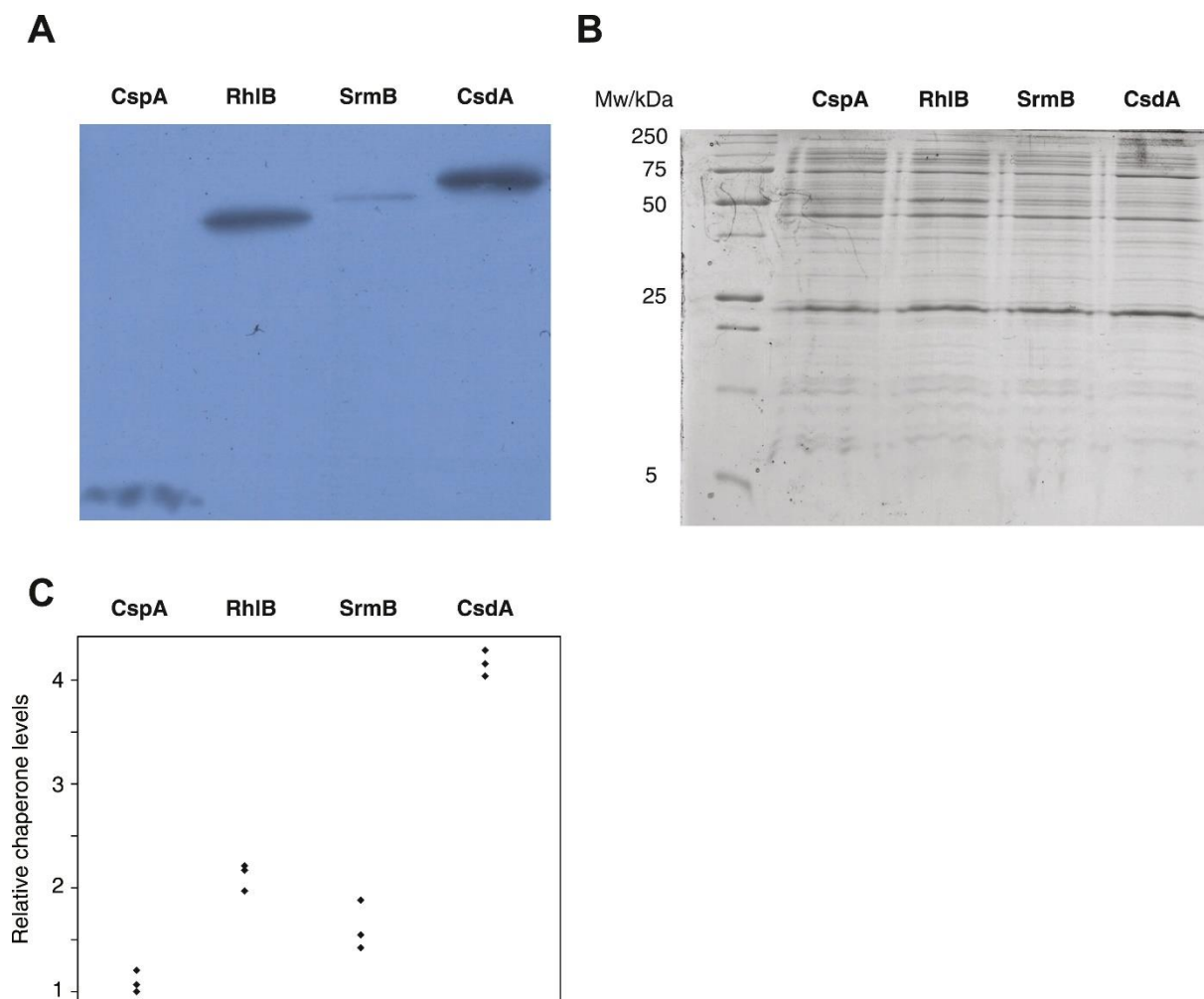


Figure 23. Relative chaperone abundances.

A) Representative Western blot for evolved $\Delta mutH$ strains overexpressing one of the focal RNA chaperones. Molecular weights (from nucleotide sequence): CspA, 7,403 kD; RhIB, 47,126 kD; SrmB, 49,914 kD; CsdA, 70,546 kD. B) Representative Coomassie-stained SDS-PAGE gel. C) Relative chaperone levels are defined as the ratio of Western blot intensity to Coomassie intensity. The lowest ratio detected across triplicate experiments in all strains was set to one. Comparing these ratios between strains overexpressing different RNA chaperones gives a semi-quantitative indication of relative chaperone abundances. For example, CsdA levels in CsdA-overexpressing cells are ~fourfold higher than CspA levels in CspA-overexpressing cells. Note that this metric does not allow conclusions about the absolute fraction of total protein that is occupied by each chaperone in the different strains. Based on and adopted from Rudan et al., (2015).

4.2. Removal of self-splicing introns from *S. cerevisiae* mitochondria triggers the retrograde response

This part of my thesis is currently under the revision.

4.2.1. Deletion of self-splicing introns from *S. cerevisiae* mitochondria lead to hyper-fusion phenotype

Mobile genetic elements frequently compromise host fitness (Werren, 2011), corrupting genetic information or disturbing adaptive gene expression patterns, sometimes to lethal effect. Despite this, mobile genetic elements are ubiquitous in most eukaryotic genomes (Hurst and Werren, 2001). In this part of research, effect on yeast fitness when mitochondrial introns are removed was explored.

Three genes of mitochondrial DNA in *S. cerevisiae* contain self-splicing introns: the 21S ribosomal RNA gene (which harbours a single group I intron named *omega*) and two protein-coding genes, *cox1* (group I: aI3, aI4, aI5 α , aI5 β ; group II: aI1, aI2, aI5 γ) and *cob* (group I: bI2, bI3, bI4, bI5; group II: bI1), both encoding components of the electron transport chain. Under a low-cost model for the persistence of self-splicing introns, removing these introns should have little, if any, effect on host fitness. Contrary to this prediction, it was found that a strain where all mitochondrial introns have been removed (I_0) exhibits stark phenotypic differences to the wild-type (WT) strain. First, yeast growth on glucose-supplemented YPD medium was measured and 30% slower post-diauxic growth of I_0 compared to the WT strain (a161_U7) was observed (Figure 24A). Chronological life span (CLS) was also measured where I_0 experienced almost two-fold longer lifespan (Figure 24B) compared to WT. To examine mitochondrial morphology and to measure mitochondrial mass 10-N-Nonyl acridine orange (NAO) fluorescent dye was used. I_0 displayed increased mitochondrial mass (Figure 24C) and almost three-fold increase in mean mitochondrial volume (Figure 24D). To visualize mitochondria in a single cell, MitoLoc plasmid was used and mitochondrial fusion phenotype of I_0 observed, characterized by a large network of branched tubules of homogeneous diameter (Figure 25). Since there are known genes for the regulation of fusion and fission processes in *S. cerevisiae* genome, their transcription levels were validated to verify this phenotype. I_0 had upregulated levels of mitofusin (*fzo1*) and the mitochondrial GTPase *mgm1* transcript levels, key regulators

of mitochondrial fusion, whereas levels of *dnm1* and *fis1*, which orchestrate mitochondrial fission, were unchanged (Figure 26). Mitochondrial inner membrane potential plays a central role in ATP production and no significant differences in I_0 compared to the WT strain, measured by 3,3'-Dihexyloxycarbocyanine iodide (DiOC6(3)) fluorescence (Figure 27A), revealing that mitochondria are functional despite grossly altered morphology. Biomarkers of mitochondrial metabolism in fact point to increased mitochondrial activity, with higher oxygen consumption (Figure 27B) and higher ATP levels (Figure 27C) during exponential growth. Despite increased activity, levels of mitochondrial superoxide are reduced (Figure 27D), likely reflecting a >7.5 fold upregulation of the mitochondrial ROS-scavenger SOD2 (qPCR, t-test $P=0.003$) (Figure 29). At the molecular level, a 10.9-fold (5.8-fold) increase in the level of mature *cox1* (*cob*) mRNA was observed (Figure 28A, B).

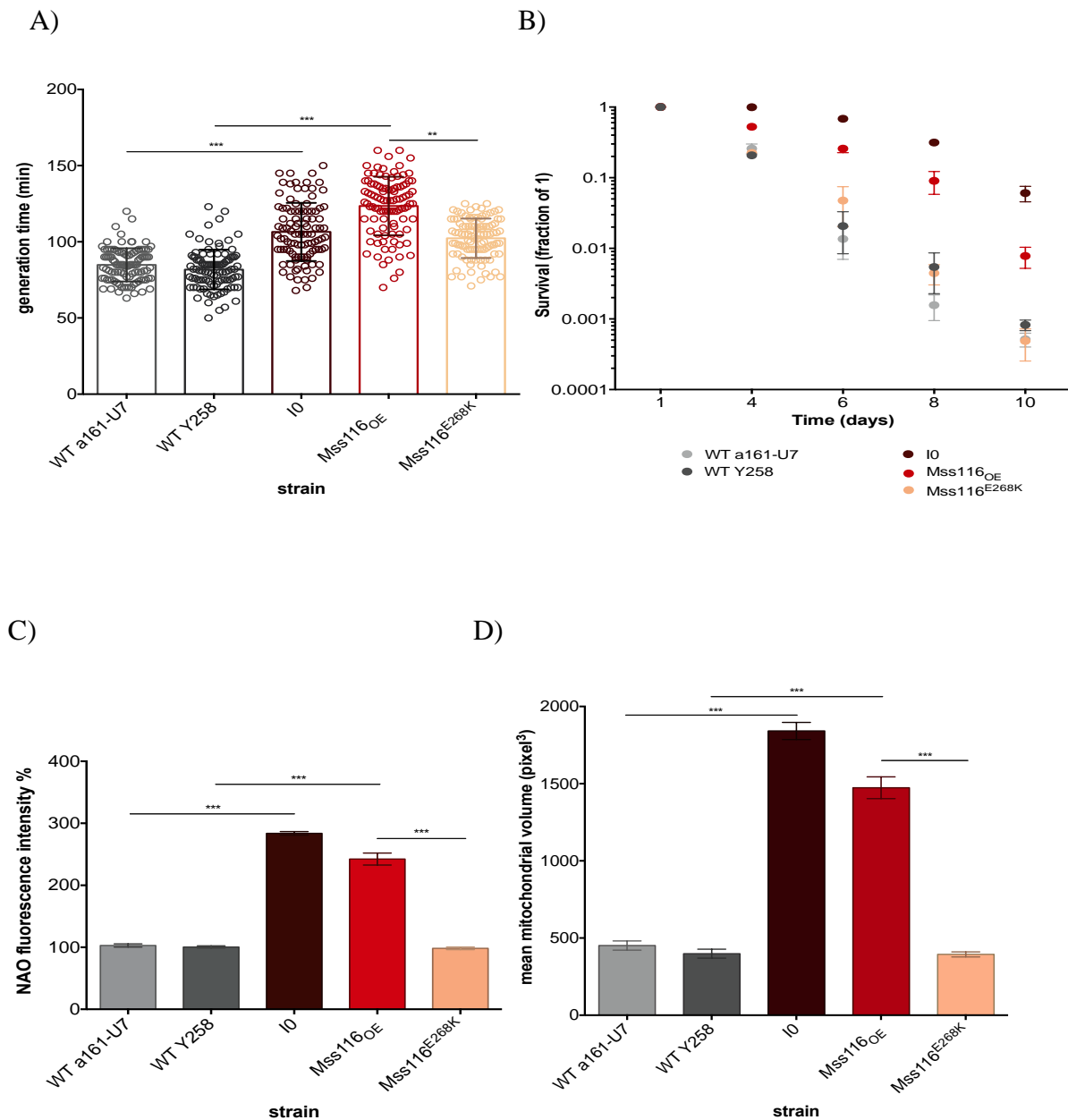


Figure 24. Phenotypic characteristics of I₀ and Mss116^{OE} strains compared with their corresponding WT strains and Mss116^{E268K} mutant: A) Generation time of I₀ and Mss116^{OE} is increased in post-diauxic shift growth. B) Chronological lifespan of I₀ and Mss116^{OE} is extended, observed as fraction of surviving cells over days in starvation. C) Mitochondrial mass is more than 2.5 fold enlarged in I₀ and Mss116^{OE} measured by flow cytometry as fluorescence intensity of cardiolipin-specific dye, NAO (10-N-Nonyl acridine orange). D) Mitochondrial volume of I₀ and Mss116^{OE} is 2.5 and 2 fold higher, respectively. The quantification of mitochondrial volume was performed using MitoLoc plugin for ImageJ in more than 500 cells. Data are mean ± SD from at least three independent cultures, each performed in triplicate. ****P* < 0.001; ***P* < 0.01; **P* < 0.05 (ANOVA plus post hoc).

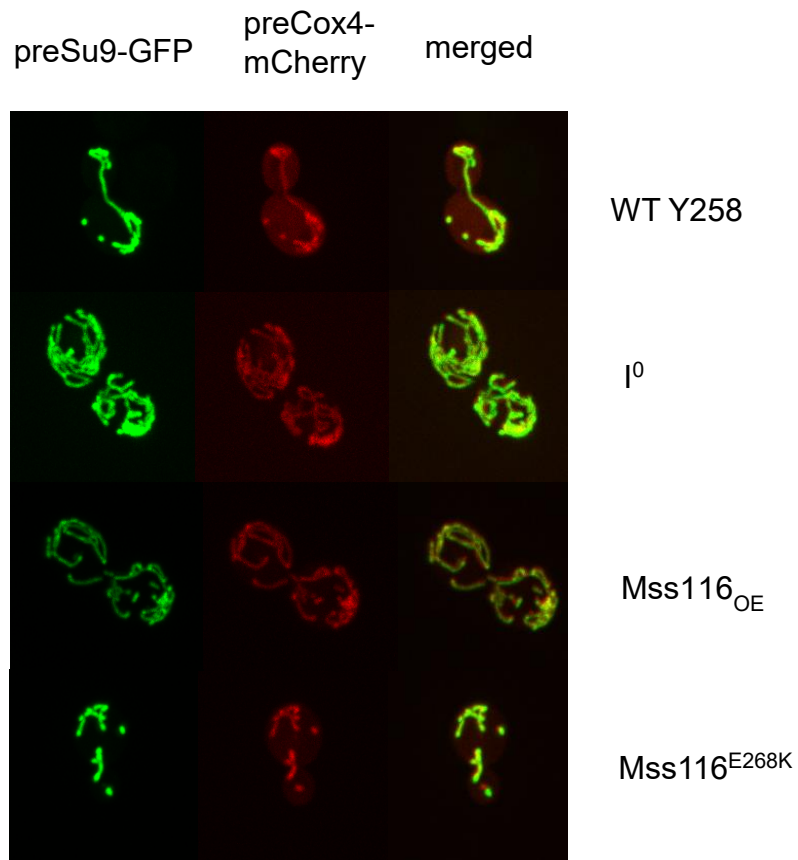


Figure 25. Representative images of cells with visualized mitochondria via preCOX4-mCherry and preSU9-GFP. This image was taken in the collaborator lab of Dr. Ira Milošević group, European Neuroscience Institute, Gottingen, and supervised by Dr. Anita Kriško.

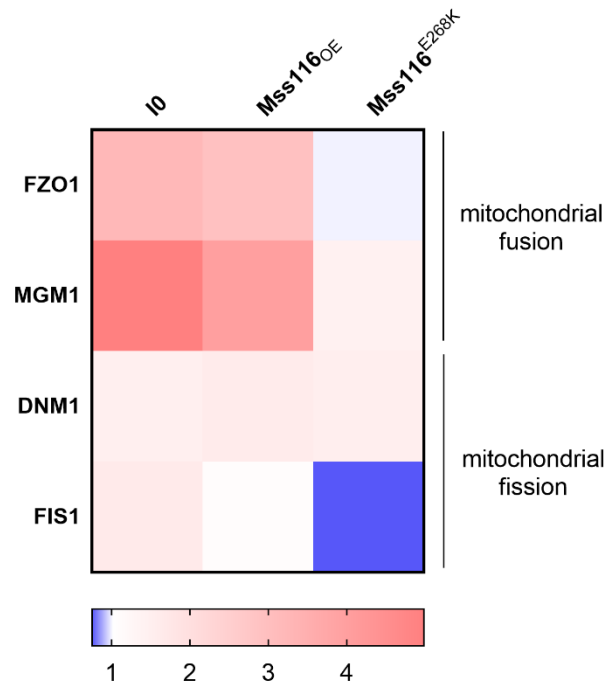


Figure 26. Transcription levels of genes regulating mitochondrial fusion and fission of I₀, Mss116^{OE} and Mss116^{E268K} strain.

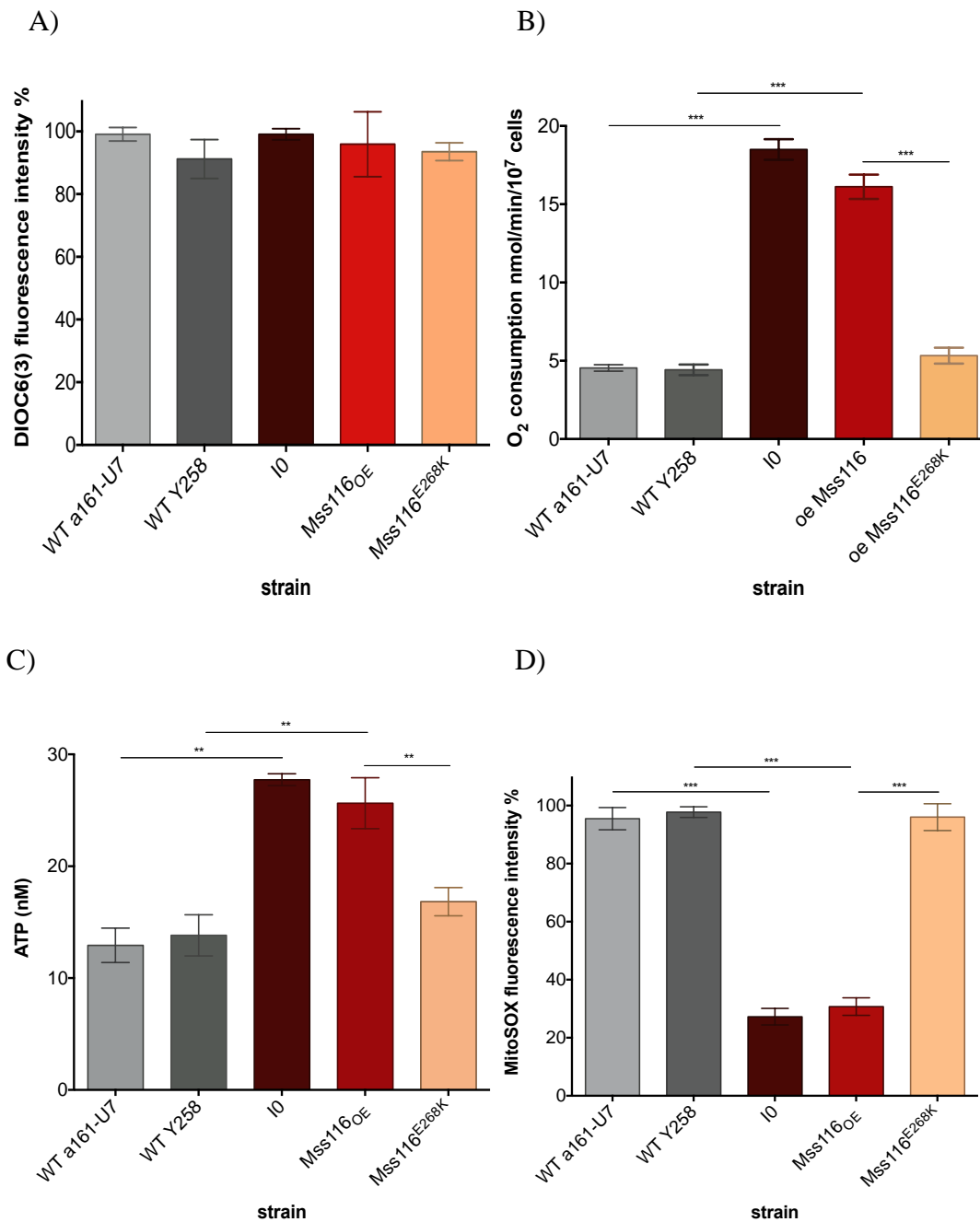


Figure 27. Increased mitochondrial activity of I₀ and Mss116^{OE} strains. A) Mitochondrial inner membrane potential measured by flow cytometry using DiOC6(3) (3,3'-Dihexyloxycarbocyanine iodide fluorescence). B) Respiration measurements of oxygen consumption. C) ATP levels are increased in I₀ and Mss116^{OE} strains. D) Mitochondrial superoxide levels measured by flow cytometry using MitoSOX fluorescence intensity display a decrease in I₀ and Mss116^{OE} strains. Data are mean \pm SD from at least three independent cultures, each performed in triplicate. *** $P < 0.001$; ** $P < 0.01$; * $P < 0.05$ (ANOVA plus post hoc).

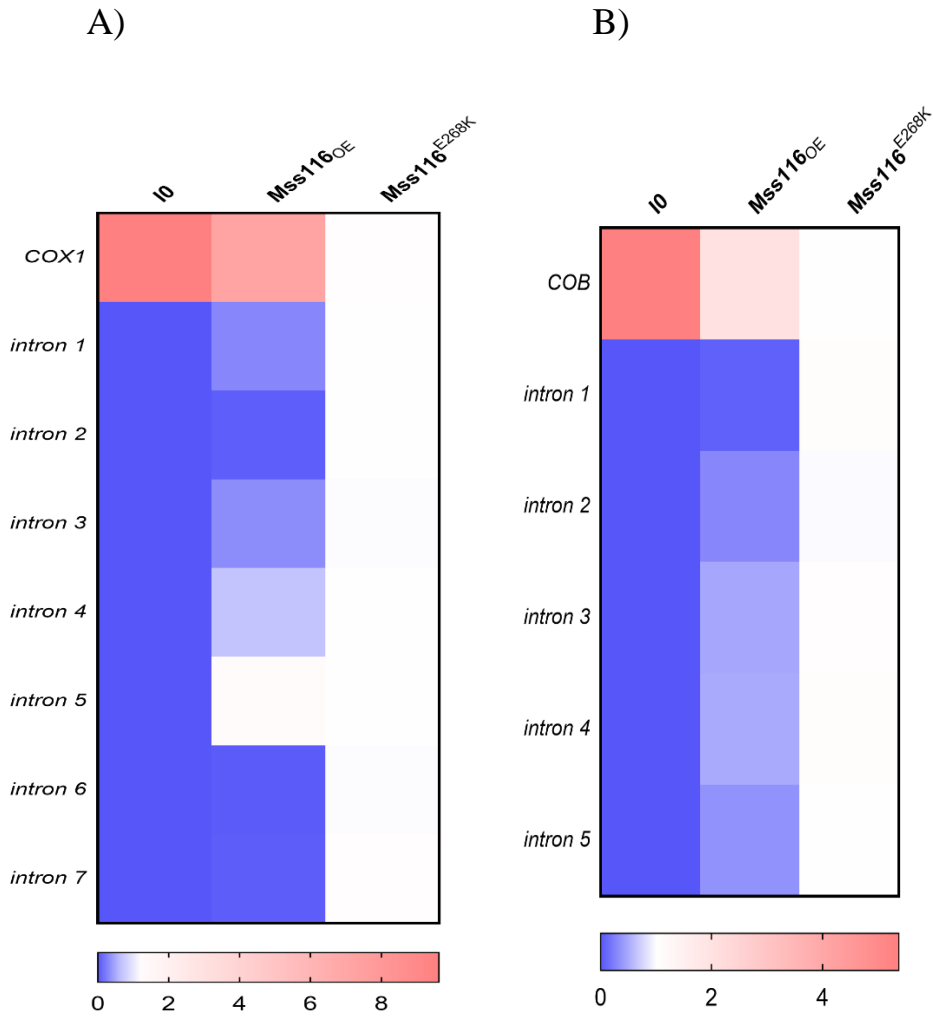


Figure 28. Transcript levels of individual introns of COX1 (A) and COB genes (B) are decreased compared to Mss116^{E268K} mutant, while level of mature *cox1* (*cob*) mRNA demonstrate 10.9-fold (5.8-fold) increase. Colour of the squares on the heat map corresponds to the mean value of the log fold change from three biological and three technical replicates. UBC6 was used for normalization.

4.2.2. Deletion of self-splicing introns from *S. cerevisiae* mitochondria activate the retrograde response

By testing different gene expression changes in *I₀* strain, induction of *cit2*, and upregulation of the two rate-limiting members of the TCA cycle, *cit1* and *idh1* was observed (Figure 29). Cit2 is coding for citrate synthase which expression is controlled by Rtg1 and Rtg2 transcription factors. Furthermore, both mitochondrially (*cox1*, *cox2*, *atp6*) and nuclearly (*cox4*, *atp1*, *sdh1*, *sdh2*) encoded parts of the respiratory chain were upregulated (Figure 29). To examine the

activation of retrograde response in the *I₀* strain, *rtg2*, the transcriptional master regulator of the retrograde response and a sensor of mitochondrial dysfunction was deleted, which resulted with suppressed *I₀* phenotype. First, chronological lifespan was measured where Δ RTG2 I_0 experienced decreased fraction of survived cells (Figure 30A) and lower oxygen consumption (Figure 30B) compared to the WT_{a161-U7} and Δ RTG2 _{a161-U7} strains. ATP levels were more than two fold decreased in Δ RTG2 I_0 strain (Figure 30C) and mitochondrial volume reduced (Figure 30D). Imaging revealed that mitochondrial shape have lost the tubular structure and adopted a large spherical shape (Figure 31), suggesting defects in the maintenance of mitochondrial ultrastructure (Paumard et al., 2002; Velours et al., 2009). Figure 32 is demonstrating transcription levels of genes included in respiratory chain, TCA cycle, retrograde response, antioxidant protection and mitochondrial fusion and fission.

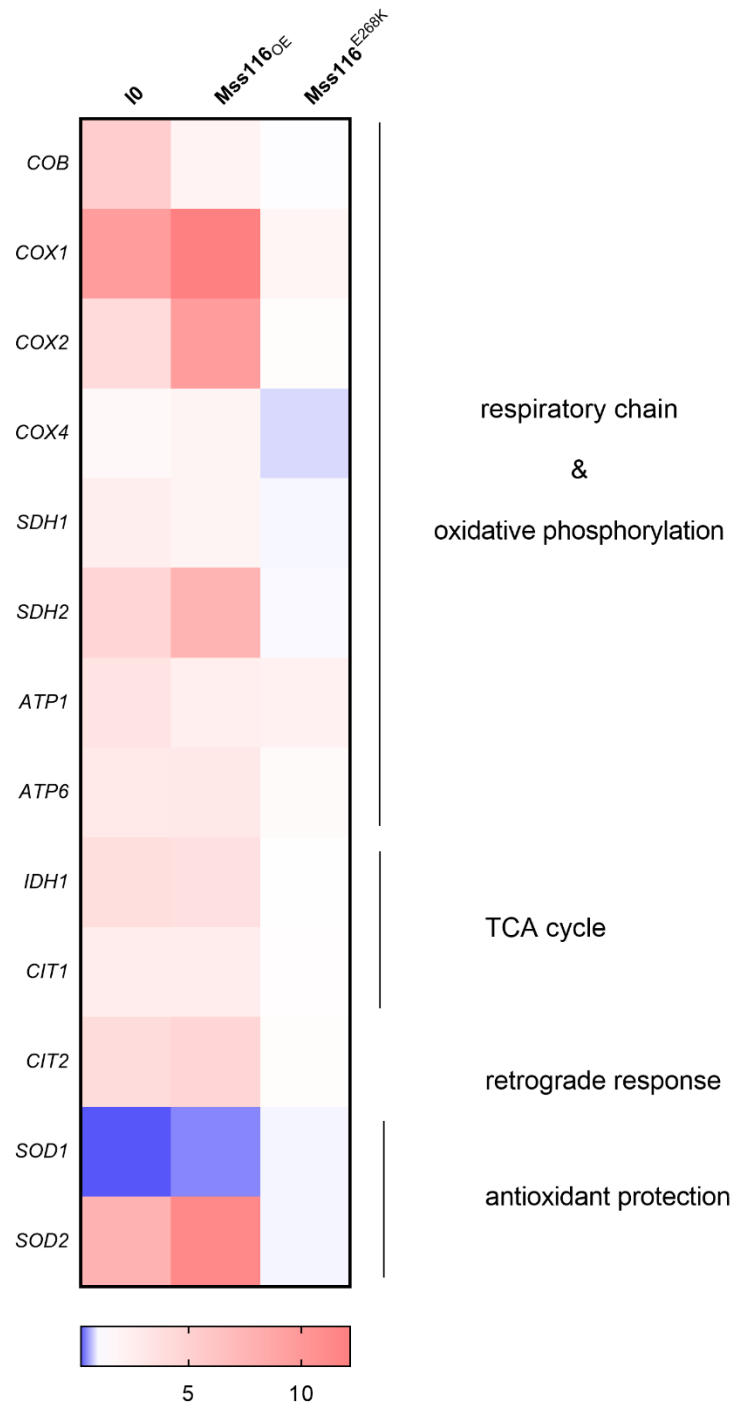


Figure 29. Quantitative real time PCR measurement of differential gene expression reveals up-regulation of the respiratory chain components, TCA cycle enzymes and mitochondrial ROS-scavenger SOD2 in I₀ and Mss116^{OE} strains. Colour of the squares on the heat map corresponds to the mean value of the log fold change from three biological and three technical replicates. UBC6 was used for normalization.

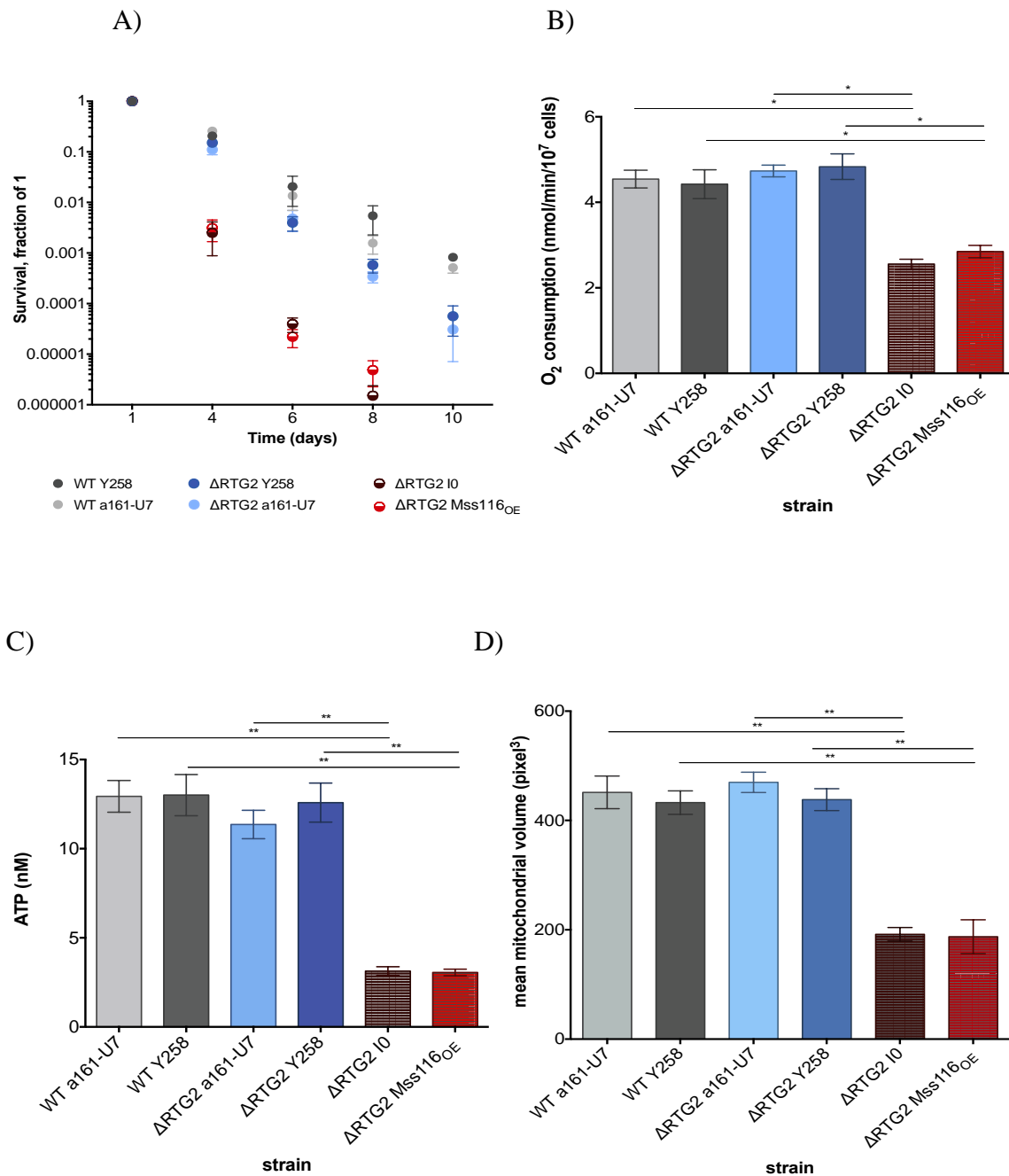


Figure 30. Phenotypic characteristics of Δ RTG2 mutants. A) Chronological lifespan of Δ RTG2_{I0} and Δ RTG2_{Mss116_{OE}} strain is decreased compared to I₀ and Mss16_{OE} strains. B) Oxygen consumption rates of Δ RTG2_{I0} and Δ RTG2_{Mss116_{OE}} strain are decreased compared to the ones in I₀ and Mss16_{OE} strains. C) ATP levels are more than two fold decreased in Δ RTG2_{I0} and Δ RTG2_{Mss116_{OE}} strain relative to I₀ and Mss16_{OE} strains. D) Mitochondrial volume of Δ RTG2_{I0} and Δ RTG2_{Mss116_{OE}} is decreased in comparison to I₀ and Mss16_{OE} strains. Data are mean \pm SD from at least three independent cultures, each performed in triplicate. *** $P < 0.001$; ** $P < 0.01$; * $P < 0.05$ (ANOVA plus post hoc).

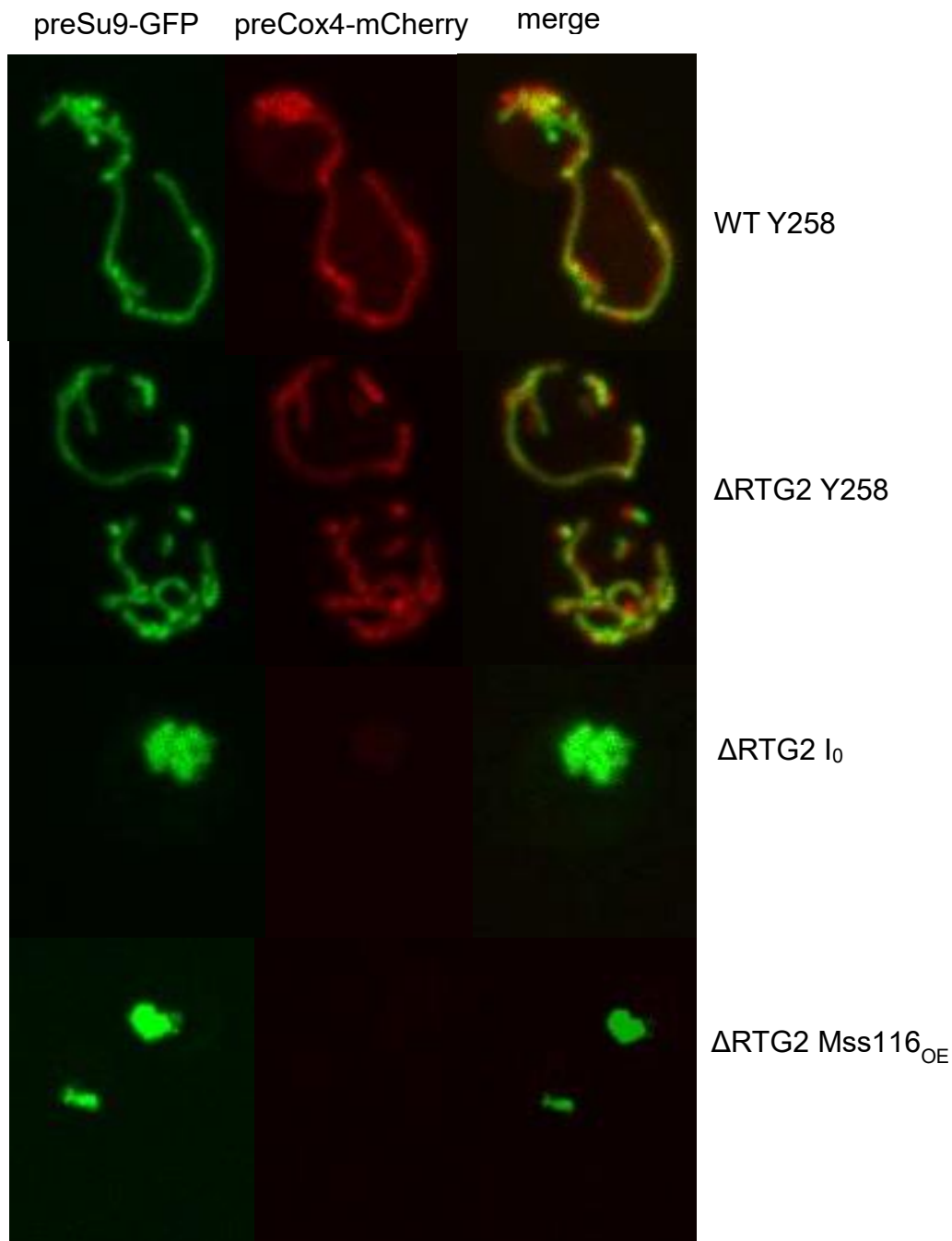


Figure 31. Representative images of cells with visualized mitochondria via preCOX4-mCherry and preSU9-GFP. Even though it has no significant effect on mitochondria in the WT background, the absence of Rtg2 has shown to be detrimental for the mitochondria of I₀ and Mss16_{OE} strains. This image was taken in the collaborator lab of Dr. Ira Milošević group, European Neuroscience Institute, Gottingen, and supervised by Dr. Anita Kriško.

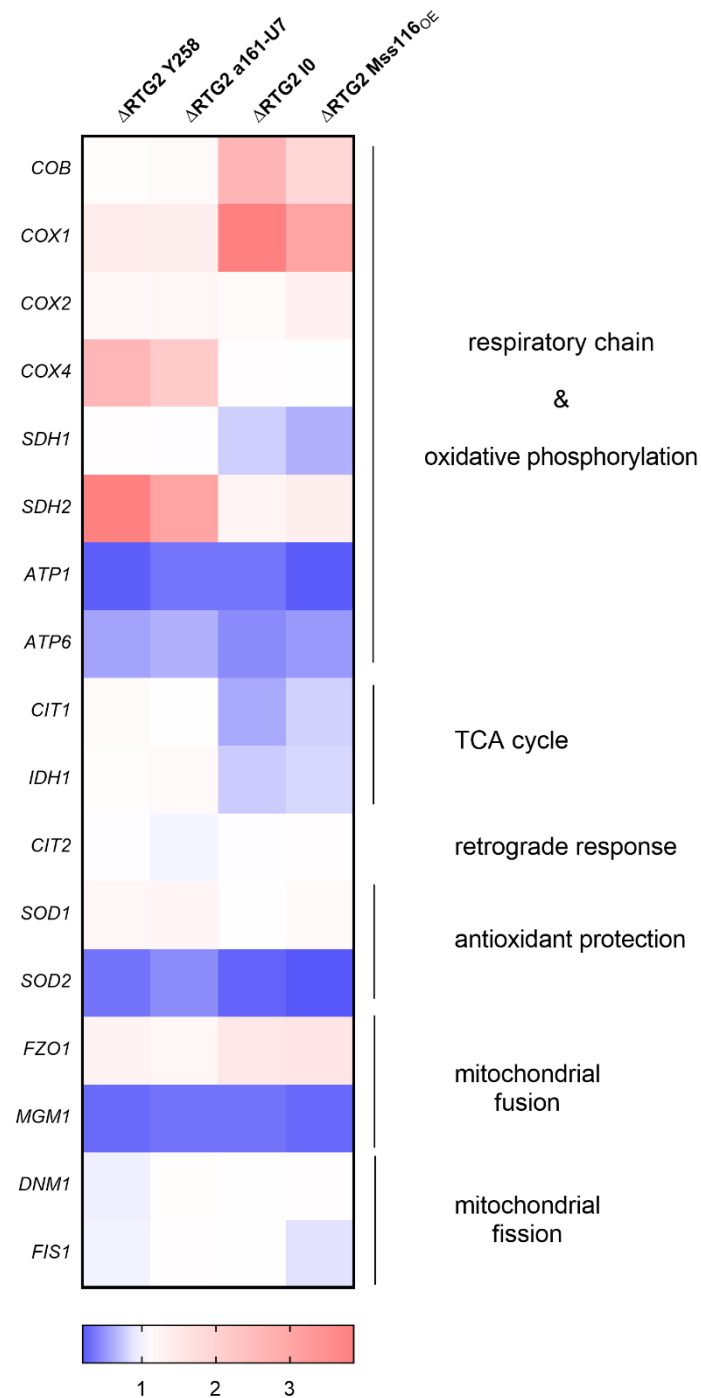


Figure 32. Transcript levels of target genes in the absence of RTG2 abolish the phenotype characteristic of I₀ and Mss116^{OE} strains. ΔRTG2_{I₀} and ΔRTG2^{Mss116} strain demonstrate down-regulation of genes involved in oxidative phosphorylation, TCA cycle, retrograde response, antioxidant protection and mitochondrial fusion. Colour of the squares on the heat map corresponds to the mean value of the log fold change from three biological and three technical replicates. UBC6 was used for normalization.

Since it is known that first three steps of the TCA cycle (involving *aco1*, *cit1*, *idh1* and *idh2*) switch from the control of the HAP genes to RTG genes under conditions of mitochondrial stress (Liu and Butow, 1999), the phenotypic changes in the strain with deleted *hap4* gene were investigated in order to confirm activation of retrograde response as the one responsible for hyper efficient transcript maturation. Deleting *hap4*, the transcriptional activator of nuclearly encoded components of the respiratory chain (as well as the TCA cycle enzymes under normal conditions) has the same effect (Figure 33 A, B, C, D), demonstrating that a nuclear response is critical for the mitochondrial phenotype to emerge. Mitochondria assume a regular tubular shape of reduced volume that is comparable to the mitochondria in the control strain (Figure 34). Consistent with prior observations, no change in TCA cycle genes was observed following *hap4* deletion (Figure 35) which indicate that an intact retrograde response, including both metabolic changes and upregulation of respiratory chain components, is necessary to generate the mitochondrial phenotype observed in the *I_o* strain.

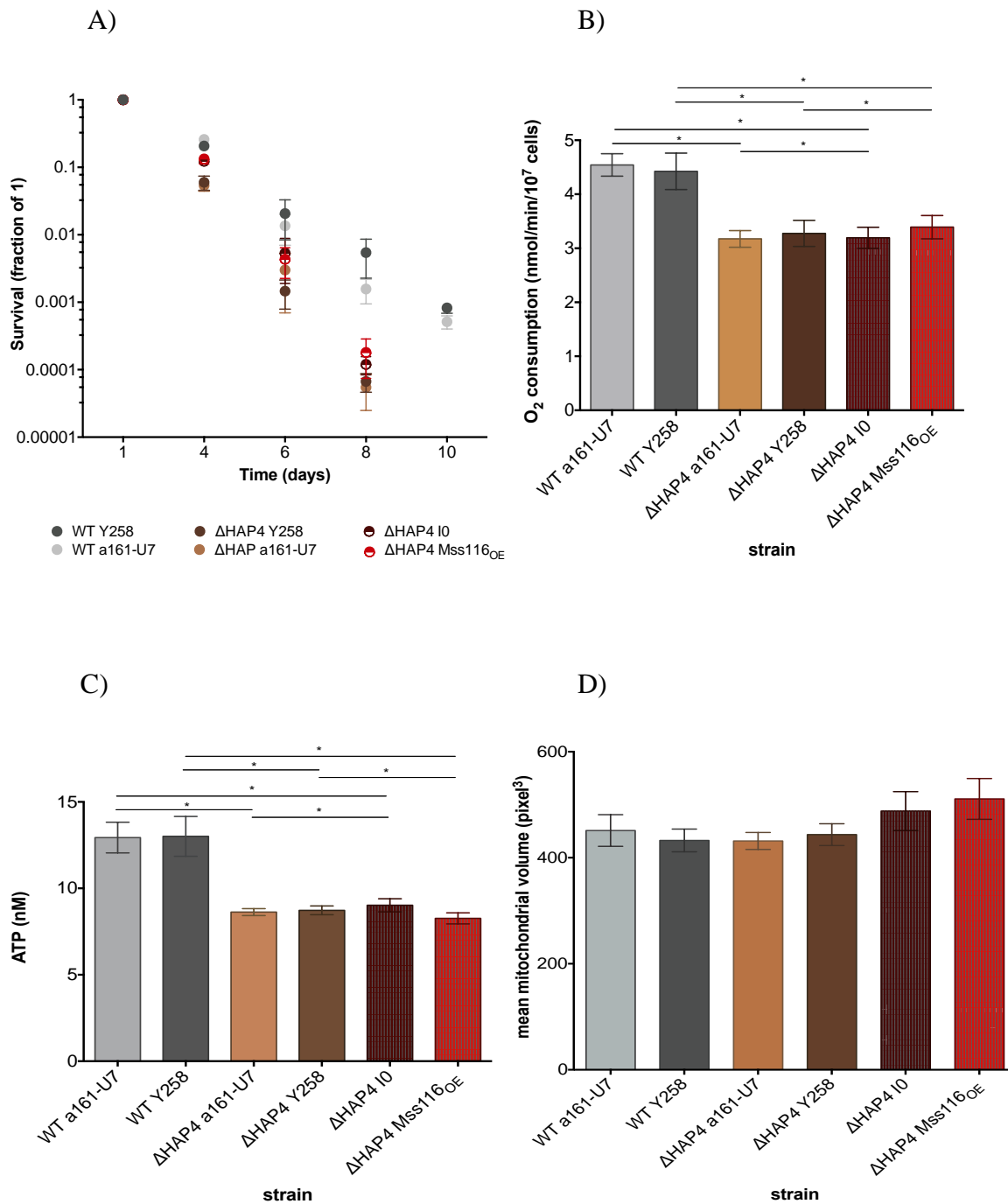


Figure 33. Phenotypic characteristics of Δ HAP4 mutants. A) Chronological lifespan display no significant differences between tested Δ HAP4 strains. B) Oxygen consumption rates of Δ HAP4 mutants demonstrate same values. C) ATP levels remain similar at each tested Δ HAP4 strain. D) Mitochondrial volume shows no significant differences between tested Δ HAP4 strains and their wild types. Data are mean \pm SD from at least three independent cultures, each performed in triplicate. *** $P < 0.001$; ** $P < 0.01$; * $P < 0.05$ (ANOVA plus post hoc).

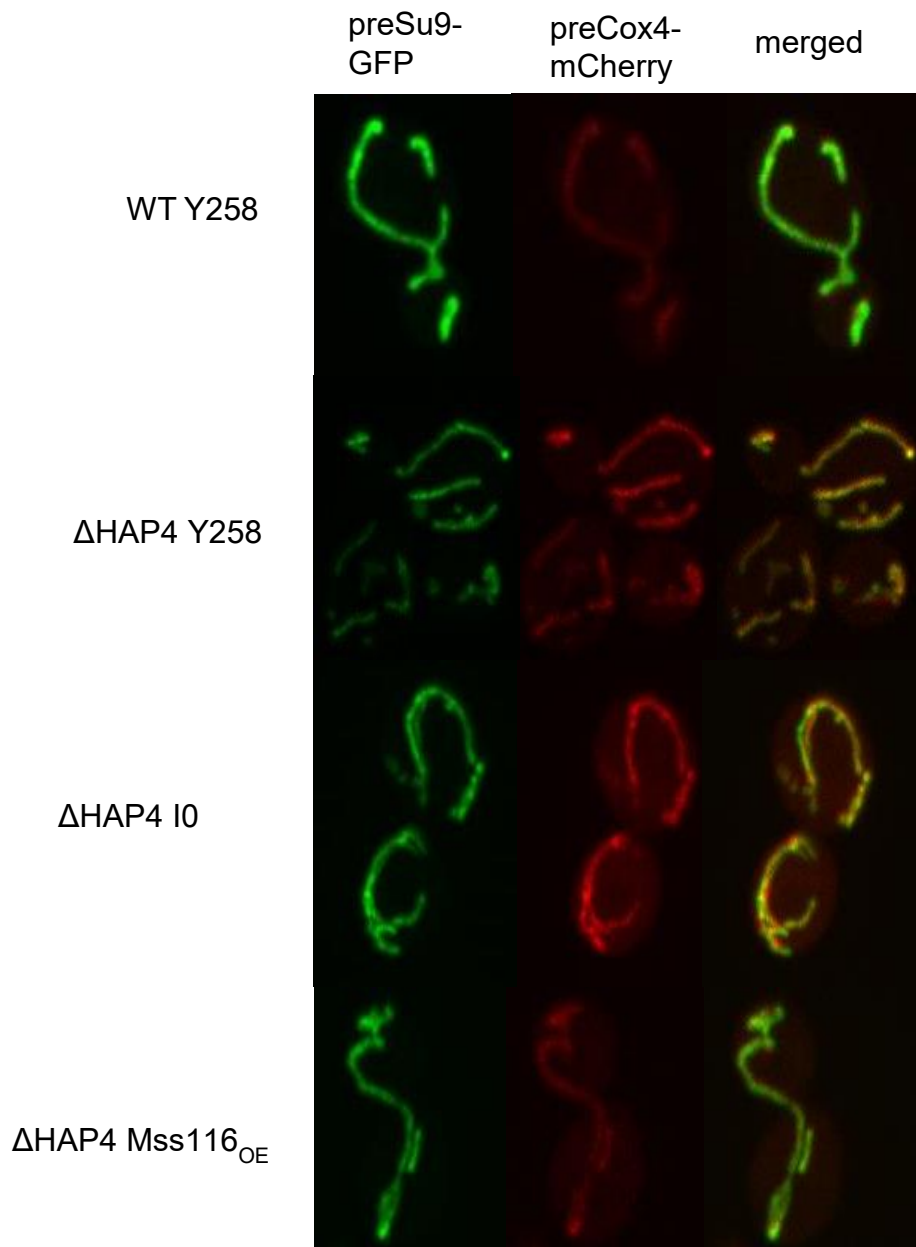


Figure 34. Representative images of cells with visualized mitochondria via preCOX4-mCherry and preSU9-GFP. The absence of Hap4 transcription factor reverses the increased mitochondrial volume in the I₀ and Mss16_{OE} strains. This image was taken in the collaborator lab of Dr. Ira Milošević group, European Neuroscience Institute, Gottingen, and supervised by Dr. Anita Kriško.

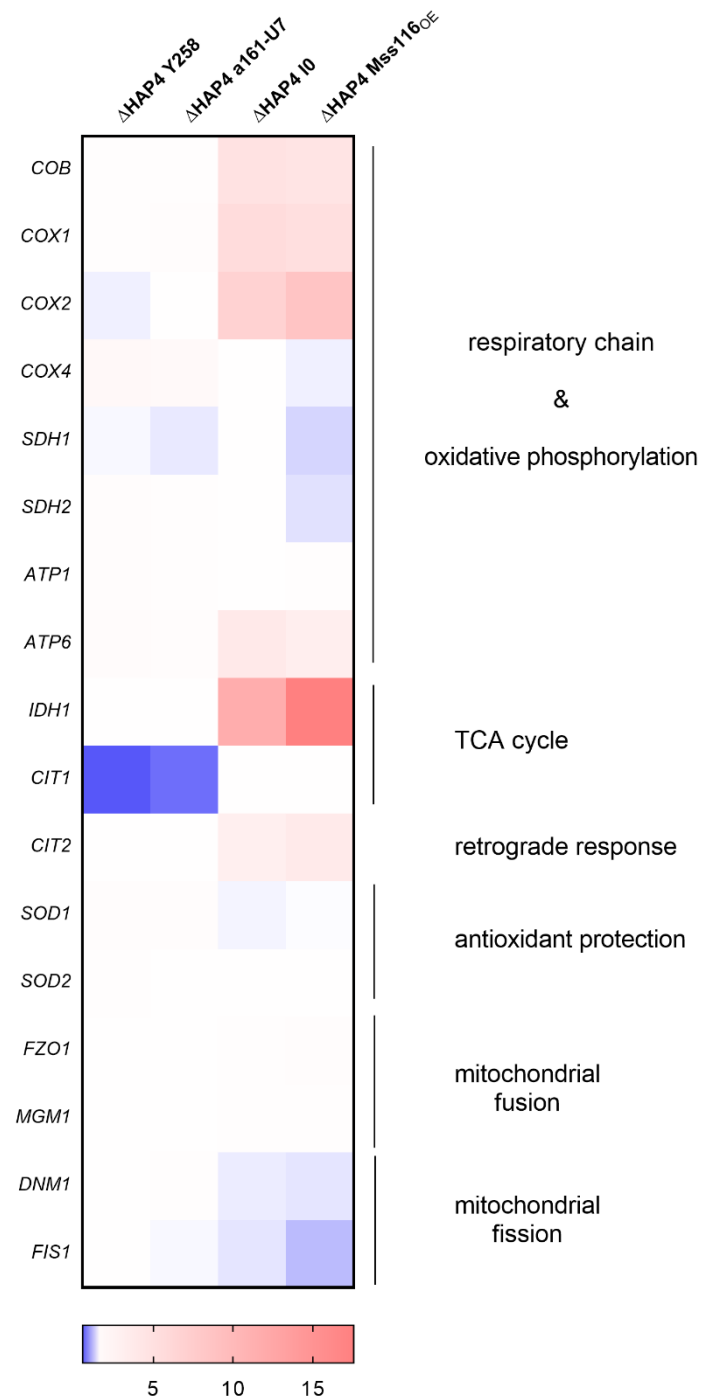


Figure 35. Transcript levels of target genes in Δ HAP4I₀ and Δ HAP4Mss116 mutants demonstrate no changes compared to the I₀ and Mss116^{OE} strain (up-regulation of TCA cycle and retrograde response). Colour of the squares on the heat map corresponds to the mean value of the log fold change from three biological and three technical replicates. UBC6 was used for normalization.

Why does the deletion of self-splicing introns lead to increased abundance of their host transcripts? One possibility is that, by deleting intronic sequence, regulatory elements that influence host gene expression were inadvertently removed. Regulatory elements here might be motifs that act in *cis* at the DNA or RNA level but also intron-encoded proteins. Both group I and group II introns self-splice *in vitro*, but auxiliary proteins are required for efficient and accurate splicing *in vivo* (Halls et al., 2007). Some of these proteins, termed maturases, are encoded in the nucleus and imported into the mitochondria. Yet others are encoded by the introns themselves and specifically act on them, for example by stabilizing salient RNA folding intermediates. By removing the introns and therefore the proteins they encode, did regulatory functions of these proteins that go beyond their core involvement in splicing was unwittingly abolished? Alternatively, rather than removing specific regulatory elements, might the act of short-circuiting the splicing process by itself interfere with normal expression? Specifically, the normal levels of transcription might be tuned to accommodate a certain proportion of mis-spliced transcripts, which are spotted by mitochondrial quality control and ultimately degraded. In *I₀*, splicing does not occur so that erroneous splicing products do not arise. As a result, production of functional *cox1/cob* mRNAs might overshoot its target and trigger a system-wide response, for example because altered COX1/COB levels upset dosage balance amongst respiratory complexes.

4.2.3. Overexpression of Mss116 RNA helicase phenocopies *I₀* strain

To test this hyper-efficient maturation hypothesis and to rule out that the removal of regulatory elements is causing mitochondrial stress, splicing efficiency was altered by orthogonal means. First, the nuclearly encoded mitochondrial DEAD box RNA helicase Mss116, which promotes splicing of all *S. cerevisiae* mitochondrial introns by remodeling or stabilizing particular RNA structures in an ATP-dependent manner, was overexpressed. Next, overexpression and mitochondrial localization of Mss116 was confirmed by flow cytometry/mass spectrometry and immunocytochemistry, respectively, using an N-terminal His-tagged version of the protein (Figure 36). Then phenotypic effects of Mss116 overexpression were characterized using an untagged version of the protein. Remarkably, the Mss116 overexpression strain (*Mss116_{OE}*) phenocopies *I₀*. *Mss116_{OE}* exhibits increased generation times (Figure 24A), extended chronological life span (Figure 24B), mitochondrial fusion (Figure 25. 26.), elevated oxygen consumption (Figure 27B), and altered ATP and ROS production (Figure 27C, D).

Transcriptional and proteomic responses are highly correlated between I_0 and $Mss116_{OE}$ (Figure 24-29). In addition, longer replicative lifespan (RLS) in $Mss116_{OE}$ was observed (Figure 37.), a more direct proxy of ageing. The RLS was not possible to measure accurately in I_0 , where separating mother and daughter cells in a timely fashion proved challenging for unknown reasons. In order to confirm role of Mss116 helicase activity in this phenotypic effects, a DEAD box mutant of Mss116 ($Mss116^{E268K}$), which lacks ATPase and therefore helicase activity was overexpressed. Results showed that it does not phenocopy I_0 (Figure 24-29). This suggests that the role of Mss116 in splicing – which relies on helicase activity – is critical rather than a recently suggested ATP-independent role in transcription elongation (Markov et al., 2014).

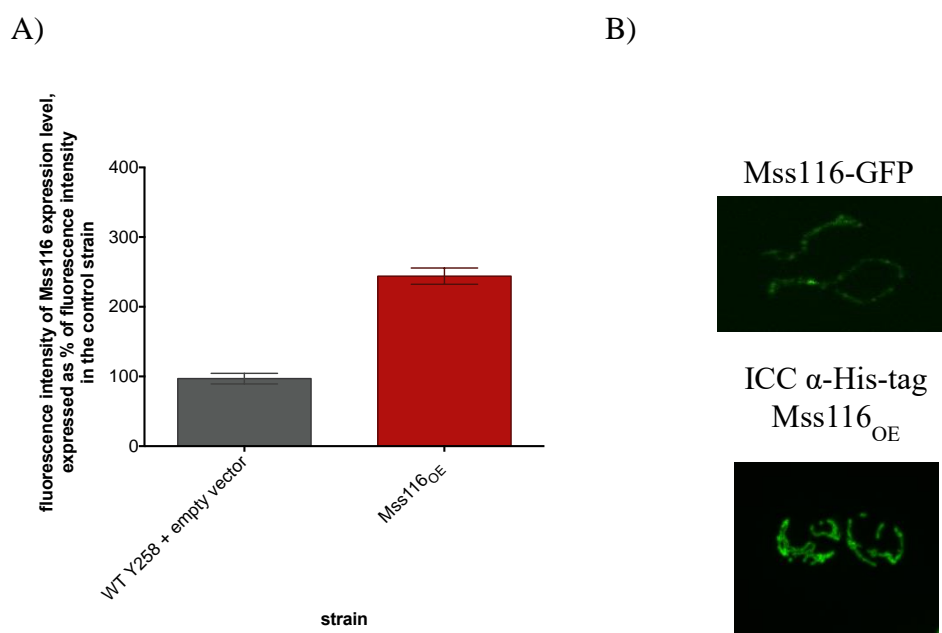


Figure 36. Mss116 is overexpressed and localized to mitochondria. (A) Expression level of Mss116 is 2.5 fold as measured by flow cytometry. The endogenous expression of Mss116 is monitored using its genomic fusion with GFP. In the case of overexpression, Mss116 was His-tagged and detected using anti-His-tag primary antibody and Alexa488-tagged secondary antibody. (B) Mss116 is localized to mitochondria, both in the WT background and in Mss116 overexpression strain.

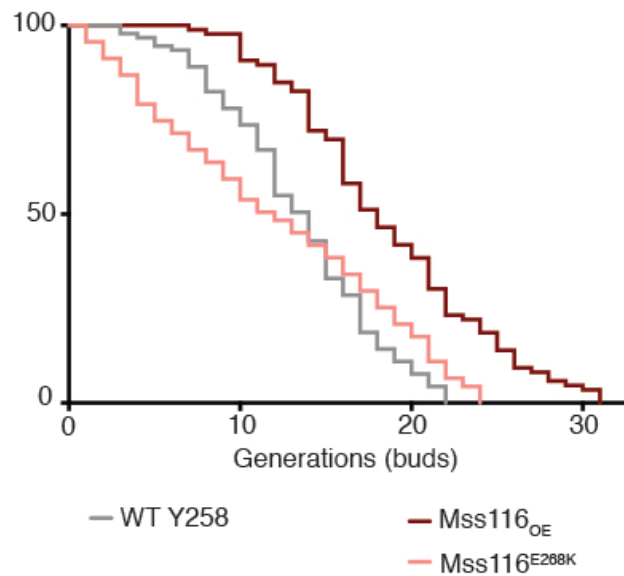


Figure 37. Median and maximal replicative lifespan of Mss116_{OE} is extended compared to the empty vector control and Mss116^{E268K}. The total number of monitored mother cells is as follows: 90 cells for the empty vector control, 86 cells for Mss116_{OE}, and 91 cells for the Mss116^{E268K}. Measurements were pooled across 3 independent experiments.

The fact that *Mss116_{OE}* – which encodes a full complement of introns – phenocopies *I₀* eliminates the hypothesis that lost DNA-level functionality explains the *I₀/Mss116_{OE}* phenotype. However, it does not explicitly rule out the possibility that intron-encoded proteins are involved, since these are absent in *I₀* but might also be reduced in *Mss116_{OE}*. To test this alternative hypothesis a plasmid bearing the sequence of each maturase alone (aI1, aI3, aI5 β , bI2, bI3) was inserted into the *I₀* strain (Figure 38). Each maturase was tagged with an N-terminal mitochondrial localization sequence. As a phenotypic read-out, mitochondrial morphology as well as metabolic changes were monitored. It was found that reintroduction of neither maturase rescues the *I₀* phenotype (Figure 39).

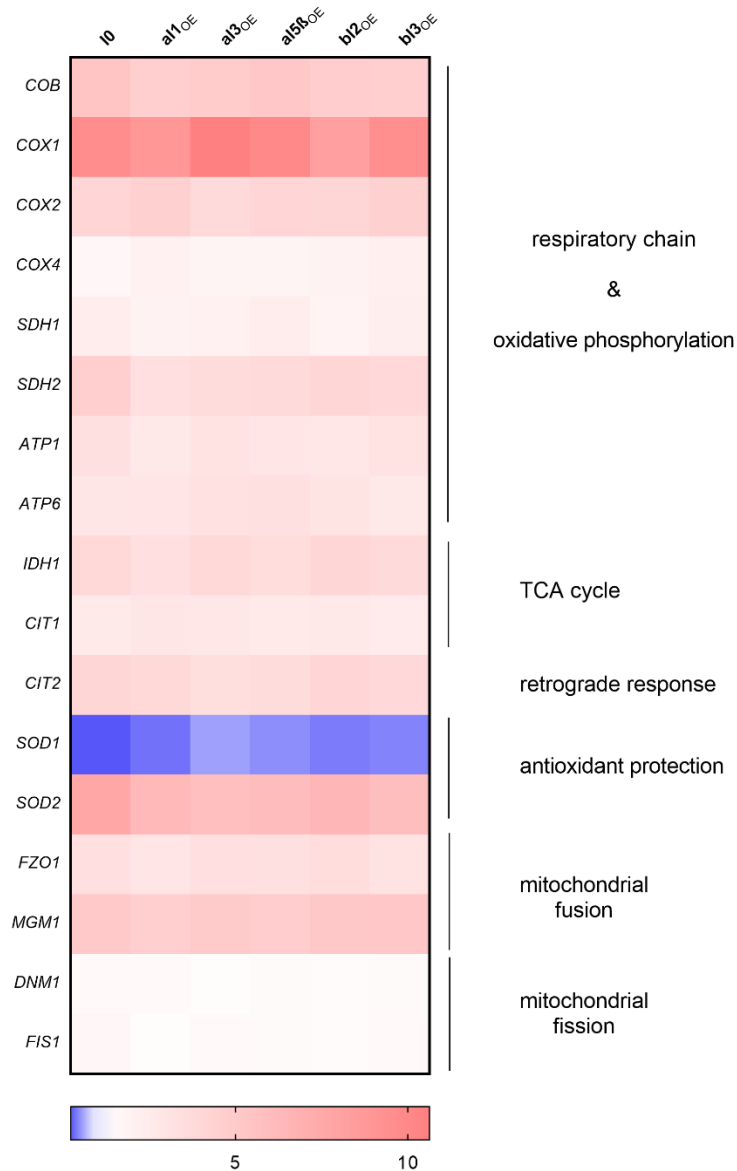
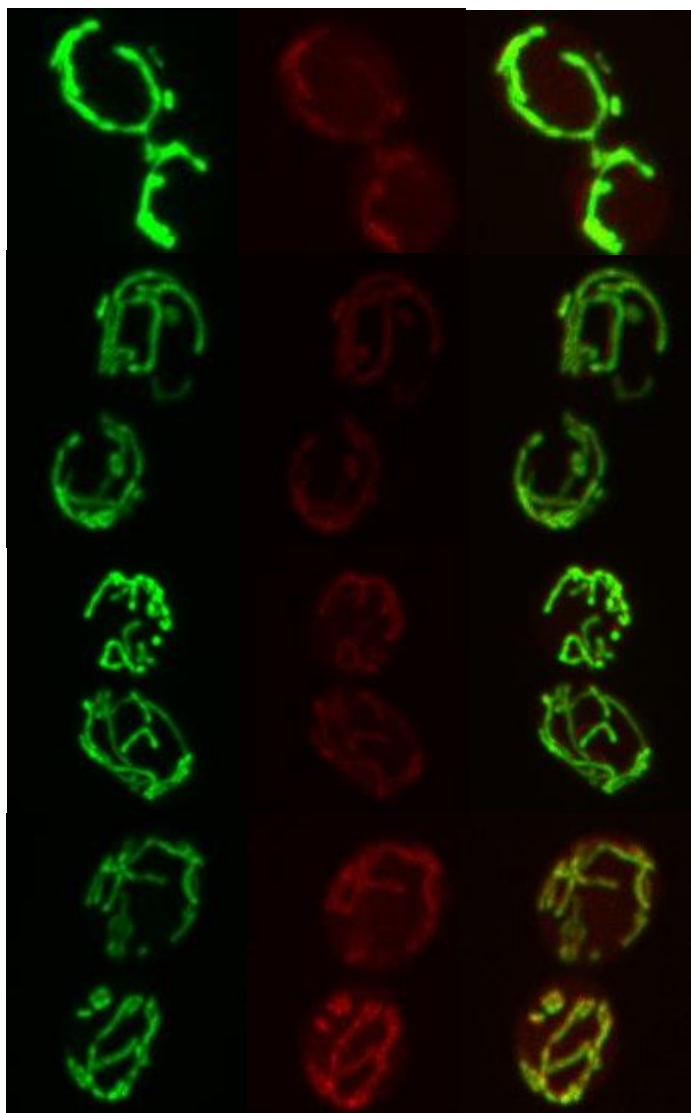


Figure 38. Overexpression of individual intron-encoded maturases does not change transcript levels observed in I_0 strain. Colour of the squares on the heat map corresponds to the mean value of the log fold change from three biological and three technical replicates. UBC6 was used for normalization.

preSu9-GFP preCox4-mCherry merged



WT a161-U7 + pYES2

I0 a1_{OE}

I0 a15_{OE}

I0 b12_{OE}

Figure 39. Representative images of cells with visualized mitochondria via preCOX4-mCherry and preSU9-GFP. Overexpression of intron-encoded maturases does not reverse the hyper-fused mitochondrial phenotype observed in I₀ strain. This image was taken in the collaborator lab of Dr. Ira Milošević group, European Neuroscience Institute, Gottingen, and supervised by Dr. Anita Kriško.

To characterize the effects of Mss116 overexpression on splicing dynamics in greater detail, qPCR was used to measure the levels of total *cox1* and *cob* transcripts as well as individual introns. For *cox1*, exon and intron (a12, a15 β) levels were monitored using RNA fluorescent *in*

situ hybridization (RNA FISH). It was found that most mitochondrial introns are strongly depleted in *Mss116_{OE}* compared to the empty vector control and relative to exons (Figure 40). The relative depletion of individual introns, however, is variable and one intron *aI5 α* is equally abundant in *Mss116_{OE}* and WT (Figure 40a). These observations are consistent with a model where initial pre mRNA abundance (and therefore nascent transcriptional output) is unchanged in *Mss116_{OE}* compared to WT and differential steady state levels are the result of post transcriptional events, with individual intron abundances determined by differential modulation of splicing kinetics in response to *Mss116* overexpression. Based on these findings, it was suggested that *Mss116_{OE}* phenocopies *I₀* because eliminating introns at the DNA level (*I₀*) and facilitating accurate and efficient excision at the RNA level (*Mss116_{OE}*) both result in abnormally efficient transcript maturation. That is, fewer transcripts are eliminated by mitochondrial quality control because splicing is erroneous or does not proceed in a timely manner, resulting in a greater number of mature *cox1/cob* mRNAs. For reasons that remain to be elucidated, increased transcript levels are then perceived as stressful and trigger the retrograde response, culminating in a multifaceted stress phenotype. In this regard it was speculated that elevated COB (COX1) levels might interfere with proper assembly and function of complex III (complex IV) and therefore constitute a deleterious dosage imbalance phenotype. That disruption of splicing homeostasis can impact normal physiological function and lead to cellular stress and disease is now well documented (Wang and Cooper, 2007). There is also increasingly detailed mechanistic knowledge of how proteins involved in splicing can alter growth and ageing via a metabolic route, exemplified by the recent finding that splicing factor 1 is a modulator of dietary restriction-induced longevity in *C. elegans* (Heintz et al., 2017). The classic model here is that loss of splicing homeostasis – through genetic, developmental, or environmental perturbation – leads to deleterious shifts in splice isoform production or precipitates increased production of erroneous transcripts that tax the quality control system and/or have direct cytotoxic effects. In other words, the disease/stress state is a high-error state. Results presented here are unusual since they demonstrate that normal splicing can be associated with high error rates and that, therefore, splicing homeostasis can also be disturbed by increasing splicing efficacy.

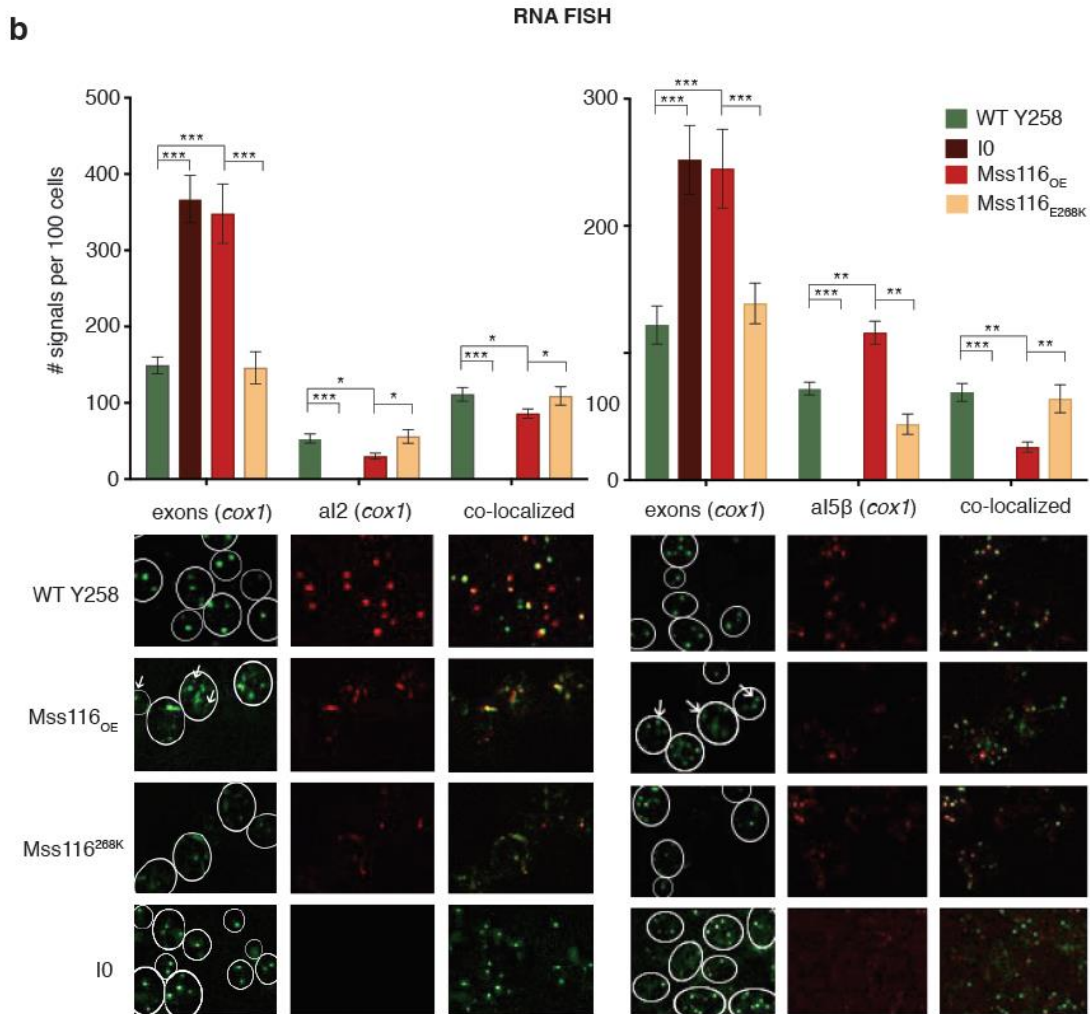
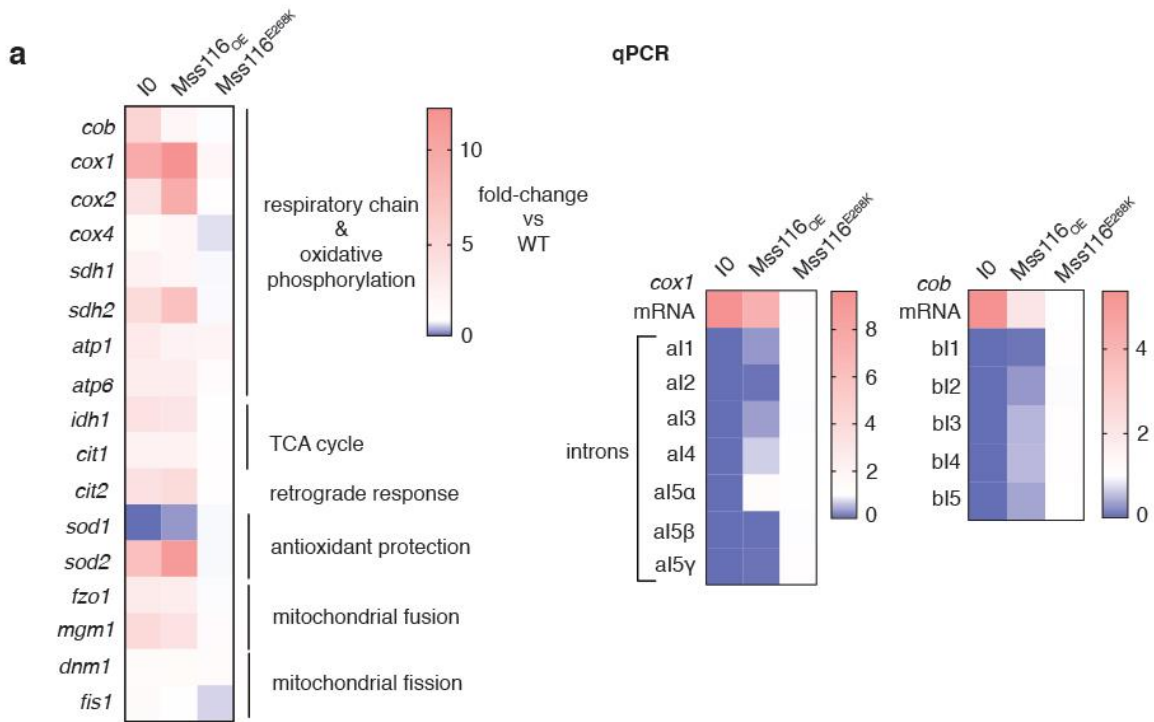


Figure 40. Transcriptional changes associated with intron removal.

Figure 40. (continued) Transcriptional changes associated with intron removal.

qPCR measurements showing upregulation of respiratory chain and oxidative phosphorylation complexes and key members of the TCA cycle, activation of the retrograde response and mitochondrial fusion (left panel). In both *cox1* (central panel) and *cob* (right panel), intron levels are specifically reduced upon overexpression of *Mss116_{OE}* but not *Mss116^{E268K}*. The colour of the squares on the heat maps corresponds to the mean value of the log fold change from three biological (each averaged over three technical replicates). UBC6 was used for normalization. (b) FISH based RNA detection (RNA-FISH) confirms the reduction of introns aI2 and aI5 β from the *cox1* transcript pool. The quantification was performed using ImageJ; green, red and green/red co-localized puncta were counted in more than 300 cells. The plot represents % of signals per 100 cells. Bar heights display the mean of three biological replicates (each averaged over three technical replicates). Error bars are standard error of the mean. ***P < 0.001; **P < 0.01; *P < 0.05 (ANOVA plus post hoc). White lines mark cell boundaries. White arrows mark examples of exonic puncta that do not co-localize with intronic puncta.

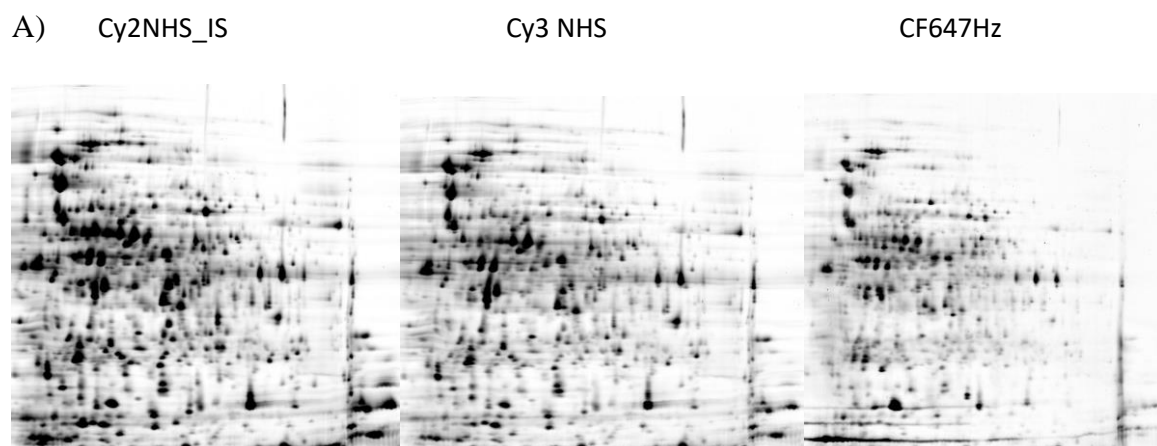
4.3. Long-term accumulation of gene polymorphisms and their effect on protein oxidability in *E.coli*

4.3.1. Elucidating correlation between *E.coli* genomic mutations and level of proteome carbonylation (preliminary results)

The data presented in this part of thesis is considering mutation accumulation to be correlated with the change in protein carbonylation (increase or decrease). Depending on the proteins whose genes are affected with mutations, the result of total carbonylation should be different. Some of possible scenarios are: a) mutation in a protein that is a part of the ribosom leading to impaired protein synthesis will result with higher level of total protein carbonylation, b)

mutation in proteins that have a role in folding and refolding of other proteins will lead to carbonylation change of their clients, c) mutation in individual protein is cause of increase or decrease of carbonylation level of that specific protein. Some mutations lead to conformational changes of a protein and could also render it more sensitive or robust to oxidation.

To answer the question if gene polymorphisms are reflected in the polymorphisms of protein oxidability, *E.coli* strains from “Long term evolution experiment” (Sniegowski et al., 1997) were chosen to work with. Those were: the ancestor REL606, the evolved mutator 10953 and the non-mutator strains 10956 sampled from the same lineage after 40,000 generations. Hypothesis in this part of my research was that accumulated mutations in the mutator strain lead to higher levels of carbonylation compared do the ancestor and the non-mutator, due to increased sensitivity of a protein to oxidation. In order to identify proteins with higher carbonylation in the mutator strain, they were separated using 2D-DIGE and compared the resulting protein spot pattern with the one of the ancestor and the non-mutator strain. After protein extraction, all samples were tagged with two fluorescent probes: Cy3NHS specific for labelling amino groups (including N-terminus), thus enabling visualization of protein expression; and hydrazide (CF647 Hz) specific for labelling carbonyl groups. Signal intensity of the hydrazide CF647 Hz dye correlates with the quantity of protein carbonyls, and is normalized to their expression level (Figure 41A; 42A). In addition, samples of each strain were pooled together into an additional sample named internal standard (IS) and labelled with Cy2NHS fluorescent dye to serve as a control for protein expression across all samples (Figure 41A; 42A). Overlap of protein expression signal and the one of carbonylation is shown in Figure 41B and 42B for non-mutator and mutator strains, respectively.



B)

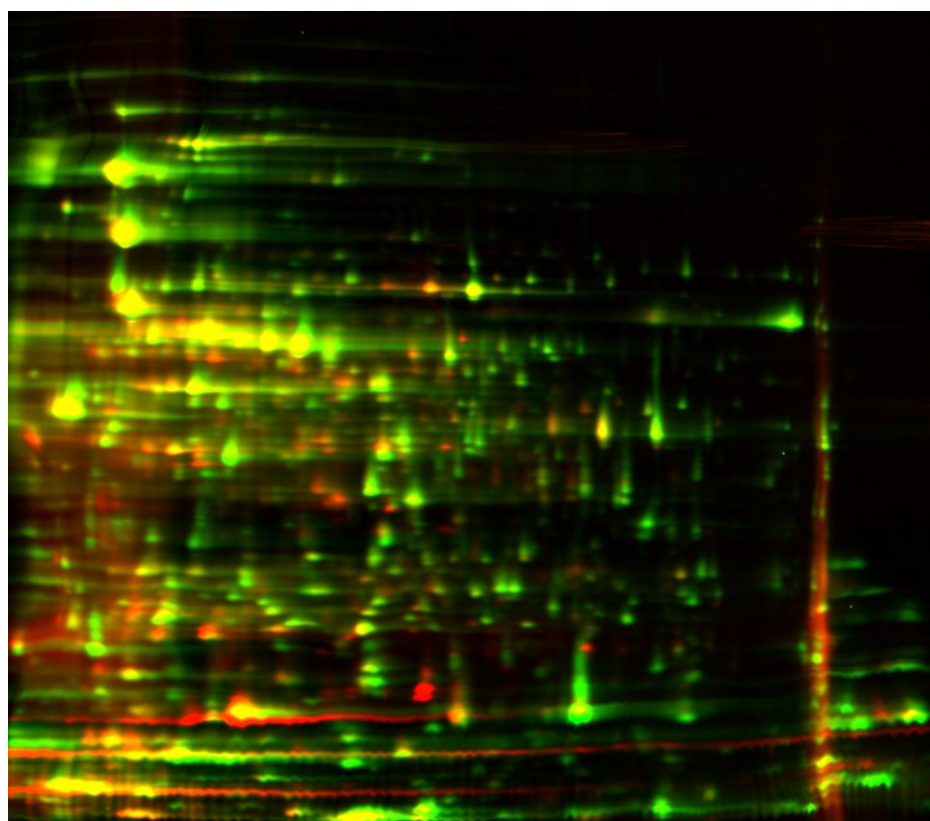


Figure 41. 2D Oxi-DIGE, non-mutator strain.

A) Protein extract labelled with Cy2NHS for internal standard, Cy3NHS for detection of protein expression levels and CF647Hz for labeling carbonylated groups. B) Cy3NHS (green signal) and CF647Hz (red signal) overlap.

4.3.2. Identification of proteins with increased/decreased carbonylation levels in mutator strain compared with ancestor and non-mutator

More than 1200 individual protein spots from mutator strain were separated by 2D-DIGE according to their isoelectric point and molecular weight. In total, 64 proteins that showed 1.5-fold change in expression or carbonylation (Figure 43), with $p \leq 0.05$ (t-test) in mutator compared with ancestor and non-mutator, were identified by mass spectrometry. Spots were sent for mass spectrometry identification in 3P5 proteomic facility, Université Paris Descartes, Institut Cochin.

All proteins identified with higher or lower carbonylation are listed in Table 9 and Table 10, respectively. There were 39 highly carbonylated proteins detected, 10 of which carrying mutation in their genes (5 synonymous, 4 non synonymous and 1 intergenic); 25 proteins with lower levels of carbonylation, 6 of which carrying mutation in their genes (2 synonymous, 3 non synonymous and 1 intergenic) (Table 9 and Table 10).

Approximately 1200 proteins in *E.coli* 40k strain were detected in the above described results and in 64 of those proteins >1.5 fold change in protein carbonylation was observed. Out of 39 proteins with increased carbonylation, 26% were also mutated in its coded genes and out of 25 proteins with decreased carbonylation, 24% had mutation(s) in their respective genes.

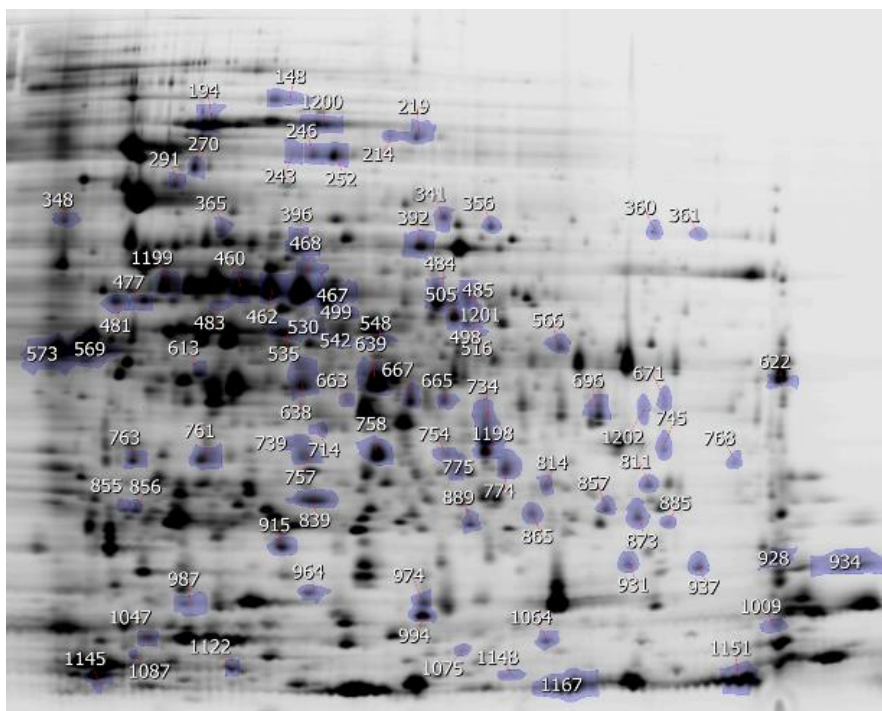


Figure 43. Spots on 2D-DIGE gel that were picked and analysed by mass spectrometry.

Table 9. Identified proteins with higher carbonylation in mutator strain, compared to ancestor and non-mutator. * stands for synonymous mutation; ** non-synonymous mutation; *** intergenic. Empty cells indicate that no significant change in the protein carbonylation level was found.

| Protein name | Mutated gene | Mutator Hz / Ancestor Hz | | Mutator Hz / Non-Mutator Hz | |
|---|--------------|--------------------------|--------------------|-----------------------------|---------|
| | | Fold change | P value | Fold change | P value |
| Elongation factor G | | 19,210 | 0,017 | | |
| Polyribonucleotide nucleotidyltransferase | pnp * | 81,537 | 0,005 | 16,277 | 0,0067 |
| Formate acetyltransferase 1 | | 8,899 | 0,007 | 2,439 | 0,0599 |
| Transketolase 1 | | 16,015 | 0,015 | | |
| Proline-tRNA ligase | | 87,646 | 0,051 | 14,792 | 0,0611 |
| Chaperone protein HscA | hscA** | 2,257 | 0,031 | 3,261 | 0,0091 |
| NAD-dependent malic enzyme | | 12,201 | 0,039 | 16,376 | 0,0366 |
| Dihydropolyllysine-residue succinyltransferase component of 2-oxoglutarate dehydrogenase complex | sucB** | 8,335 | 3*10 ⁻⁸ | 5,519 | 0,00001 |
| Paraquat-inducible protein B | pqiB ** | 6,113 | 0,006 | 2,5073 | 0,0684 |
| ATP synthase subunit alpha | | 2,060 | 0,031 | 2,288 | 0,0213 |
| Enolase | | 5,405 | 0,018 | 5,587 | 0,0189 |
| Isocitrate lyase | | 2,863 | 0,018 | 5,832 | 0,0069 |
| UDP-N-acetylglucosamine 1-carboxyvinyltransferase | lpxD** | 6,378 | 0,011 | 6,284 | 0,0112 |
| 3-oxoacyl-[acyl-carrier-protein] synthase 2 | | 6,378 | 0,011 | 6,284 | 0,0112 |

| | | | | | |
|---|---------|--------|-------------|--------|--------------------|
| Glutamate-1-semialdehyde 2,1-aminomutase | | 3,892 | 0,004 | 5,510 | 0,0022 |
| Ribosome-binding ATPase YchF | | 4,380 | 0,016 | 11,373 | 0,0079 |
| 6-phosphogluconate dehydrogenase, decarboxylating | gnd* | 29,573 | 0,001 | 73,508 | 0,0011 |
| Acetate kinase | ackA* | 7,616 | 0,048 | | |
| Succinyl-CoA ligase [ADP- forming] subunit beta | | 2,190 | 0,041 | 3,261 | 0,016 |
| Protease 7 | | 3,651 | 0,003 | 3,284 | 0,004 |
| Acetate kinase | | 11,264 | 0,027 | 8,462 | 0,030 |
| Outer membrane protein F | ompF*** | 10,676 | 0,007 | 7,062 | 0,009 |
| tRNA-modifying protein YgfZ | | 3,624 | 0,005 | 8,152 | 0,002 |
| Acetyl-coenzyme A carboxylase carboxyl transferase subunit beta | | 18,500 | 0,008 | 25,134 | 0,008 |
| Acetyl-coenzyme A carboxylase carboxyl transferase subunit alpha | | 13,702 | 0,0009 | 6,928 | 0,001 |
| 2-dehydro-3- deoxyphosphooctonate aldolase | | 2,382 | 0,030 | 3,172 | 0,016 |
| 30S ribosomal protein S2 | | 4,408 | 0,013 | 2,016 | 0,099 |
| Outer membrane protein A | | 5,713 | 0,003 | 6,402 | 0,0033 |
| Histidine-binding periplasmic protein | | 5,878 | 0,026 | 6,475 | 0,024 |
| Sugar phosphatase YidA | | 5,878 | 0,026 | 6,475 | 0,024 |
| Elongation factor P-like protein | | 5,878 | 0,026 | 6,475 | 0,024 |
| D-ribose-binding periplasmic protein | | 18,547 | 0,0000 3 | 12,463 | 3*10 ⁻⁵ |

| | | | | | |
|---|-------|--------|--------|--------|--------|
| Fatty acid metabolism regulator protein | | 20,537 | 0,0006 | 21,962 | 0,0006 |
| Purine nucleoside phosphorylase DeoD-type | | 2,912 | 0,023 | 7,091 | 0,006 |
| FKBP-type 22 kDa peptidyl-prolyl cis-trans isomerase | | 9,475 | 0,002 | 5,982 | 0,0041 |
| 3-oxoacyl-[acyl-carrier-protein] reductase FabG | fabG* | 5,691 | 0,0001 | 6,1204 | 0,0001 |
| Single-stranded DNA-binding protein | | 2,158 | 0,008 | 4,541 | 0,0017 |
| Outer membrane lipoprotein SlyB | | | | 19,261 | 0,0157 |
| Cell division protein FtsA | | 8,530 | 0,0156 | 4,325 | 0,0281 |

Table 10. Identified proteins with lower carbonylation in mutator strain, compared to ancestor and non-mutator. * stands for synonymous mutation; ** non-synonymous mutation; *** intergenic. Empty cells indicate that no significant change in the protein carbonylation level was found.

| Protein name | Mutated gene | Mutator Hz / Ancestor Hz | | Mutator Hz / Non-Mutator Hz | |
|--|---------------------|---------------------------------|---------|------------------------------------|---------|
| | | Fold change | P value | Fold change | P value |
| Pyruvate kinase I | pykF* | | | -4,7352 | 0,0327 |
| Periplasmic oligopeptide-binding protein | oppA** | -6,891 | 0,0062 | -72,437 | 0,0074 |
| Acetate kinase | | | | -1,1055 | 0,8458 |
| Outer membrane protein C | | | | -9,5079 | 0,0232 |
| Outer membrane protein A | | -222,42 | 0,0238 | -117,45 | 0,0300 |
| D-tagatose-1,6-bisphosphate aldolase subunit GatY | | -7,538 | 0,0006 | -41,682 | 0,0010 |

| | | | | | |
|---|---------|---------|----------------------|---------|---------|
| FKBP-type peptidyl-prolyl cis-trans isomerase SlyD | | -5,821 | 0,0002 | -5,5637 | 0,0045 |
| Uridine phosphorylase | | -3,117 | 0,03511 | -5,8525 | 0,0083 |
| Succinate dehydrogenase iron-sulfur subunit | sdhB** | -3,235 | 0,0053 | -4,5233 | 0,0538 |
| Molybdate-binding periplasmic protein | modA** | -2,863 | 0,0008 | -7,0947 | 0,0036 |
| FKBP-type 22 kDa peptidyl-prolyl cis-trans isomerase | | | | -12,252 | 0,0577 |
| 3-oxoacyl-[acyl-carrier-protein] reductase FabG | | -6,556 | 0,0015 | -12,276 | 0,0142 |
| Osmotically-inducible protein Y | | -4,6683 | 0,0012 | -5,1027 | 0,04850 |
| 30S ribosomal protein S5 | | -9,339 | 0,0094 | | |
| Single-stranded DNA-binding protein | | -78,636 | 0,0017 | -50,514 | 0,0001 |
| DNA protection during starvation protein | | -6,498 | 0,0001 | -1,7803 | 0,2500 |
| Outer membrane lipoprotein SlyB | | -6,0991 | 0,04159 | | |
| Iron-binding protein IscA | | -17,925 | 0,0055 | -2,9647 | 0,0254 |
| Cold shock-like protein CspE | | -158,22 | 0,0054 | -151,31 | 0,0084 |
| Cold shock-like protein CspB | | -12,919 | 1,6*10 ⁻⁵ | -24,019 | 0,0001 |
| 50S ribosomal protein L7/L12 | | -86,730 | 0,04874 | -37,862 | 0,0003 |
| D-ribose-binding periplasmic protein | | -15,779 | 0,0049 | -423,89 | 0,0024 |
| UDP-3-O-(3-hydroxymyristoyl) glucosamine N-acyltransferase | lpxD* | -2,133 | 0,0032 | -3,6382 | 0,0223 |
| Glucose-1-phosphate thymidyltransferase 1 | | -3,606 | 0,00039 | -4,1841 | 0,0001 |
| D-tagatose-1,6-bisphosphate aldolase subunit GatY | gatY*** | -7,538 | 0,00064 | -41,682 | 0,001 |

Proteins that displayed an increase in their carbonylation levels in the mutator relative to ancestor and non-mutator and do not carry mutation in their genes were also identified, however they do carry mutations in polypeptides reported to interact with them transiently or permanently. One such example is ATP synthase. ATP synthase is the main enzyme in oxidative phosphorylation consisting of two regions: F_0 (a, b and c subunits) and F_1 (α , β , γ , δ and ϵ subunits), all shown in Figure 44. Mutator strain from LTEE carries intergenic mutation between *atpG* (28 bp distance), coding for ATP synthase gamma chain and the *atpA* (23 bp distance), coding for ATP synthase subunit alpha, which has a 2-fold increase in carbonylation level compared with the one in ancestor. Another mutation is found in the F_1 region, *atpB* gene (non-synonymous mutation L28P), coding for ATP synthase subunit a, which plays a direct role in the translocation of protons across the membrane. Since both, F_1 and F_0 complexes are rotary motors and its subunits are in constant interactions, it is likely to expect that mutation in gene coding for one subunit of the protein will result with eventually conformational changes in the interaction partners. This is likely to render it more susceptible to oxidative damage, manifested as increased level of carbonylation.

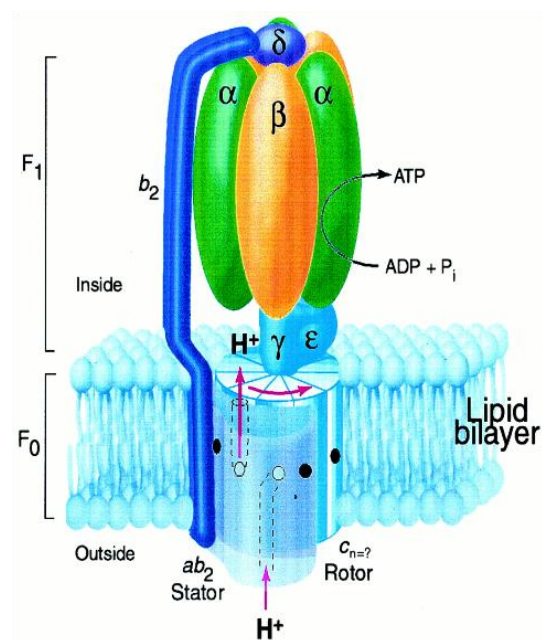


Figure 44. Rotary model of ATP synthase based on the subunit composition of the *E. coli* enzyme. Adopted from Jiang et al., (2001).

5. DISCUSSION

Proteins that are misfolded or have compromised stability due to certain mutations can be buffered by molecular chaperones, so that harmful effects of mutations are masked. The aim of this research was to test whether RNA chaperones play a similar role in buffering mutations.

Results of this study showed that DEAD box RNA helicases can improve fitness of mutator *E.coli* bacteria whose relative fitness was impaired compared to the control strains. This phenomenon was confirmed with another RNA chaperone, cold shock protein A, responsible for stabilization of mRNAs. By performing competition experiments and calculating relative fitness it was demonstrated that buffering by RNA chaperones occurs at the organismal level where helicase and nucleic acid-binding activity are required for buffering by DBRHs and CspA, respectively.

In order to understand the molecular basis of mutation buffering and its relationship with phenotype, it is crucial to first understand how different chaperones interact with different RNAs. In this work it is established that buffering by RNA chaperones is done at the organismal level, that DHRHs and CspA require helicase activity and nucleic acid binding activity, respectively, to perform buffering. Further, *lamB* and *rplS* are identified as mutations especially responsive to buffering, and as such they could be valuable to further research of this phenomenon. Correlation of base pairing probabilities, among other metrics for quantifying mutational impact on RNA secondary structure, suggest severe impact of *rplS^{syn}*, thus implicating this mutation as a possible cause of fitness loss. Similarly, *lamB* was predicted to have the most severe effects on the local RNA structure of all the mutations in the evolved *ΔmutH* strain, as indicated by the maximum local base pair distance (d_{\max}). However, these measurements can only tell us about the mutation impact on RNA structure; whether the resulting defects can be rescued by chaperones, or whether these defects have any impact on the organismal level, is beyond the scope of this measurement. In order to quantify the reliability of any structural predictor one would have to study a far larger set of characterized mutations which are both deleterious and amenable to buffering.

RNA chaperone activity might be beneficial through stabilizing, destabilizing, or remodelling affected structures in the transcript or by affecting the way these transcripts interact with other transcripts and/or RNA-binding proteins (Pan and Russell, 2010).

In the case of *lamB*, it is possible that local increase in stability caused by the mutation causes a temporary block in translation which is resolved by RNA chaperones.

A more complex scenario is also possible, one in which the non-synonymous *lamB* mutation results in a dominant negative protein product, in which case the mutation is buffered by the overexpressed RNA chaperone facilitation degradation of the mutant LamB protein mRNA, thereby ameliorating fitness defects. In order to distinguish between these scenarios, this study should be followed up by thorough and targeted experiments, such as measuring levels of LamB, which is predicted to decrease in upon chaperone overexpression. However, there are still issues that need to be considered. First, it should be established if the RNA buffering is direct or indirect i.e. is it a result of interaction between RNA chaperons and the RNA itself or the RNA chaperones mediate buffering through interactions with cell components other than the RNA. Some mutations could be a buffering target by both protein and RNA chaperones. One possible example would be a protein helping rescue a misfolded protein while an RNA chaperone removes the translational roadblocks responsible for misfolding. Therefore, clarifying the contributions of both protein and RNA chaperones to mutation buffering will be of great interest in future research.

In addition, RNA structure can be affected by both synonymous and non-synonymous mutations through, in case of non-synonymous mutations, changes arising in the sequence, even if the amino acid change is selectively neutral, or through changes in translation kinetics and folding, affecting fitness at protein level, in case of synonymous mutations (Plotkin and Kudla, 2011). Therefore, whether the mutation is synonymous or non-synonymous cannot be used as a reliable factor based on which mutations can be classified as candidates for buffering by RNA chaperones.

Lastly, similar to protein chaperones, RNA chaperones are likely to act through a range of mechanisms. Therefore, another challenge in the future will be identifying the general principles of the RNA chaperone mutational mediated buffering. Findings presented here should be taken as a stepping stone to continue the investigation and meet this challenge. Recent advances in high throughput probing of RNA secondary structures and RNA-protein interactions have made this challenge a realistic one. Ultimately, we should clarify the consequences of this mechanistically diverse activity of RNA chaperones on not just RNA biogenesis, but also evolution and evolvability.

Further research will be required to tease apart how individual introns affect overall mis-splicing burden. It is evident from population genomic analysis of different *S. cerevisiae* strains that some introns are fixed across extant populations whereas others exhibit presence/absence polymorphism (Wolters et al., 2015). This seems to suggest that the removal of at least some introns is insufficiently stressful to be purged by natural selection. At the same time, studies of *su3*, the second DEAD box RNA helicase present in yeast mitochondria, suggest that the deleterious effect of removing individual introns while possibly idiosyncratic is at least partially cumulative. Deletion of *su3*, a component of the mitochondrial degradosome, decreases levels of mature *cox1/cob* mRNA and compromises respiratory capacity, but less so where more introns had been removed from the mitochondrial DNA (Golik et al., 1995). Importantly at least for the combinations tested – severity was found to depend on the number but not identity of the *cox1* or *cob* introns present.

In addition to providing a deeper insight into post-transcriptional gene regulation in mitochondria, our findings have implications for understanding the evolutionary persistence of self-splicing introns and perhaps mobile elements more generally. The phenotypic effects run counter to the notion that self-splicing introns are low-cost passengers and instead demonstrate that these selfish elements are firmly embedded in the organization of mitochondrial gene expression. Their presence is expected and their forced removal compromises normal expression of their host genes. These observations can be explained by an evolutionary lock-in model where the primordial colonization of an intron-free *cox1/cob* ancestor by a self splicing intron led to a drop in *cox1/cob* mRNA levels and favoured compensatory mutations that increased *cox1/cob* transcription to restore mRNA abundance back to their original levels. When these introns are forcefully removed, however, this hard wired upregulation turns maladaptive. There no longer is a pool of transcripts targeted for degradation leading to excess levels of mature mRNA. Suggested evolutionary lock-ins of this type might provide an unappreciated mechanism to facilitate the longer-term persistence of genetic parasites. This argument might in principle extend to nuclear introns: if, for a given dosage-sensitive gene, mis-splicing is common and transcription levels are set to compensate, intron loss might be deleterious and prevented by purifying selection even though the intron makes no adaptive contribution to gene regulation.

Aim of third part of the thesis was to elucidate the molecular basis of protein sensitivity to oxidative damage, in particular protein carbonylation. The system of *E.coli* bacterial cells with accumulated over 1000 mutations during 40,000 generations of *in vitro* evolution presented us with endless possibilities to observe and study the ones with effects on protein oxidation susceptibility. At the level of total protein carbonylation, increased levels in the mutator strain was observed compared with the ancestor and non-mutator, which strongly suggested a major effect of accumulated mutations on protein oxidability.

Since, these are preliminary results of screening the proteome carbonylation, there are still some open questions that need to be answered. For example, what is the percentage of mutated genes that are also expressed and detectable using this method? What is the contribution of mutations in individual proteins crucial for the maintaining the cell compared to proteome enrichment for carbonylation.

Until now, only mutations in coding regions were related to carbonylation status of proteins. Indirect effects of genetic polymorphisms on protein carbonylation was also observed, such as ATP synthase with mutation in F_O region, one intergenic mutation, and carbonylated subunit in F₁ region. Elucidation of this interplay between mutation and carbonylation of different subunits and/or proteins would require analyse of interaction partners, where this effect is observed.

In order to elucidate impact of the mutations on protein susceptibility to oxidation, it is necessary to determine how many of mutated genes in *E.coli* 40k strain are expressed at the level above 2D Oxi-DIGE detection threshold.

Conclusion based on these results is that mutational impact on protein sensitivity to carbonylation is not a consistent pattern; it is rather a complex form of interactions between proteins whose coded genes are subjected to mutations or are not.

6. CONCLUSIONS

Both RNA and protein homeostasis are of great importance to maintain the cell (prokaryotic or eukaryotic) in balance. They can be also disrupted by mutations that have an impact on RNA/protein conformation with phenotypic consequences. On the protein level, detrimental mutation effect can be buffered by protein chaperones with no impairment of phenotype.

The results presented in Chapter 4.1 provide, for the first time, evidence of RNA chaperone mediated mutation buffering by measuring the relative fitness of *E.coli* strains. Performing competition experiments, it was shown that growth rate of two low-fitness mutator strains (40k and $\Delta mutH$) was improved by overexpression of three DEAD-box RNA helicases (RhlB, SrmB, CsdA) and the cold shock protein CspA, respectively. Not a single identical mutation has been identified between 40k and $\Delta mutH$ strain, suggesting that RNA chaperone buffering occur across a broad range of substrates. Mutations that have shown to be individually deleterious were found in *lamB* and *rplS* gene and their compromised fitness rescued by DBRHs and CspA overexpression.

The main question that arises after revealing the phenotypic effects of mutation buffering by RNA chaperones is: what is the molecular basis of this phenomenon? There are several aspects to examine the mechanism of RNA chaperone competence in concealing the effects of deleterious mutations. First is analysing transcriptome of *E.coli* strains (wild type and mutator) in the presence of RNA chaperone overexpression followed by the proteome level analyses. Next thing that would be of the particular interest for this study is identification of protein-RNA interactions using individual-nucleotide resolution cross-linking and immunoprecipitation (iCLIP), enabling association of RNA chaperones and their respective substrates. This approach would allow us to perceive RNA chaperone binding preferences to RNA molecules with or without certain mutations. Further studies that could reveal molecular mechanism of mutation buffering include identification of mutations (synonymous and nonsynonymous) that are privileged buffered by the RNA chaperone activity. The data presented here indicate the relevance of synonymous mutations in this context. Individual synonymous mutation in the *rplS* gene has shown decline in the relative fitness and the rescue by DBRHs. Therefore, producing the mutant libraries of selected genes and introducing them into *E.coli*, sequester the ones that decrease the fitness in competitions experiments and increase the same one in the presence of

RNA chaperone overexpressions would provide us with more information in comprehending this mechanism.

Another interesting aspect of this study is the evolution one. Accumulation of genetic changes drive the evolution and in parallel alter the sequences coding for diverse RNA chaperones whose preferences toward their target substrates could be modified. In which direction this phenomenon focus the evolution require additional investigation in the future.

An important role of RNA quality control in the lifespan of eukaryotic organism, *S.cerevisiae*, was demonstrated in the Chapter 4.2, showing that more efficient splicing of mitochondrial introns from COX1 and COB gene by Mss116 DEAD-box RNA helicase overexpression results with prolonged chronological lifespan compared to the wild type strain. Both *S.cerevisiae* strains, the one with deleted mitochondrial introns (*I₀*) and the one with overexpressed Mss116, showed increased generation time, prolonged CLS, mitochondrial fusion phenotype, increased oxygen consumption, higher levels of ATP and increased levels of mature cox1 and cob mRNA compared with their levels in the wild type. Further results led to conclusion that this phenotypic changes are controlled by activation of the retrograde response. By deleting *rtg2* gene, mitochondrial volume and mitochondrial spherical shape were reduced in the tested *S.cerevisiae* strain.

RNA splicing homeostasis was perceived here in unconventional fashion. For the first time it was shown that efficient splicing or forced intron removal of yeast mitochondrial mRNAs can activate the stress response and affect phenotype. It is known that introducing the minor stress (ROS, heat shock, calorie restriction) can activate pathways to promote organism longevity. Here, it is demonstrated that more efficient splicing can also activate stress response and prolonge both, CLS and RLS.

In order to understand more how disruption of RNA splicing homeostasis affect phenotype, further studies including the analyses of intronic polymorphisms and RNA chaperone involvement would be of great benefit.

The objective of this studies was also to explore molecular bases of protein resistance or sensitivity to oxidative damage by measuring carbonylation levels. Data presented in Chapter 4.3 demonstrates that only 5% of detected proteins using 2D Oxi-DIGE method had significant change (increase or decrease) of protein carbonylation in the mutator strain compared with non-

mutator. Although, 26% of the proteins with increased level and 24% of the ones with decreased carbonylation level contain a mutation in their coded genes. Since data presented here also point out proteins with altered carbonylation levels and their interaction partners carrying certain polymorphisms in their coded genes, suggested underlying mutation-based impact on carbonylation is not straightforward. One approach for revealing whether DNA polymorphisms reflect in polymorphisms of protein oxidability is to examine individual protein level of carbonylation by introducing diverse types of mutations in the coded gene.

DNA polymorphisms can certainly influence organismal fitness and phenotype modifying RNA, protein homeostasis or by crosstalk among DNA, RNA and protein level. In order to understand the biological effect of this crosstalk, studying the RNA chaperone function in the mutation buffering regarding protein sensitivity to oxidation could result with some valuable insights. By identification of target proteins that are crucial in displaying certain diseases with detecting their conformation changes, carbonylation level and related gene polymorphisms, we could design a predictive model for the early diagnostic.

7. REFERENCES

- Anfinsen, C. B. (1973). Principles that govern the folding of protein chains. *Science*, 181(4096), 223-230.
- Bae, W., Jones, P. G., & Inouye, M. (1997). CspA, the major cold shock protein of *Escherichia coli*, negatively regulates its own gene expression. *Journal of bacteriology*, 179(22), 7081-7088.
- Bae, W., Xia, B., Inouye, M., & Severinov, K. (2000). *Escherichia coli* CspA-family RNA chaperones are transcription antiterminators. *Proceedings of the National Academy of Sciences*, 97(14), 7784-7789.
- Barrick, J. E., Yu, D. S., Yoon, S. H., Jeong, H., Oh, T. K., Schneider, D., Lenski R. E. & Kim, J. F. (2009). Genome evolution and adaptation in a long-term experiment with *Escherichia coli*. *Nature*, 461(7268), 1243.
- Barton, A. A. (1950). Some aspects of cell division in *Saccharomyces cerevisiae*. *Microbiology*, 4(1), 84-86.
- Bessenyei, B., Marka, M., Urban, L., Zeher, M., & Semsei, I. (2004). Single nucleotide polymorphisms: aging and diseases. *Biogerontology*, 5(5), 291-303.
- Bonnefoy, N., Remacle, C., & Fox, T. D. (2007). Genetic transformation of *Saccharomyces cerevisiae* and *Chlamydomonas reinhardtii* mitochondria. *Methods in cell biology*, 80, 525-548.
- Bradford, M. M. (1976). A rapid and sensitive method for the quantitation of microgram quantities of protein utilizing the principle of protein-dye binding. *Analytical biochemistry*, 72(1-2), 248-254.
- Burtner, C. R., & Kennedy, B. K. (2010). Progeria syndromes and ageing: what is the connection?. *Nature reviews Molecular cell biology*, 11(8), 567-578.
- Burtner, C. R., Murakami, C. J., Kennedy, B. K., & Kaerberlein, M. (2009). A molecular mechanism of chronological aging in yeast. *Cell cycle*, 8(8), 1256-1270.
- Butterfield, D. A., & Stadtman, E. R. (1997). Protein oxidation processes in aging brain. *Advances in Cell Aging and Gerontology*, 2, 161-191.

- Carrington, J. L. (2007). The biology of aging: Observations and principles.
- Casanueva, M. O., Burga, A., & Lehner, B. (2012). Fitness trade-offs and environmentally induced mutation buffering in isogenic *C. elegans*. *Science*, 335(6064), 82-85.
- Chapman, E., Farr, G. W., Usaite, R., Furtak, K., Fenton, W. A., Chaudhuri, T. K., Hondorp, E. R., Matthews R. G., Wolf, G. S., Yates, J. R., Pypaert, M. & Horwich, A. L. (2006). Global aggregation of newly translated proteins in an *Escherichia coli* strain deficient of the chaperonin GroEL. *Proceedings of the National Academy of Sciences*, 103(43), 15800-15805.
- Charollais, J., Pflieger, D., Vinh, J., Dreyfus, M., & Iost, I. (2003). The DEAD-box RNA helicase SrmB is involved in the assembly of 50S ribosomal subunits in *Escherichia coli*. *Molecular microbiology*, 48(5), 1253-1265.
- Chen, X. J., & Butow, R. A. (2005). The organization and inheritance of the mitochondrial genome. *Nature reviews. Genetics*, 6(11), 815.
- Collins, T. J. (2007). ImageJ for microscopy. *Biotechniques*, 43(1 Suppl), 25-30.
- Cutler, R. G. (1991). Antioxidants and aging. *The American journal of clinical nutrition*, 53(1), 373S-379S.
- da Cunha, F. M., Torelli, N. Q., & Kowaltowski, A. J. (2015). Mitochondrial retrograde signaling: triggers, pathways, and outcomes. *Oxidative medicine and cellular longevity*, 2015.
- Dalle-Donne, I., Giustarini, D., Colombo, R., Rossi, R., & Milzani, A. (2003). Protein carbonylation in human diseases. *Trends in molecular medicine*, 9(4), 169-176.
- de la Cruz, J., Kressler, D., & Linder, P. (1999). Unwinding RNA in *Saccharomyces cerevisiae*: DEAD-box proteins and related families. *Trends in biochemical sciences*, 24(5), 192-198.
- De Magalhaes, J. P. (2011). The biology of ageing: a primer. *An Introduction to Gerontology*. Cambridge University Press, Cambridge, UK, 21-47.
- Death, A., Notley, L., & Ferenci, T. (1993). Derepression of LamB protein facilitates outer membrane permeation of carbohydrates into *Escherichia coli* under conditions of nutrient stress. *Journal of bacteriology*, 175(5), 1475-1483.

- Del Campo, M., Mohr, S., Jiang, Y., Jia, H., Jankowsky, E., & Lambowitz, A. M. (2009). Unwinding by local strand separation is critical for the function of DEAD-box proteins as RNA chaperones. *Journal of molecular biology*, 389(4), 674-693.
- Ding, Y., & Lawrence, C. E. (2003). A statistical sampling algorithm for RNA secondary structure prediction. *Nucleic acids research*, 31(24), 7280-7301.
- Dinner, A. R., Šali, A., Smith, L. J., Dobson, C. M., & Karplus, M. (2000). Understanding protein folding via free-energy surfaces from theory and experiment. *Trends in biochemical sciences*, 25(7), 331-339.
- Dobson, C. M. (2001). The structural basis of protein folding and its links with human disease. *Philosophical Transactions of the Royal Society of London B: Biological Sciences*, 356(1406), 133-145.
- Downs, W. D., & Cech, T. R. (1996). Kinetic pathway for folding of the Tetrahymena ribozyme revealed by three UV-inducible crosslinks. *Rna*, 2(7), 718-732.
- Dukan, S., Farewell, A., Ballesteros, M., Taddei, F., Radman, M., & Nyström, T. (2000). Protein oxidation in response to increased transcriptional or translational errors. *Proceedings of the National Academy of Sciences*, 97(11), 5746-5749.
- Elles, L. M. S., & Uhlenbeck, O. C. (2007). Mutation of the arginine finger in the active site of Escherichia coli DbpA abolishes ATPase and helicase activity and confers a dominant slow growth phenotype. *Nucleic acids research*, 36(1), 41-50.
- Epstein, C. B., Waddle, J. A., Hale, W., Davé, V., Thornton, J., Macatee, T. L., Garner, H. R. & Butow, R. A. (2001). Genome-wide responses to mitochondrial dysfunction. *Molecular Biology of the Cell*, 12(2), 297-308.
- Esser, C., Alberti, S., & Höhfeld, J. (2004). Cooperation of molecular chaperones with the ubiquitin/proteasome system. *Biochimica et Biophysica Acta (BBA)-Molecular Cell Research*, 1695(1), 171-188.
- Fares, M. A., Moya, A., & Barrio, E. (2004). GroEL and the maintenance of bacterial endosymbiosis. *Trends in Genetics*, 20(9), 413-416.
- Fares, M. A., Ruiz-González, M. X., Moya, A., Elena, S. F., & Barrio, E. (2002). Endosymbiotic bacteria: groEL buffers against deleterious mutations. *Nature*, 417(6887), 398-398.

- Fedor, M. J., & Williamson, J. R. (2005). The catalytic diversity of RNAs. *Nature reviews. Molecular cell biology*, 6(5), 399.
- Fedorova, O., & Pyle, A. M. (2012). The brace for a growing scaffold: Mss116 protein promotes RNA folding by stabilizing an early assembly intermediate. *Journal of molecular biology*, 422(3), 347-365.
- Foury, F., Roganti, T., Lecrenier, N., & Purnelle, B. (1998). The complete sequence of the mitochondrial genome of *Saccharomyces cerevisiae*. *FEBS letters*, 440(3), 325-331.
- Freitas, A. A., & de Magalhaes, J. P. (2011). A review and appraisal of the DNA damage theory of ageing. *Mutation Research/Reviews in Mutation Research*, 728(1), 12-22.
- Genga, A., Bianchi, L., & Foury, F. (1986). A nuclear mutant of *Saccharomyces cerevisiae* deficient in mitochondrial DNA replication and polymerase activity. *Journal of Biological Chemistry*, 261(20), 9328-9332.
- Ghazi, A., Henis-Korenblit, S., & Kenyon, C. (2007). Regulation of *Caenorhabditis elegans* lifespan by a proteasomal E3 ligase complex. *Proceedings of the National Academy of Sciences*, 104(14), 5947-5952.
- Giegé, R., Frugier, M., & Rudinger, J. (1998). tRNA mimics. *Current opinion in structural biology*, 8(3), 286-293.
- Gietz, R. D., & Schiestl, R. H. (2007). High-efficiency yeast transformation using the LiAc/SS carrier DNA/PEG method. *Nature protocols*, 2(1), 35.
- Goffeau, A., Barrell, B. G., Bussey, H., Davis, R. W., Dujon, B., Feldmann, H., Galibert, F., Hoheisel, J. D., Jacq, C., Johnston, M., Louis, E. J., Mewes, H. W., Murakami, Y., Philippsen, P., Tettelin, H., & Oliver, S. G., (1996). Life with 6000 genes. *Science*, 274(5287), 546-567.
- Golik, P., Szczepanek, T., Bartnik, E., Stepień, P. P., & Lazowska, J. (1995). The *S. cerevisiae* nuclear gene SUV3 encoding a putative RNA helicase is necessary for the stability of mitochondrial transcripts containing multiple introns. *Current genetics*, 28(3), 217-224.
- Grimsrud, P. A., Xie, H., Griffin, T. J., & Bernlohr, D. A. (2008). Oxidative stress and covalent modification of protein with bioactive aldehydes. *Journal of Biological Chemistry*, 283(32), 21837-21841.

- Halls, C., Mohr, S., Del Campo, M., Yang, Q., Jankowsky, E., & Lambowitz, A. M. (2007). Involvement of DEAD-box proteins in group I and group II intron splicing. Biochemical characterization of Mss116p, ATP hydrolysis-dependent and-independent mechanisms, and general RNA chaperone activity. *Journal of molecular biology*, 365(3), 835-855.
- Hamosh, A., King, T. M., Rosenstein, B. J., Corey, M., Levison, H., Durie, P., & Macek, M. (1992). Cystic fibrosis patients bearing both the common missense mutation, Gly→ Asp at codon 551 and the Δ F508 mutation are clinically indistinguishable from Δ F508 homozygotes, except for decreased risk of meconium ileus. *American journal of human genetics*, 51(2), 245.
- Harman, D. (1956). Aging: a theory based on free radical and radiation chemistry. *Journal of gerontology*, 11(3), 298-300.
- Hartl, F. U. (2016). Cellular homeostasis and aging. *Annual review of biochemistry*, 85, 1-4.
- Hartl, F. U., & Hayer-Hartl, M. (2009). Converging concepts of protein folding in vitro and in vivo. *Nature structural & molecular biology*, 16(6), 574-581.
- Hartl, F. U., Bracher, A., & Hayer-Hartl, M. (2011). Molecular chaperones in protein folding and proteostasis. *Nature*, 475(7356), 324.
- Hasty, P., Campisi, J., Hoeijmakers, J., Van Steeg, H., & Vijg, J. (2003). Aging and genome maintenance: lessons from the mouse?. *Science*, 299(5611), 1355-1359.
- Heintz, C., Doktor, T. K., Lanjuin, A., Escoubas, C., Zhang, Y., Weir, H. J., Dutta, S., Silva-García, C. G., Bruun, G. H., Morantte, I., Hoxhaj, G., Manning, B. D., Andresen, B. S., & Mair, W. B. (2017). Splicing factor 1 modulates dietary restriction and TORC1 pathway longevity in *C. elegans*. *Nature*, 541(7635), 102.
- Herrero, A., & Barja, G. (1997). Sites and mechanisms responsible for the low rate of free radical production of heart mitochondria in the long-lived pigeon. *Mechanisms of ageing and development*, 98(2), 95-111.
- Herschlag, D. (1995). RNA chaperones and the RNA folding problem. *Journal of Biological Chemistry*, 270(36), 20871-20874.
- Hillier, B. J., Rodriguez, H. M., & Gregoret, L. M. (1998). Coupling protein stability and protein function in *Escherichia coli* CspA. *Folding and Design*, 3(2), 87-93.

- Hoeijmakers, J. H. (2009). DNA damage, aging, and cancer. *New England Journal of Medicine*, 361(15), 1475-1485.
- Hong, E. L., Balakrishnan, R., Dong, Q., Christie, K. R., Park, J., Binkley, G., Costanzo M. C., Hirschman, J. E. & Cherry, J. M. (2007). Gene Ontology annotations at SGD: new data sources and annotation methods. *Nucleic acids research*, 36(suppl_1), D577-D581.
- Huertas-Vazquez, A., Plaisier, C. L., Geng, R., Haas, B. E., Lee, J., Greevenbroek, M. M., Pajukanta, P. et al. (2010). A nonsynonymous SNP within PCDH15 is associated with lipid traits in familial combined hyperlipidemia. *Human genetics*, 127(1), 83.
- Hunger, K., Beckering, C. L., Wiegeshoff, F., Graumann, P. L., & Marahiel, M. A. (2006). Cold-induced putative DEAD box RNA helicases CshA and CshB are essential for cold adaptation and interact with cold shock protein B in *Bacillus subtilis*. *Journal of bacteriology*, 188(1), 240-248.
- Hurst, G. D., & Werren, J. H. (2001). The role of selfish genetic elements in eukaryotic evolution. *Nature reviews. Genetics*, 2(8), 597.
- Hyun, M., Lee, J., Lee, K., May, A., Bohr, V. A., & Ahn, B. (2008). Longevity and resistance to stress correlate with DNA repair capacity in *Caenorhabditis elegans*. *Nucleic acids research*, 36(4), 1380-1389.
- Ingram, V. M. (1956). A specific chemical difference between the globins of normal human and sickle-cell anaemia haemoglobin. *Nature*, 178(4537), 792-794.
- Jarmoskaite, I., Bhaskaran, H., Seifert, S., & Russell, R. (2014). DEAD-box protein CYT-19 is activated by exposed helices in a group I intron RNA. *Proceedings of the National Academy of Sciences*, 111(29), E2928-E2936.
- Jiang, W., Hermolin, J., & Fillingame, R. H. (2001). The preferred stoichiometry of c subunits in the rotary motor sector of *Escherichia coli* ATP synthase is 10. *Proceedings of the National Academy of Sciences*, 98(9), 4966-4971.
- Jiang, W., Hou, Y., & Inouye, M. (1997). CspA, the major cold-shock protein of *Escherichia coli*, is an RNA chaperone. *Journal of Biological Chemistry*, 272(1), 196-202.
- Kaeberlein, M., Burtner, C. R., & Kennedy, B. K. (2007). Recent developments in yeast aging. *PLoS genetics*, 3(5), e84.

- Kennell, J. C., Moran, J. V., Perlman, P. S., Butow, R. A., & Lambowitz, A. M. (1993). Reverse transcriptase activity associated with maturase-encoding group II introns in yeast mitochondria. *Cell*, 73(1), 133-146.
- Kerner, M. J., Naylor, D. J., Ishihama, Y., Maier, T., Chang, H. C., Stines, A. P., & Hartl, F. U. (2005). Proteome-wide analysis of chaperonin-dependent protein folding in *Escherichia coli*. *Cell*, 122(2), 209-220.
- Khemici, V., & Carpousis, A. J. (2004). The RNA degradosome and poly (A) polymerase of *Escherichia coli* are required in vivo for the degradation of small mRNA decay intermediates containing REP-stabilizers. *Molecular microbiology*, 51(3), 777-790.
- Kispal, G., Sipos, K., Lange, H., Fekete, Z., Bedekovics, T., Janáky, T., ... & Lill, R. (2005). Biogenesis of cytosolic ribosomes requires the essential iron-sulphur protein Rli1p and mitochondria. *The EMBO journal*, 24(3), 589-598.
- Koga, H., Kaushik, S., & Cuervo, A. M. (2011). Protein homeostasis and aging: The importance of exquisite quality control. *Ageing research reviews*, 10(2), 205-215.
- Krisko, A., & Radman, M. (2010). Protein damage and death by radiation in *Escherichia coli* and *Deinococcus radiodurans*. *Proceedings of the National Academy of Sciences*, 107(32), 14373-14377.
- Krisko, A., & Radman, M. (2013). Biology of extreme radiation resistance: the way of *Deinococcus radiodurans*. *Cold Spring Harbor perspectives in biology*, 5(7), a012765.
- Lahaye, A., Stahl, H., Thines-Sempoux, D., & Foury, F. (1991). PIF1: a DNA helicase in yeast mitochondria. *The EMBO Journal*, 10(4), 997.
- Lambowitz, A. M., Caprara, M. G., Zimmerly, S., & Perlman, P. S. (1999). Group I and group II ribozymes as RNPs: clues to the past and guides to the future. *COLD SPRING HARBOR MONOGRAPH SERIES*, 37, 451-486.
- Lasserre, J. P., Dautant, A., Aiyar, R. S., Kucharczyk, R., Glatigny, A., Tribouillard-Tanvier, D., Pitayu, L. et al. (2015). Yeast as a system for modeling mitochondrial disease mechanisms and discovering therapies. *Disease models & mechanisms*, 8(6), 509-526.
- Lee, S. S., Vizcarra, I. A., Huberts, D. H., Lee, L. P., & Heinemann, M. (2012). Whole lifespan microscopic observation of budding yeast aging through a microfluidic dissection platform. *Proceedings of the National Academy of Sciences*, 109(13), 4916-4920.

- Lenski, R. E. (1988). Experimental studies of pleiotropy and epistasis in *Escherichia coli*. I. Variation in competitive fitness among mutants resistant to virus T4. *Evolution*, 42(3), 425-432.
- Lenski, R. E. (1991). Quantifying fitness and gene stability in microorganisms. *Biotechnology (Reading, Mass.)*, 15, 173-192.
- Levine, R. L. (2002). Carbonyl modified proteins in cellular regulation, aging, and disease 2, 3. *Free Radical Biology and Medicine*, 32(9), 790-796.
- Lind, P. A., Berg, O. G., & Andersson, D. I. (2010). Mutational robustness of ribosomal protein genes. *Science*, 330(6005), 825-827.
- Linder, P., Lasko, P. F., Ashburner, M., Leroy, P., Nielsen, P. J., Nishi, K., & Slonimski, P. P. (1989). Birth of the DEAD box. *Nature*, 337(6203), 121-122.
- Lindstrom, D. L., & Gottschling, D. E. (2009). The mother enrichment program: a genetic system for facile replicative life span analysis in *Saccharomyces cerevisiae*. *Genetics*, 183(2), 413-422.
- Lipinski, K. A., Kaniak-Golik, A., & Golik, P. (2010). Maintenance and expression of the *S. cerevisiae* mitochondrial genome—from genetics to evolution and systems biology. *Biochimica et Biophysica Acta (BBA)-Bioenergetics*, 1797(6), 1086-1098.
- Lithgow, G. J., White, T. M., Melov, S., & Johnson, T. E. (1995). Thermotolerance and extended life-span conferred by single-gene mutations and induced by thermal stress. *Proceedings of the National Academy of Sciences*, 92(16), 7540-7544.
- Liu, Z., & Butow, R. A. (1999). A transcriptional switch in the expression of yeast tricarboxylic acid cycle genes in response to a reduction or loss of respiratory function. *Molecular and Cellular Biology*, 19(10), 6720-6728.
- Liu, Z., Sekito, T., Špírek, M., Thornton, J., & Butow, R. A. (2003). Retrograde signaling is regulated by the dynamic interaction between Rtg2p and Mks1p. *Molecular cell*, 12(2), 401-411.
- Longo, V. D. (1997). The pro-senescence role of Ras2 in the chronological life span of yeast. Los Angeles: University of California Los Angeles, 112-153.

- López-Otín, C., Blasco, M. A., Partridge, L., Serrano, M., & Kroemer, G. (2013). The hallmarks of aging. *Cell*, 153(6), 1194-1217.
- Lorenz, R., Bernhart, S. H., Zu Siederdisen, C. H., Tafer, H., Flamm, C., Stadler, P. F., & Hofacker, I. L. (2011). ViennaRNA Package 2.0. *Algorithms for Molecular Biology*, 6(1), 26.
- Lu, J., Aoki, H., & Ganoza, M. C. (1999). Molecular characterization of a prokaryotic translation factor homologous to the eukaryotic initiation factor eIF4A. *The international journal of biochemistry & cell biology*, 31(1), 215-229.
- Moll, I., Grill, S., Gründling, A., & Bläsi, U. (2002). Effects of ribosomal proteins S1, S2 and the DeaD/CsdA DEAD-box helicase on translation of leaderless and canonical mRNAs in *Escherichia coli*. *Molecular microbiology*, 44(5), 1387-1396.
- Morimoto, R. I. (2008). Proteotoxic stress and inducible chaperone networks in neurodegenerative disease and aging. *Genes & development*, 22(11), 1427-1438.
- Mortimer, R. K., & Johnston, J. R. (1959). Life span of individual yeast cells. *Nature*, 183(4677), 1751-1752.
- Mounolou, J. C., Jakob, H., & Slonimski, P. P. (1966). Mitochondrial DNA from yeast “petite” mutants: Specific changes of buoyant density corresponding to different cytoplasmic mutations. *Biochemical and biophysical research communications*, 24(2), 218-224.
- Narayanan, L., Fritzell, J. A., Baker, S. M., Liskay, R. M., & Glazer, P. M. (1997). Elevated levels of mutation in multiple tissues of mice deficient in the DNA mismatch repair gene Pms2. *Proceedings of the National Academy of Sciences*, 94(7), 3122-3127.
- Newman, A. (1998). RNA splicing. *Current Biology*, 8(25), R903-R905.
- Nyström, T. (2005). Role of oxidative carbonylation in protein quality control and senescence. *The EMBO journal*, 24(7), 1311-1317.
- Pan, C., & Russell, R. (2010). Roles of DEAD-box proteins in RNA and RNP folding. *RNA biology*, 7(6), 667-676.
- Paumard, P., Vaillier, J., Couлары, B., Schaeffer, J., Soubannier, V., Mueller, D. M., Velours, J., et al. (2002). The ATP synthase is involved in generating mitochondrial cristae morphology. *The EMBO journal*, 21(3), 221-230.

- Perry, S. W., Norman, J. P., Barbieri, J., Brown, E. B., & Gelbard, H. A. (2011). Mitochondrial membrane potential probes and the proton gradient: a practical usage guide. *Biotechniques*, 50(2), 98.
- Plotkin, J. B., & Kudla, G. (2011). Synonymous but not the same: the causes and consequences of codon bias. *Nature reviews. Genetics*, 12(1), 32.
- Prud'homme-Généreux, A., Beran, R. K., Iost, I., Ramey, C. S., Mackie, G. A., & Simons, R. W. (2004). Physical and functional interactions among RNase E, polynucleotide phosphorylase and the cold-shock protein, CsdA: evidence for a 'cold shock degradosome'. *Molecular microbiology*, 54(5), 1409-1421.
- Py, B., Higgins, C. F., Krisch, H. M., & Carpousis, A. J. (1996). A DEAD-box RNA helicase in the Escherichia coli RNA degradosome. *Nature*, 381(6578), 169.
- Queitsch, C., Sangster, T. A., & Lindquist, S. (2002). Hsp90 as a capacitor of phenotypic variation. *Nature*, 417(6889), 618.
- Quinlan, A. R., & Hall, I. M. (2010). BEDTools: a flexible suite of utilities for comparing genomic features. *Bioinformatics*, 26(6), 841-842.
- Radford, S. E., & Dobson, C. M. (1999). From computer simulations to human disease. *Cell*, 97(3), 291-298.
- Riordan, J. R., Rommens, J. M., Kerem, B. S., Alon, N., & Rozmahel, R. (1989). Identification of the cystic fibrosis gene: cloning and characterization of complementary DNA. *Science*, 245(4922), 1066.
- Rohner, N., Jarosz, D. F., Kowalko, J. E., Yoshizawa, M., Jeffery, W. R., Borowsky, R. L. & Tabin, C. J. (2013). Cryptic variation in morphological evolution: HSP90 as a capacitor for loss of eyes in cavefish. *Science*, 342(6164), 1372-1375.
- Rossi, D. J., Bryder, D., Seita, J., Nussenzweig, A., Hoeijmakers, J., & Weissman, I. L. (2007). Deficiencies in DNA damage repair limit the function of haematopoietic stem cells with age. *Nature*, 447(7145), 725.
- Rudan, M., Schneider, D., Warnecke, T., & Krisko, A. (2015). RNA chaperones buffer deleterious mutations in E. coli. *Elife*, 4, 1-16.

- Russell, R. (2008). RNA misfolding and the action of chaperones. *Frontiers in bioscience: a journal and virtual library*, 13, 1.
- Russell, R., Jarmoskaite, I., & Lambowitz, A. M. (2013). Toward a molecular understanding of RNA remodeling by DEAD-box proteins. *RNA biology*, 10(1), 44-55.
- Rutherford, S. L. (2003). Between genotype and phenotype: protein chaperones and evolvability. *Nature reviews. Genetics*, 4(4), 263.
- Rutherford, S. L., & Lindquist, S. (1998). Hsp90 as a capacitor for morphological evolution. *Nature*, 396(6709), 336.
- Sambrook, J., Fritsch, E. F., & Maniatis, T. (1989). *Molecular cloning: a laboratory manual* (No. Ed. 2). Cold spring harbor laboratory press.
- Sawitzke, J. A., Thomason, L. C., Bubunencko, M., Li, X. T., Costantino, N., & Court, D. L. (2013). Recombineering: highly efficient in vivo genetic engineering using single-strand oligos. *Methods Enzymol*, 533, 157-177.
- Sekito, T., Thornton, J., & Butow, R. A. (2000). Mitochondria-to-nuclear signaling is regulated by the subcellular localization of the transcription factors Rtg1p and Rtg3p. *Molecular Biology of the Cell*, 11(6), 2103-2115.
- Semrad, K. (2010). Proteins with RNA chaperone activity: A world of diverse proteins with a common task—impediment of RNA misfolding. *Biochemistry research international*, 2011.
- Shama, S., Lai, C. Y., Antoniazzi, J. M., Jiang, J. C., & Jazwinski, S. M. (1998). Heat stress-induced life span extension in yeast. *Experimental cell research*, 245(2), 379-388.
- Sies, H., Cadenas, E., Symons, M. C. R., & Scott, G. (1985). Oxidative stress: damage to intact cells and organs. *Philosophical transactions of the Royal Society of London. Series B, Biological sciences*, 617-631.
- Singleton, M. R., Dillingham, M. S., & Wigley, D. B. (2007). Structure and mechanism of helicases and nucleic acid translocases. *Annu. Rev. Biochem.*, 76, 23-50.
- Sniegowski, P. D., Gerrish, P. J., & Lenski, R. E. (1997). Evolution of high mutation rates in experimental populations of *E. coli*. *Nature*, 387(6634), 703.
- Sohal, R. S., & Allen, R. G. (1990). Oxidative stress as a causal factor in differentiation and aging: a unifying hypothesis. *Experimental gerontology*, 25(6), 499-522.

- Stuart, G. R., Oda, Y., de Boer, J. G., & Glickman, B. W. (2000). Mutation frequency and specificity with age in liver, bladder and brain of lacI transgenic mice. *Genetics*, 154(3), 1291-1300.
- Sutphin, G. L., Olsen, B. A., Kennedy, B. K., & Kaeberlein, M. (2011). Genome-wide analysis of yeast aging. In *Aging Research in Yeast* (pp. 251-289). Springer Netherlands.
- Szilard, L. (1959). On the nature of the aging process. *Proceedings of the National Academy of Sciences*, 45(1), 30-45.
- Tanner, N. K., & Linder, P. (2001). DExD/H box RNA helicases: from generic motors to specific dissociation functions. *Molecular cell*, 8(2), 251-262.
- Tenaillon, O., Barrick, J. E., Ribeck, N., Deatherage, D. E., Blanchard, J. L., Dasgupta, A., ... & Schneider, D. (2016). Tempo and mode of genome evolution in a 50,000-generation experiment. *Nature*, 536(7615), 165-170.
- Tenaillon, O., Rodríguez-Verdugo, A., Gaut, R. L., McDonald, P., Bennett, A. F., Long, A. D., & Gaut, B. S. (2012). The molecular diversity of adaptive convergence. *Science*, 335(6067), 457-461.
- Thomas, P. J., Qu, B. H., & Pedersen, P. L. (1995). Defective protein folding as a basis of human disease. *Trends in biochemical sciences*, 20(11), 456-459.
- Tokuriki, N., & Tawfik, D. S. (2009). Chaperonin overexpression promotes genetic variation and enzyme evolution. *Nature*, 459(7247), 668-673.
- Tokuriki, N., Stricher, F., Serrano, L., & Tawfik, D. S. (2008). How protein stability and new functions trade off. *PLoS Computational Biology*, 4(2), e1000002.
- Turk, E. M., Das, V., Seibert, R. D., & Andrulis, E. D. (2013). The mitochondrial RNA landscape of *Saccharomyces cerevisiae*. *PLoS One*, 8(10), e78105.
- Turner, A. M. W., Love, C. F., Alexander, R. W., & Jones, P. G. (2007). Mutational analysis of the *Escherichia coli* DEAD box protein CsdA. *Journal of bacteriology*, 189(7), 2769-2776.
- Vallenet, D., Belda, E., Calteau, A., Cruveiller, S., Engelen, S., Lajus, A., Rouy, Z. et al. (2012). MicroScope—an integrated microbial resource for the curation and comparative analysis of genomic and metabolic data. *Nucleic acids research*, 41(D1), D636-D647.

- Vanzo, N. F., Li, Y. S., Py, B., Blum, E., Higgins, C. F., Raynal, L. C., Carpousis, A. J. et al. (1998). Ribonuclease E organizes the protein interactions in the Escherichia coli RNA degradosome. *Genes & development*, 12(17), 2770-2781.
- Velours, J., Dautant, A., Salin, B., Sagot, I., & Brèthes, D. (2009). Mitochondrial F₁F₀-ATP synthase and organellar internal architecture. *The international journal of biochemistry & cell biology*, 41(10), 1783-1789.
- Vidovic, A., Supek, F., Nikolic, A., & Krisko, A. (2014). Signatures of conformational stability and oxidation resistance in proteomes of pathogenic bacteria. *Cell reports*, 7(5), 1393-1400.
- Vijg, J., & Dollé, M. E. (2002). Large genome rearrangements as a primary cause of aging. *Mechanisms of ageing and development*, 123(8), 907-915.
- Vowinckel, J., Hartl, J., Butler, R., & Ralser, M. (2015). MitoLoc: A method for the simultaneous quantification of mitochondrial network morphology and membrane potential in single cells. *Mitochondrion*, 24, 77-86.
- Wang, G. S., & Cooper, T. A. (2007). Splicing in disease: disruption of the splicing code and the decoding machinery. *Nature reviews. Genetics*, 8(10), 749-761.
- Welsh, M. J., & Smith, A. E. (1993). Molecular mechanisms of CFTR chloride channel dysfunction in cystic fibrosis. *Cell*, 73(7), 1251-1254.
- Werren, J. H. (2011). Selfish genetic elements, genetic conflict, and evolutionary innovation. *Proceedings of the National Academy of Sciences*, 108 (Supplement 2), 10863-10870.
- Wielgoss, S., Barrick, J. E., Tenailon, O., Wisner, M. J., Dittmar, W. J., Cruveiller, S., Schneider, D. et al. (2013). Mutation rate dynamics in a bacterial population reflect tension between adaptation and genetic load. *Proceedings of the National Academy of Sciences*, 110(1), 222-227.
- Wisner, M. J., Ribeck, N., & Lenski, R. E. (2013). Long-term dynamics of adaptation in asexual populations. *Science*, 342(6164), 1364-1367.
- Wolf, A. B., Caselli, R. J., Reiman, E. M., & Valla, J. (2013). APOE and neuroenergetics: an emerging paradigm in Alzheimer's disease. *Neurobiology of aging*, 34(4), 1007-1017.

Wolters, J. F., Chiu, K., & Fiumera, H. L. (2015). Population structure of mitochondrial genomes in *Saccharomyces cerevisiae*. *BMC genomics*, 16(1), 451.

Xie, Z., Zhang, Y., Zou, K., Brandman, O., Luo, C., Ouyang, Q., & Li, H. (2012). Molecular phenotyping of aging in single yeast cells using a novel microfluidic device. *Aging cell*, 11(4), 599-606.

Zimmerly, S., & Semper, C. (2015). Evolution of group II introns. *Mobile DNA*, 6(1), 7.

8. CURRICULUM VITAE

Name: Marina

Surname: Rudan

E-mail: marina.rudan@yahoo.com

Education:

2012 -2018 PhD student, Department of Biology, Faculty of Science, University of Zagreb, Croatia

2010 - Graduated at Laboratory for Sediments and Marine Sedimentology at Institute of Oceanography and Fisheries in Split. Graduation thesis: Sediments of Croatian part of the Adriatic sea

2004 - 2009. University of Split, Center of Marine Studies, Marine biology and ecology at Institute of Oceanography and Fisheries in Split, Croatia

Positions:

2012 – 2017 PhD student, Macromolecular homeostasis in aging, Mediterranean Institute for Life Sciences, Split, Croatia

2011-2012 volunteer, Biology of robustness and Molecular basis of intrinsic aging and its prevention, Mediterranean Institute for Life Sciences, Split, Croatia

Publications:

Perić, M., Lovrić, A., Šarić, A., Musa, M., Dib, P. B., Rudan, M., Nikolić, A., Sobočanec, S., Mikecin, A-M., Dennerlein, S., Milošević, I., Vlahoviček, K., Raimundo, N. & Kriško A. (2017). TORC1-mediated sensing of chaperone activity alters glucose metabolism and extends lifespan. *Aging Cell*.

Perić, M., Dib, P. B., Dennerlein, S., Musa, M., Rudan, M., Lovrić, A., Nikolić A., Šarić A., Sobočanec, S., Mačak, Ž., Raimundo N. & Kriško A. (2016). Crosstalk between cellular compartments protects against proteotoxicity and extends lifespan. *Scientific reports*, 6, 28751.

Rudan, M., Schneider, D., Warnecke, T., & Kriško, A. (2015). RNA chaperones buffer deleterious mutations in *E. coli*. *Elife*, 4, 1-16.